P-05-197

Forsmark site investigation

Fracture mineralogy

Results from fracture minerals and wall rock alteration in boreholes KFM01B, KFM04A, KFM05A and KFM06A

Björn Sandström, Department of Geology,
Earth Sciences Centre, Göteborg University

Eva-Lena Tullborg, Terralogica AB

December 2005

Svensk Kärnbränslehantering AB
Swedish Nuclear Fuel
and Waste Management Co
Box 5864
SE-102 40 Stockholm Sweden
Tel 08-459 84 00
+46 8 459 84 00
Fax 08-661 57 19
+46 8 661 57 19

ISSN 1651-4416
SKB P-05-197

Forsmark site investigation

Fracture mineralogy

Results from fracture minerals and wall rock alteration in boreholes KFM01B, KFM04A, KFM05A and KFM06A

Björn Sandström, Department of Geology,
Earth Sciences Centre, Göteborg University

Eva-Lena Tullborg, Terralogica AB

December 2005

Keywords: Fracture mineralogy, Sequence of events, Low temperature minerals, Stable isotopes, Calcite, Redox conditions, Wall rock alteration, AP PF 400-04-32.

Abstract

Fracture mineral investigations have been carried out on samples from drill cores KFM01B, KFM04A, KFM05A and KFM06A. Open as well as sealed fractures have been sampled in order to identify the fracture minerals typical for the area and to distinguish between different fracture mineral generations and their formation conditions.

The analyses carried out and reported in this P-report include microscopy, electron microscopy (SEM-EDS), X-ray diffraction (XRD) as well as different chemical analyses of fractures filling material. Fracture calcites have been paid special attention since they occur in many fractures and can be formed during various conditions. Stable isotope results as well as chemical composition and morphology of the calcites can provide palaeohydrogeological information.

The most common fracture minerals in the area are calcite, chlorite, quartz, adularia (low-temperature K-feldspar), laumontite, prehnite, epidote, hematite, pyrite and clay minerals. Amongst the clay minerals, the most common is corrensite, which is a mixed layer clay with alternating layers of chlorite and smectite/vermiculite. Other clay minerals, less common, are illite, smectite, saponite and mixed-layer illite/smectite.

From the examined drill cores, 6 different generations of fracture mineralizations have been distinguished: 1) quartz-epidote-chlorite, 2) prehnite-laumontite-calcite-adularia-chlorite/corrensite, 3) euhedral quartz-adularia-albite, 4) calcite and pyrite, 5) asphaltite 6) calcite-clay minerals. The present understanding is that Generation 1 is clearly separated in time from Generation 2. The latter probably represents one prolonged and intense period of hydrothermal alteration and formation of new fractures in the area. Subsequently, after a period of dissolution, Generations 3 and 4 have precipitated, as a result of a younger period of hydrothermal circulation probably grading into low temperatures < 100°C. The asphaltite in Generation 5 has an organic origin and is most likely Phanerozoic. The precipitation of clay minerals and calcites in Generation 6 may have occurred during the Paleozoic to Neogene. The formation of new fractures is mostly associated with Generations 1, 2 and 3.

Generation 1 is mostly found in subhorizontal or steep NW striking fractures and Generation 2 in steep NE striking fractures, while the later generations are found in most orientations but preferably in horizontal to subhorizontal fractures.

The wall rock alteration is most extensive around the fractures of Generation 1 and 2. The dominant alteration is saussuritization of the plagioclase and chloritization of the biotite while the K-feldspar is relatively unaltered. The altered wall rock is red-stained due to micro-grains of hematite, mainly hosted in the plagioclase. The altered wall rock extends from less than 1 cm up to 10 cm away from the fractures.

A minor study on sediment-like fracture fillings was also carried out showing that the fracture filling material was partly gouge, partly quartz and adularia from Generation 3, i.e. the fillings were not sediments. Altered pitchblende has also been found in a special study of one uranium enriched fracture filling.

Sammanfattning

Sprickmineralogiska undersökningar har utförts på prover från borrkärnorna KFM01B, KFM04A, KFM05A och KFM06A. Såväl öppna som läkta sprickor har provtagits i syfte att identifiera sprickmineral samt för att skilja ut olika sprickmineral-generationer och deras bildningsmiljö.

De analyser som redovisas i denna P-rapport omfattar mikroskopi (polariserat ljus), elektronmikroskopi (SEM-EDS) röntgendiffraktion (XRD) och kemiska analyser av sprickfyllnadsmaterial. Sprickfyllnadskalciter har ägnats speciellt intresse eftersom de förekommer i många sprickor och dessutom representerar flera olika generationer och därmed olika bildningsmiljöer. Stabila isotoper samt kemisk sammansättning och kristall-morfologi har utnyttjats för att särskilja olika generationer och för att där så är möjligt ge palaeohydrogeologisk information.

De vanligaste sprickmineralen i området är: kalcit, klorit, kvarts, adularia (låg temperatur kalifältspat), laumontit, prehnit, epidot, hematit, pyrit och lermineral. Corrensit, som är ett blandskiktsmineral med alternerande lager av klorit och smektit eller vermikulit, är det vanligaste lermineralet. Andra lermineral som också identifierats är illit, smektit, saponit och ett blandskiktsmineral bestående av smektit och illit-lager.

Från de undersökta borrkärnorna har 6 olika generationer av sprickmineraliseringar urskiljts: 1) kvarts-epidot-klorit, 2) prehnit-laumontit-kalcit-adularia-klorit/corrensit, 3) euhedral kvarts-adularia-albit-analcim, 4) kalcit-pyrit 5) asfaltit (bergbeck) 6) lermineral, kalcit. Generation 1 är klart separerad i tid från Generation 2. Den senare representerar sannolikt en omfattande (kanske utdragen) period av hydrotermal omvandling och nybildning av sprickor. Efter en period av upplösning följer ytterligare en period av sprickbildning med omvandling/utfällning (Generation 3 och 4) under såväl reaktivering av tidigare sprickor som nybildning av sprickor. Denna period är yngre än Generation 2 och 3 och sträcker sig sannolikt in i temperaturer ner mot lågtemperatur-området (< 100 °C). Asfaltiten i Generation 5 har ett organiskt ursprung och är troligtvis fanerozoisk. Utfällningar av lågtemperatur-mineral (Generation 6) utgörs av olika mineral som kan vara utfällda under mycket skiftande betingelser med bildningsåldrar som kan variera från paleozoikum till neogen. Bildandet av nya sprickor har varit koncentrerat till Generation 1, 2 och 3. Generation 1 återfinns mest i subhorisontella eller branta NW-strykande sprickor och Generation 2 i branta NE sprickor medan senare generationer återfinns i de flesta riktningarna men mestadels i horisontella till subhorisontella.

Sidobergsomvandlingen är mest omfattande runt sprickorna i Generation 1 och 2 med en utbredning mellan < 1 cm upp till 10 cm ut från sprickorna. Omvandlingen består mest av saussuritisering av plagioklas, kloritisering av biotit samt en rödfärgning som uppstår på grund av att mikrokorn av hematit har bildats, oftast i plagioklasen. Kalifältspaten är oftast relativt oomvandlad. En mindre studie av sedimentliknande sprickfyllnader har också utförts vilken visade att materialet var dels gouge, dels kvarts och adularia från Generation 3, dvs inte något sediment. Omvandlad pechblände har också hittats i en specialstudie av en sprickfyllnad med förhöjd uranhalt.

Contents

1 Introduction

This document reports the results gained by the detailed study of fracture minerals from drill cores from boreholes KFM01B, KFM04A, KFM05A and KFM06A at the Forsmark site. The document is also an update of the sequence of fracture mineral generations based on the results from boreholes KFM01A, KFM02A, KFM03A and KFM03B /Sandström et al. 2004/. The work was carried out in accordance with activity plan SKB PF 400-04-32. In Table 1-1 controlling documents for performing this activity are listed. Both activity plan and method descriptions are SKB's internal controlling documents.

Mapping of fractures and fracture minerals is carried out on all cored boreholes within the site investigation program and this information serves as a basis for the fracture mineral study /Berglund et al. 2004, Petersson et al. 2004a, Petersson et al. 2004c, Petersson et al. 2005/ However, identifying fracture minerals macroscopically can be very difficult, especially considering clay minerals and other very fine grained mineral coatings. Regular drill core mapping (Boremap) has been carried out on the KFM01B, KFM04A, KFM05A and KFM06A drill cores, whereby fracture minerals have been mapped and identified although a number of non-identified fracture fillings have been noted. Several of these fillings have been sampled for XRD (X-Ray Diffractometry) identification and the results are accounted for in Appendix VII. In addition, the mineralogical characteristics of differently orientated fracture orientation sets and zones have been analysed. Furthermore, calcites were sampled since they provide palaeohydrogeological information. A major intention with the fracture mineralogy study has been to establish a relative sequence of low-temperature events in the bedrock.

The locations for the boreholes studied are shown in a map together with the bedrock geology of the Forsmark area (Figure 1-1).

The orientations of the fractures examined in this report were extracted from the BIPS-files created during the Boremap mapping. For more extensive statistical analyses of fracture orientations, data of fractures identified during the Boremap mapping of KFM01A, KFM02A, KFM03A and KFM03B were extracted together with the data from KFM01B, KFM04A, KFM05A and KFM06A from SICADA.

The flow logging has been used as a tool for selection of samples of hydraulically conductive fractures.

Table 1-1. Controlling documents for performance of the activity.

Activity Plan	**Number**	**Version**
Sprickmineralogiska undersökningar	AP PF 400-04-32	1.0
Method descriptions	**Number**	**Version**
Sprickmineralogi	SKB MD 144.000	1.0

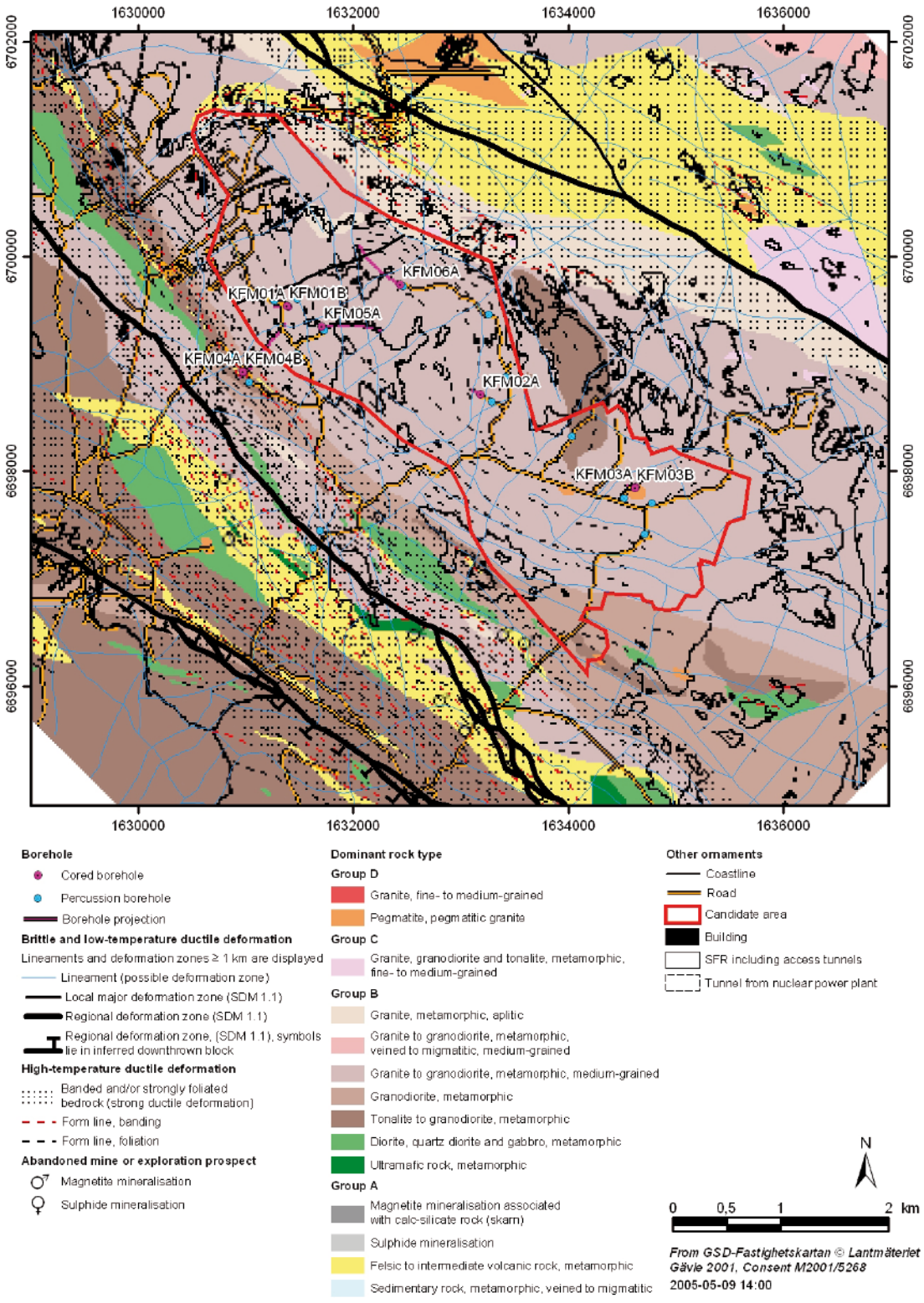

Figure 1-1. *Bedrock geology of the Forsmark area with projections of the boreholes KFM01A, KFM01B, KFM02A, KFM03A, KFM03B, KFM04A, KFM04B, KFM05A, KFM06A /SKB GIS database 2005/.*

2 Objective and scope

The basic idea behind the fracture mineral study is to:

- Identify fracture minerals.
- Distinguish different fracture mineral generations, their parageneses and determine their relative ages.
- Relate the different fracture generations to the structural geological model, i.e. to the deformation zones and fracture orientation sets.
- Provide mineralogical and geochemical information for the hydrogeochemical modelling.
- Contribute palaeohydrogeological evidences, mainly based on calcite geochemistry and stable isotope composition to the hydrogeochemical modelling.
- Support background information for the selection of samples within the Transport Programme (measurements of porosity, Kd, diffusivity etc).

3 Equipment

3.1 Description of equipment/interpretation tools

- Rock saw
- Steel knife
- Tweezers
- Digital camera (Olympus C3020 Zoom)
- Petrographic Microscope (Leica DMRXP)
- Stereo microscope (Leica MZ12)
- Digital microscope camera (Leica DFC 280)
- Scanner (Epson 4180 Photo) and polarizing filters
- Computer software (e.g. Corel Draw 9, Microsoft Word 2003, Microsoft Excel 2003, BIPS Image Viewer 2.51, StereoWin 1.2)
- Analytical balance (Sartorius 2004 MP)
- Scanning electron microscope (Zeiss DSM 940) with EDS (Oxford Instruments Link)
- ICP-MS (Hewlett-Packard HP 4500)
- Cetac LSX-200 Laser Ablation System
- Mass spectrometer (VG Prism Series II)

The equipment listed above is located at the Earth Sciences Centre, Göteborg University, Sweden. Other instruments used are listed below together with respective laboratories:

- Micromass Optima Isotope Mass Spectrometer – Institute for Energy Technology, Norway.
- Isotope Ratio Mass Spectrometer (Finnigan MAT DeltaXP) – Institute for Energy Technology, Norway.
- Thermal Ionization Mass Spectrometer – TIMS (Finnigan MAT 261) – Institute for Energy Technology, Norway.

4 Execution

4.1 General

Fracture filling samples suitable for microscopy were selected from the drill cores KFM01B, KFM04A, KFM05A and KFM06A. In a few cases, samples were selected from previous drill cores in order to clarify relations or to get better statistics in the chemical analyses. Fractures assumed to have been filled with minerals of different generations were preferred. Totally 67 samples were chosen from representative fractures. From these samples, 46 thin sections and 12 surface sections were made. The selection of the samples was more based on the information expected to be yielded from each sample than to get a statistic overview of the drill core. Fractures with well preserved open fracture surfaces were sampled as well.

- The thin-sections have been used to identify mineral parageneses of different fracture filling generations. The division into different generations has been based on textural and mineralogical observations, e.g. cross-cutting relations and dissolution/replacement textures. Ductile, semi-ductile and brittle deformation has been noted as well. Chemical compositions have been used in order to separate different generations of e.g. chlorite and calcites.
- The stable C, O and Sr isotope composition in calcite has been used to distinguish generations and to estimate formation conditions for the different mineral generations.
- The data of fracture orientations extracted from SICADA has been used to obtain a statistical basis from which the fracture mineralogy can be correlated to different fracture orientation sets. The dialogue with the drill core logging geologists has been important during the interpretation of the SICADA data.
- The sampled fractures have also been examined with emphasis on the deformation zone model (DFM) and the fracture mineralogy of individual zones has been described.

4.2 Selection of samples

Samples have been selected on different grounds:

- For mineralogical identification; the sampling has usually been initiated by the geologists carrying out the drill core logging. XRD analyses are performed on many of these samples, but they are also used for thin section preparation and subsequent microscopy.
- Samples selected for mineralogical studies (thin section preparation); these samples often show complex sealing and coatings and they are usually chosen to represent several generations of fracture mineralization. These samples include the asphaltite that is collected for chemical and stable isotope analyses.
- Samples of open fracture surfaces (preferably with euhedral crystals of calcite and pyrite precipitated on the surface). These samples are selected for the calcite study including stable isotopes, trace element composition and morphological determinations.
- Hydraulically conductive fractures are sampled based e.g. on the flow logging. Priority is given to fractures within the sections sampled for groundwater chemistry.
- A problem encountered in the fracture filling studies is the small sample volumes. The representativity of the samples can therefore not be quantified which needs to be considered in the subsequent interpretations.

4.3 Analytical work

Thin-sections with a thickness of 30 µm were prepared and analysed with optical microscope and scanning electron microscope (SEM) equipped with an energy dispersive spectrometer (EDS). In order to study minerals grown in the open space in some fractures, fracture surfaces were also prepared and examined by SEM-EDS. Additional fracture surfaces were only briefly examined with stereomicroscope. The SEM-EDS analyses were conducted at Earth Sciences Centre, Göteborg University, and are described in /Sandström et al. 2004/.

The XRD analyses were performed by Dr. Sven Snäll at SGU in Uppsala according to /Petersson et al. 2004b/.

Fracture calcites were hand picked by tweezers or scraped by a steel knife and analysed for stable carbon, oxygen and strontium isotope composition and trace element composition on leachate. Trace element analyses have also been made in situ. The stable carbon and oxygen isotope analyses were carried out at Earth Sciences Centre, Göteborg University. The method is described in /Sandström et al. 2004/. The Sr isotope analyses were performed at the Institute for Energy Technology in Norway (IFE), and are described in /Sandström et al. 2004/. The ICP-MS analyses on calcites leachates were made by Earth Sciences Centre, Göteborg University, according to the procedure described in /Sandström et al. 2004/. The in situ analyses were carried out by Laser ablation ICP-MS on 200 µm thick polished thin sections. The laser used was a Cetac LSX-200 Laser Ablation System and the ICP-MS was the above described. The laser operated with 50% effect and 1 Hz frequency. The spot size was 100 µm and a NIST 612 glass was used as a calibration standard with ^{44}Ca as an internal standard.

Carbon isotopic analyses on asphaltite were carried out by IFE, Norway. The analytical procedure for the $\delta^{13}C$ analyses was as follows: The sample was grinded to a fine powder in an agate mortar and approximately 1.5 mg was transferred to a 9x15 mm tin capsule. The combustion of the sample in the presence of O_2 and Cr_2O_3 at 1700°C was done in a Carlo Erba NCS 2500 element analyser. Reduction of NO_x to N_2 was done in a Cu oven at 650°C. H_2O was removed in a chemical trap of $KMnO_4$ before separation of N_2 and CO_2 in a 2 m Poraplot Q GC column. N_2 and CO_2 were directly injected on-line to a Micromass Optima, Isotope Ratio Mass Spectrometer for determination of $\delta^{13}C$. The precision of the results are ± 0.2‰. The analyses are checked with analyses of USGS-24 standard.

Chemical analyses of powdered fracture filling material were made by Analytica AB in Luleå. The analytical technique is described in /Petersson et al. 2004b/

The Mössbauer analyses were carried out by Prof. Hans Annersten at Uppsala University according to the following method: 20–40 mg sample were pressed into Cu-holders between low absorbing Mylar films and mounted in the magic angle 54.7 degrees to avoid textural effects from the flaky phyllosilicates. This results in symmetric absorption doublets and will make the fitting of a strong overlapping absorption line more easy. Measuring time for each sample was 1–3 days depending on the iron content. Each spectrum, 512 channels each were analysed in computer and fitted using a least square fitting program that provides the Mössbauer parameters centroid shift, quadrupole splitting, magnetic hyperfine field and intensity. Velocity scale of the spectrometer is calibrated against metallic iron. Centroid shifts for ferrous iron are around 1.12 mm/s and for ferric iron between 0.35–0.45 mm/s. Quadrupole splitting are generally much higher for ferrous iron, 2.60 mm/s, while splitting from ferric iron is between 0.60–1.0 mm/s. However ferric iron quadrupole splitting in epidote group minerals are the highest measured for ferric iron in silicates, 2.0 mm/s.

This is an important diagnostic feature for identifying epidote in rock samples by use of Mössbauer spectroscopy. Magnetite and hematite are identified from their large magnetic hyperfine field 48 and 51 T respectively. Oxidation degree of the sample is calculated from the intensity ratio between the ferric iron and ferrous iron absorption pattern assuming similar recoil free fractions.

4.4 Data handling

The types of data produced at the fracture mineralogy investigation and eventual treatment/ storage are listed below:

- Information from thin section microscopy; Identified minerals and a qualitative judgement on occurrence of each mineral are stored in SICADA. The order of mineralization (different generations) in individual samples is relative. Therefore a reference to this report is given in SICADA instead of actual data.
- Descriptions, corresponding to Appendix 1, of each thin section including photos and if present SEM pictures are stored in the SICADA file archive.
- Stable isotopes (O, C and Sr) are stored as reported from the laboratory, in a table for analyses of stable isotopes, without further processing.
- Chemical analyses (ICP-MS and LA-ICP-MS) of calcite leachates, calcite samples and fracture fillings in general are stored in SICADA data tables as reported from the laboratory without further processing.
- The results from Mössbauer analyses and calculated oxidation factors are stored in the SICADA file archive. The expressions used for the calculations are given in Appendix VIII.
- Mineral identifications and quantitative analyses by X-ray diffraction are stored in data tables in SICADA. The analyses are stored as reported from the laboratory without further processing.

All data in SICADA are traceable by the Activity Plan Number.

4.5 Nonconformities

The activity has been performed according to the activity plan without any significant nonconformities.

5 Results

The results from the present study are presented in appendices to this report. They are:

Appendix I: Results from microscopy including order of mineralizations.

Appendix II: SEM-EDS analyses of different fracture minerals.

Appendix III: Stable isotopes analyses of calcites including O, C and Sr isotopes.

Appendix IV: ICP-MS analyses on calcite leachates.

Appendix V: LA-ICP-MS analyses on calcite samples.

Appendix VI: Stable C isotopes in asphaltite samples.

Appendix VII: XRD analyses.

Appendix VIII: Mössbauer analyses.

Appendix IX: Chemical analyses of fracture fillings.

Due to the problem with small amount of fracture filling material and existence of different generations of the same mineral in one sample, some of the analyses may represent mixtures of different generations or contaminations from other minerals.

Some revision of the fracture generation sequence has been done since the previous report /Sandström et al. 2004/. Some of the previous generations have been combined while others have been split into different generations.

5.1 Minerals identified

A list of the fracture minerals identified within the Forsmark area is presented below (the XRD and SEM-EDS information referred to is published in /Petersson et al. 2004b, Sandström et al. 2004/ and in Appendix II and VII in this report). The abundance of different fracture minerals in Forsmark varies highly, the relative abundance can be summarized as follows: most common are calcite, chlorite/corrensite, laumontite and quartz which are followed by prehnite, adularia, epidote, hematite, pyrite and clay minerals (in no particular order). The rest of the minerals have only been found as minor occurrences but can be more common in particular zones, like asphaltite.

Albite (Na-Plagioclase) ($NaAlSi_3O_8$) is often found in fracture fillings together with hydrothermal K-feldspar (adularia). The fillings can be brick-red due to hematite staining.

Analcime ($NaAlSi_2O_6 \times H_2O$) has colourless, usually trapetzohedral crystals (like garnet). Analcime is stable at temperatures up to 200°C in the presence of quartz, but can in other assemblages exist at temperatures up to 600°C /Liou 1971/. In Forsmark, relatively big crystals have been found in some fractures (in the order of 5 to 10 mm).

Apophyllite ($(K,Na)Ca_4Si_8O_{20}F \times 8H_2O$) is a hydrothermal sheet silicate with white to silvery surface. It is detected in some fractures at Forsmark. Based on a few SEM-EDS analyses it seems to be relatively pure K-Ca-apophyllite.

Asphaltite ("bergbeck" in Swedish). The term is here used in a broad sense, meaning black, highly viscose to solid hydrocarbons with low U and Th content.

Baryte ($BaSO_4$) occurs in Forsmark as small grains and as small inclusions in galena.

Calcite ($CaCO_3$) occurs abundantly in Forsmark in different assemblages and with different crystal shape. The calcite generally shows low contents of Mg, Mn and Fe.

Chalcopyrite ($CuFeS_2$) occurs in Forsmark as small grains together with pyrite, galena and sphalerite.

Chlorite ($(Mg,Fe,Al)_3(Si,Al)_4O_{10}(OH)_2$) occurs abundantly in Forsmark as a usually dark-green mineral found in several associations. XRD identifies the chlorite as clinochlore but large variations in FeO/MgO ratios are indicated from SEM-EDS analyses (from 6 down to < 1). The occurrence of K, Na and Ca in many of the chlorite samples indicates possible ingrowths of clay minerals, mostly corrensite. The Mn and Ti contents in the chlorites are usually low but a few samples have TiO_2 values between 1 and 1.5%.

Epidote ($Ca_2Al_2Fe(SiO_4)(Si_2O_7)(O,OH)_2$) occurs as a green filling in sealed fractures. According to the SEM-EDS analyses, the Fe-oxide content varies between 8 and 14% given as FeO. In reality, however, most of the Fe in epidote is Fe^{3+}.

Fluorite (CaF_2). Violet fluorite is found in a few fractures.

Galena (PbS) is mainly found on fracture surfaces and has cubic or octahedral crystals. The mineral occurs together with pyrite in Forsmark and can have small inclusions of baryte.

K-feldspar ($KAlSi_3O_8$) is usually adularia (the low- temperature form) but is also found as wall rock fragments in breccias showing typical microcline twinnings, Like in albite the colour can be brick-red due to hematite staining. Occurs also greenish in a fine-grained mixture with quartz.

Hematite (Fe_2O_3) is common in the Forsmark fractures but the amount is relatively low (does not often turn up in the diffractograms). However, micro-grains of hematite cause intense red-staining of many fracture coatings.

Laumontite ($CaAl_2Si_4O_{12} \times 4H_2O$) is a common zeolite mineral in the Forsmark area. It shows a prismatic shape and is brittle. The mineral is white, but is mostly coloured red by micro-grains of hematite, although white varieties are observed as well. Zeolites have open structures suitable for ion exchange.

Pitchblende (UO_2) is an often massive, granular form of uraninite, in Forsmark so far only found in one fracture together with hematite and chlorite.

Prehnite ($Ca_2Al_2Si_3O_{10}(OH)_2$) occurs as a light greyish green to grey or white, hydrothermal mineral. The Fe content varies between 1 and 5.5 weight % (given as FeO). Like in epidote most of the Fe is Fe^{3+}. The upper limit of stability in natural environment is c 380°C /Liou et al. 1983/.

Pyrite (FeS_2) is found in many fractures as small euhedral, cubic crystals grown on open fracture surfaces.

Quartz (SiO_2) has been identified in many of the analysed samples, often as very small and occasionally hematite stained, euhedral crystals covering the fracture walls. They often have a greyish sugary appearance but can also be transparent and then appear to have the colour of the wall rock.

Sphalerite (ZnS) has been found in a few fractures and is often associated with galena.

Clay minerals

Corrensite ($(Mg,Fe)_9(Si,Al)_8O_{20}(OH)_{10} \times H_2O$) is a chlorite-like mixed-layer clay with layers of chlorite and smectite/vermiculite, usually with a ratio of 1:1. Based on XRD analyses, some of the corrensite samples show irregular ordering in the layering, indicating either that they have not reached perfect corrensite crystallinity or that they are altered. Corrensite is the clay mineral most frequently found, and as mentioned above often found together with chlorite. This is a swelling type of clay like mixed-layer illite/smectite and saponite (see below).

Illite ($(K, H_2O)Al_2[(Al,Si)Si_3O_{10}](OH)_2$) occurs as micro – to cryptocrystalline, micaceous-flakes, and is usually light grey in colour.

Mixed-Layer clays. Mixed-layer clay with layers of illite and smectite has been identified in some fractures. XRD analyses show a 3:2 ratio of illite/smectite.

Saponite ($Mg_3(Si_4O_{10})(OH)_2 \times nH_2O$). This is a variety of swelling smectite.

5.2 Sequence of fracture mineralizations

Table 5-1 shows the compilation of relative sequences of mineralizations in the analyzed samples. From this compilation, together with data from /Sandström et al. 2004/ it is obvious that minerals like quartz, adularia, chlorite and calcite occur as several generations. It can also been seen that e.g. epidote belongs to the oldest generation in the thin sections studied, whereas lower temperature minerals like e.g. zeolites and clay minerals are found in later generations. From the microscopy results, a general sequence of fracture mineral generations in the Forsmark area has been established. Selected deformation zones and the different fracture orientation sets are individually dealt with. The deformation zones are defined in /SKB 2005b/ and the fracture orientation sets in /La Pointe et al. 2005/. The deformation zones in KFM06A were not yet defined when this report was written.

Table 5-1. Relative chronological relations between fracture minerals in individual samples from KFM01B, KFM04A, KFM05A and KFM06A, result from microscopy.

Sample	Ep	Qz	Pr	Ana	Lau	Hm	Chl	Kfsp	Alb	Ca	Py	Clay	X	Fracture set	Deformation Zone
KFM01B															
28,65		1						1,2						HZ	ZFMNE00A2
417,53	1						2			2				n.a.	ZFMNS0404
KFM04A															
171,62		2*						1		1,2				NW	ZFMNE00A2
179,70		2*								1,4		3		NE	
197,95	1	1,3*				1		1	1	4				NW	
212,77	1	1,2,3*				1	1Mg	1,2		2,4			1’	NW	ZFMNE00A2
226,20	1	1,3*			2		1,2Fe	1	1	4				NW	
226,98	1	1			2	2	1							n.a.	
244,46					1	2		2		2				NE	
247,00		2			1,2		2			3				NE	
263,25		1*		2								3’’		NE	
294,50		1*								2				n.a.	
296,50		2*			1					3	4	4’’		NE	
306,40		3*			1					2,4	4			NE	
347,32					1,2	1				1,3				NE	
414,10	1	1,2*		3	1	1		1		1,4				NE	ZFMNE1188
415,30		2*		3	1					5	4			NE	ZFMNE1188
KFM05A															
105,41		1*						1		2			2^{A}	n.a.	ZFMNE00A2
109,75		1*								1	1	2’’	1^{A}	HZ	ZFMNE00A2
111,56		1*						1				1’’’	2^{A}	HZ	ZFMNE00A2
146,40		1*								1	1	1’’		NE	
232,95		1			2	1		1		3		4’’		NE	
395,75			1			3		3		2,4		5’’		NE	
428,00	1	1,2*						1		3		4’’		NE	ZFMNE0401
689,33			1,2			1		1						NE+NW	
692,00	1		2			2	1	1,2		3			$1’,1^{T},1^{x}$	NW+NE	
702,42		2		1	1			2				4’’,5’’	3^{C}	NE	
737,78	1	2	2					2						HZ	
938,00		1,3*	1		1,2	1		1	1			1’’,4’’		NE	ZFMNE062A

Sample	Ep	Qz	Pr	Lau	Hm	Chl	Kfsp	Alb	Ca	Py	Clay	X	Fracture set	Deformation Zone
KFM06A														
102,62									1		2	3^{A}	NS	n.d.
106,18		1*							2	2		3^{A}	NS	n.d.
106,94		1*					1			1		1^{G},1^{S},1^{C},1^{B},2^{A}	NS	n.d.
110,49		1*,4*							2	2		2^{G},3^{A}	NS	n.d.
110,53		1*,3*							2			4^{A}	NS	n.d.
110,72		1*							2	2		2^{G},3^{A}	NS	n.d.
111,40		2*							1	1		1^{G}	NS	n.d.
142,27		1*							1,2	2			NE	n.d.
142,93		1*							2	3		3^{S},4^{A}	NE	n.d.
145,62		2				2	2		1	2	2	2'''	NS	n.d.
170,06									1	1	1		NS	n.d.
187,68		1	2		1		1	1	2,3,4				NE	n.d.
199,66		1*							2	2			NS	n.d.
201,94		1				1	1				1''	1'''	NS	n.d.
220,22		2*			1	3	1	1			3		NE	n.d.
223,33	1	3			3	2	3				2''		NE	n.d.
260,81	1												HZ	n.d.
268,48		1							1				HZ	n.d.
268,77	1												HZ	n.d.
317,43				1									NE	n.d.
324,54		2			1		1	1	3,4				NE	n.d.
331,88		1							1,2	1			NE	n.d.
332,62		2*			1		1	1	3	3			NE	n.d.
336,68		2*			1	3	1,2		3	3	3''		NE	n.d.
348,06		1							2				NE	n.d.
352,27		1							2	2			NS	n.d.
356,53		1*							1	1			NS	n.d.
404,99									2	2	1''		EW	n.d.
503,44		1					1	1	1			1^{bi}	NE	n.d.
568,94					1	2	1		3		2''		NE	n.d.
620,14					1	2	1	1			2''		NE	n.d.
622,31		1*				1	1	1			1''		NS	n.d.
653,26		2			1		1	1	3	3			NE	n.d.
743,39		1*							2	2			NE	n.d.
768,87			1		2						2		NE	n.d.
770,32		1				1	1		1		1''		NE	n.d.
794,78									2	1			EW	n.d.
963,99					1	1	1				1		NE	n.d.

Ep = epidote, Qz = quartz, Pr = prehnite, Ana = analcime, Lau = laumontite, Hm = hematite, Chl = chlorite, Kfsp = k-feldspar, Alb = albite, Ca = calcite, Py = pyrite, ' = apatite, '' = corrensite, ''' = illite, * = euhedral quartz, ^{A} = asphaltite, ^{T} = titanite, ^{x} = allanite, ^{C} = chalcopyrite, ^{S} = sphalerite, ^{B} = baryte, ^{G} = galena, ^{bi} = biotite, n.a. = not visible in BIPS, n.d. = not defined.

From the results presented in Table 5-1, 6 different generations of fracture mineralizations have been distinguished in the Forsmark area (Table 5-2). No correlation between depth and fracture minerals has been found except for asphaltite and clay minerals which are more abundant in the upper parts of the drill cores. Since the clay minerals mostly are found in hydraulically conductive fractures and zones, this is probably due to the higher abundance of hydraulically conductive fractures/zones closer to the surface and not the depth itself. Where hydraulically conductive zones occur at large depths, clay minerals are also found, e.g. has illite been identified by XRD in KFM05A 985.80–985.92 m (Appendix VII).

Table 5-2. Generations of fracture mineralizations presented with decreasing age. Only the most common minerals are presented in this table.

Generation	Characteristic minerals
1	Epidote, quartz, chlorite.
2	Prehnite, laumontite, calcite, adularia, hematite, chlorite.
3	Euhedral quartz.
4	Calcite, pyrite, corrensite.
5	Asphaltite.
6	Clay minerals, calcite.

5.2.1 Generation 1

The oldest generation in the area mainly consists of cataclasite of epidote and quartz (Figure 5-1), locally partly mylonitized. K-feldspar, Fe-chlorite and in some fractures fluorite have also crystallized during this period. The altered rock fragments in the catacla-

Figure 5-1. *Epidote sealed cataclasite. The diameter of the drill core is c 5 cm, KFM06A 268.77–268.82 m.*

sites mostly contain quartz, K-feldspar and albite. A later cataclastic reactivation, usually accompanied by hematitization causing red-staining, has been observed in some samples. The FeO content in the epidote varies between 8.4 and 15.6% and shows large variations between different samples as well as between adjacent crystals. It seems as Generation 1 represents a period during which P-T conditions gradually moved from semi-ductile to brittle under greenschist facies. Experimental studies have shown that the lower temperature limit for epidote is c 350°C when it is replaced by prehnite /Liou et al. 1983/. $^{40}Ar/^{39}Ar$ data from biotite show that cooling below 300°C occurred between 1,704 and 1,635 Ma /Page et al. 2004/ and is therefore suggested as the minimum age of Generation 1. Together with the epidote, a Fe-rich chlorite (FeO ≈ 30%) often occurs. Under crossed polars, this chlorite has a deep blue colour (Figure 5-2). The fractures of Generation 1 are almost exclusively sealed and are surrounded by highly altered wall rock. The wall rock alteration consists of saussuritized plagioclase, chloritized biotite and to a lesser degree sericitized K-feldspar. The chlorite replacing the biotite in the altered wall rock has the same chemical composition as the chlorite in the fractures. The red-colouring of the altered wall rock comes from hematite staining of the plagioclase (Section 5.5).

Generation 1 occurs most abundantly in the upper 170 m borehole length of KFM01B, between 400 and 600 meter in KFM02A /Berglund et al. 2004, Carlsten et al. 2004, Sandström et al. 2004/ and in the part of KFM04A where the borehole cuts the SE-NW striking zone /Petersson et al. 2004c/ constituting the western border of the candidate area. Generation 1 is less represented in KFM05A and KFM06A. Boremap data extracted from SICADA (boreholes KFM01A, KFM01B, KFM02A, KFM03A, KFM04A, KFM05A and KFM06A) show that the epidote-sealed fractures of Generation 1 have two main orientations, one distinct population with a steep dip striking NW-SE and one more diffuse population striking NE-SW with a moderate dip towards NW (Figure 5-3). The epidote filled fractures are often parallel or subparallel to the foliation.

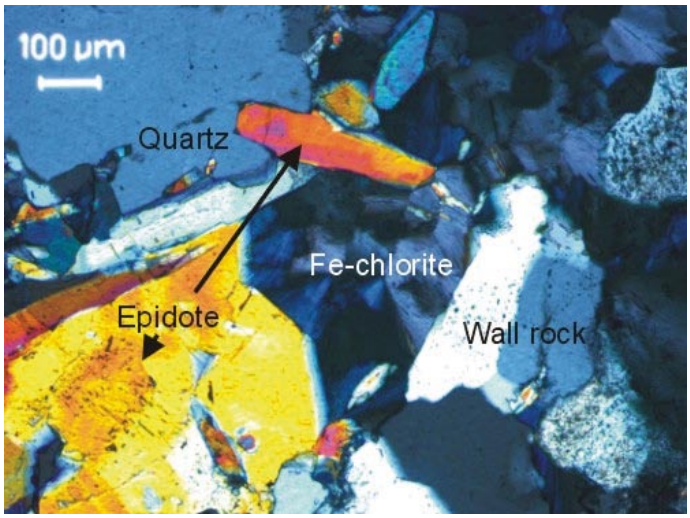

Figure 5-2. *Epidote together with Fe-rich chlorite and partly recrystallized quartz. Photomicrograph with crossed polars. KFM05A 692.00–692.15 m.*

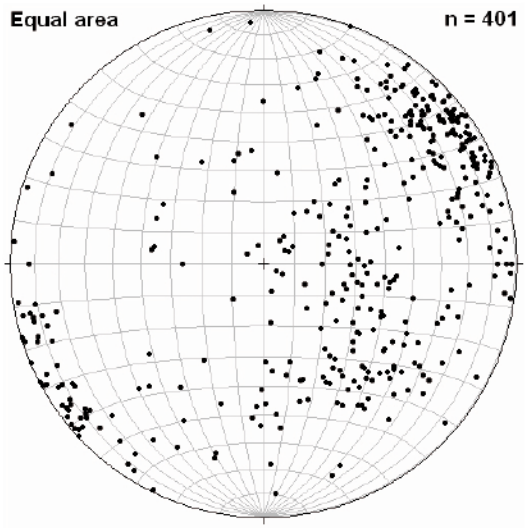

Figure 5-3. *Stereographic plot showing poles to planes with epidote filled fractures from KFM01A, KFM01B, KFM02A, KFM03A, KFM04A, KFM05A and KFM06A. Two main fracture orientations can be seen, one steep with a SE-NW strike and one striking towards NE-SW with a moderate dip towards NW.*

5.2.2 Generation 2

This is a sequence of hydrothermal mineralizations which previously has been divided into two different generations /Sandström et al. 2004/. It has now been reviewed as a single event although extended in time and with episodes of different hydrothermal intensity. The sequence involves a first phase of hematite stained adularia and albite followed by prehnite and succeeded by a third phase consisting of laumontite, calcite, adularia, quartz and micro-grains of hematite. Chlorite and corrensite have crystallized during the entire hydrothermal event although most intensively during a late phase of reactivation of the fractures.

The thin, brick-red adularia sealed fractures which in addition also contain albite, quartz and calcite in various proportions, are characteristic for the Forsmark area. The red staining is caused by micro-grains of hematite. The thin sealed brick-red adularia fillings can be seen to pre-date the prehnite (Figure 5-4 and 5-5). However, in some samples prehnite has crystallized together with the adularia. Prehnite occurs also in the altered wall rock adjacent to the adularia sealed fractures. This indicates that the crystallization took place under approximately the same conditions.

Figure 5-4. *Brick-red adularia and hematite filled fracture cut by a prehnite filled fracture. The diameter of the drill core is c 5 cm. KFM05A 689.33–689.61 m.*

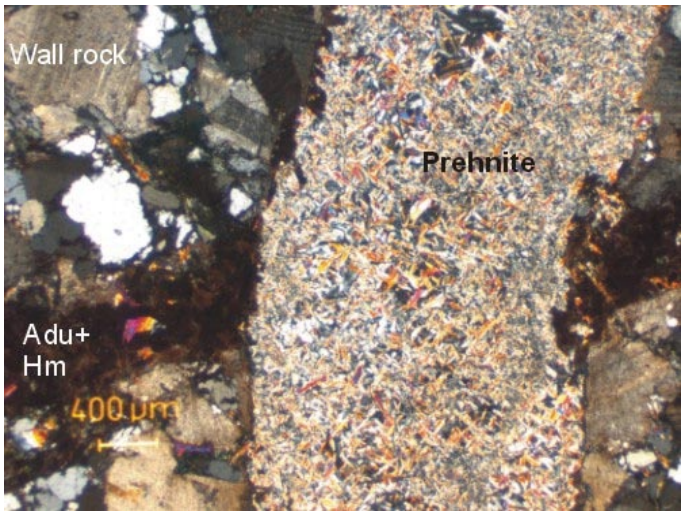

Figure 5-5. *Thin fracture filled with adularia (adu) and hematite (hm) cut by a prehnite filled fracture. Some prehnite is also present in the adularia filled fracture. Photomicrograph with crossed polars. KFM05A 689.33–689.61 m.*

The appearance of new fracture orientations contemporary with the crystallization of laumontite indicate formation of new fractures during this period, often cutting the foliation and older epidote sealed fractures. The Generation 2 fractures are steep and strike NE-SW or N-S (Figure 5-6). The formation of new fractures is further supported by the fact that laumontite often occurs as the first crystallized mineral in many fractures. This fracture formation was entirely brittle and laumontite has sealed zones of brecciated rock. These brecciated zones are in the order of centimetres to metres in width (Figure 5-7).

The calcites of Generation 2 are often heavily deformed and have thick (>> 1 µm) and curved twins (Figure 5-8). This indicates deformation temperatures above c 200°C /Ferrill 1991, Burkhard 1993/.

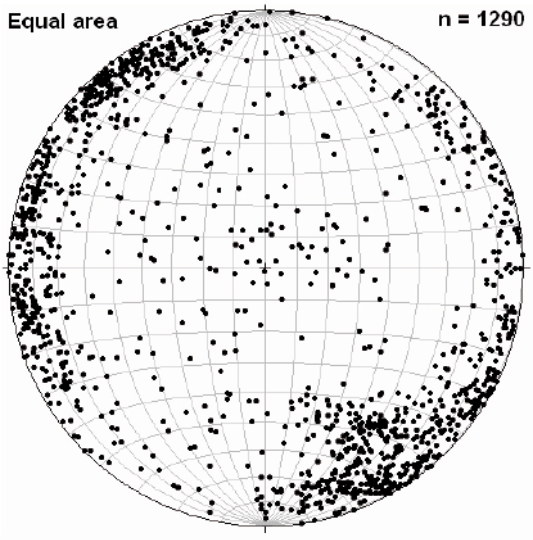

Figure 5-6. *Laumontite filled fractures. Stereographic plot showing poles to planes. Data from KFM01A, KFM01B, KFM02A, KFM03A, KFM03B, KFM04A, KFM05A and KFM06A.*

Figure 5-7. *Laumontite sealed breccia. The diameter of the drill core is c 5 cm. KFM04A 24.46–244.58 m.*

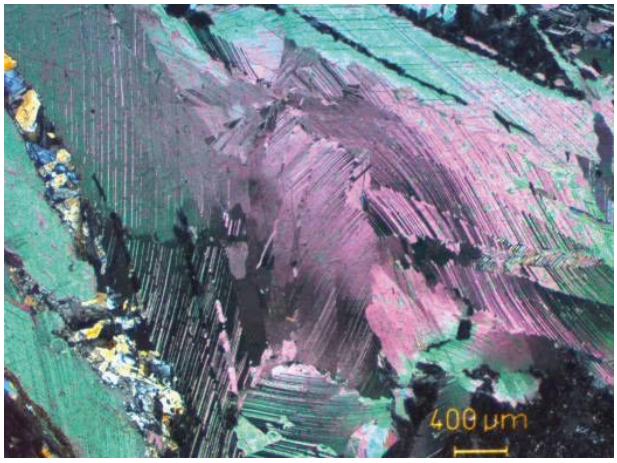

Figure 5-8. *Prismatic calcite crystals with highly deformed and curved twins, the yellow-blue mineral to the left in the figure is prehnite. Photomicrograph with crossed polars. KFM05A 395.75–395.85 m.*

Most of the calcites from Generation 2 have $\delta^{13}C$ values between –2 and –7 ‰ (Figure 5-9) which is typical for hydrothermal precipitation of calcite /Tullborg 1997, Hoefs 2004/ and implies that no or only minor addition of biogenic carbon has taken place. The $\delta^{18}O$ values vary between –7 and –18 ‰. The large variation can be explained by high temperatures during the crystallization of the calcite which caused exchange of oxygen isotopes between the fluid and the silicates along the flow paths and in the wall rock. This exchange is highly dependent on the fluid/rock ratio which has varied between different fractures. The $^{87}Sr/^{86}Sr$ ratios of the calcites from Generation 2 are between 0.707 and 0.711 and can clearly be distinguished from younger calcites (Figure 5-10). The total Sr content in these hydrothermal calcites varies between 103 and 334 ppm (Appendix IV and V) and is significantly higher than in younger calcites.

The REE chemistry of the analysed calcites separates into two groups of which the hydrothermal calcites in Generation 2 are less enriched in the LREEs compared to later calcites (Figure 5-11). A negative Ce anomaly is also evident in many of the hydrothermal calcites. This is probably due to oxidizing conditions during the circulation of the fluids from which the calcite has precipitated. During this circulation, the less soluble oxidized Ce^{4+} has separated from the other REEs.

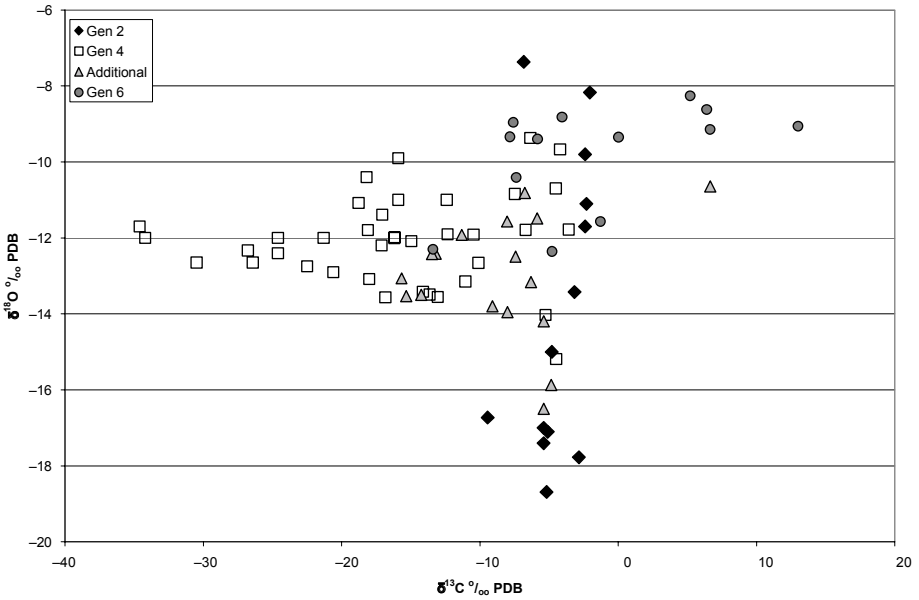

Figure 5-9. *$\delta^{13}C/\delta^{18}O$ values for calcites from KFM01B, KFM04A, KFM05A and KFM06A plotted together with data from KFM01A, KFM02A and KFM03A /Sandström et al. 2004/. For the samples marked additional, it has not been possible to confirm to which generation they belong.*

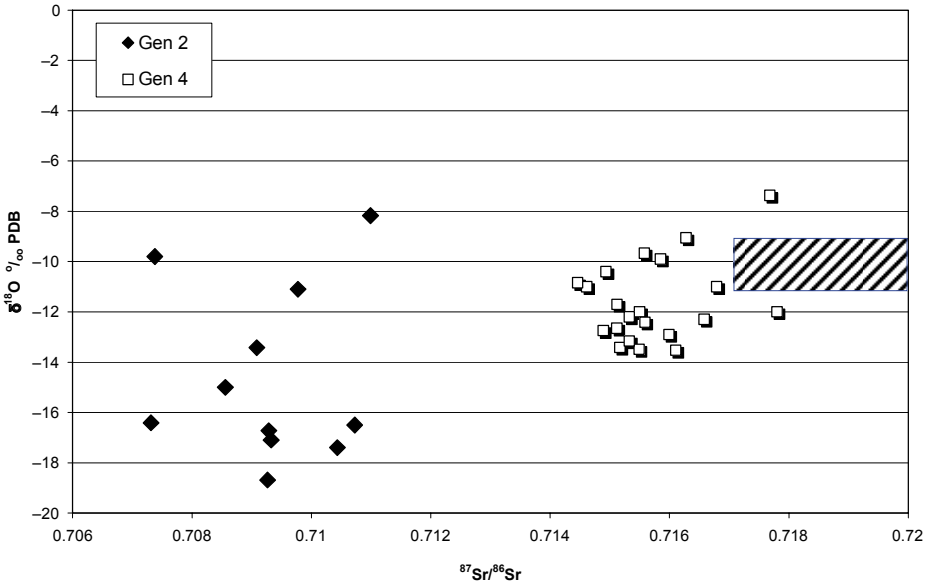

Figure 5-10. *$^{87}Sr/^{86}Sr$ versus $\delta^{18}O$ plot for calcites from KFM01A, KFM01B, KFM02A, KFM04A and KFM05A. The area with shaded lines represents calcite in equilibrium with present day meteoric water at present temperatures at the Forsmark site. Some of the samples plotted as Generation 4 with $\delta^{18}O$ values higher than –11‰ may represent calcites from Generation 6.*

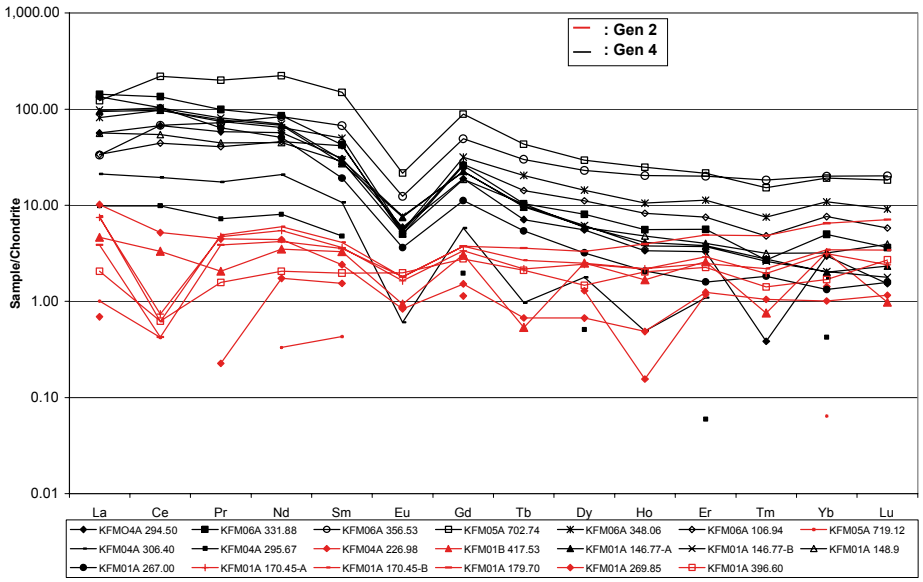

Figure 5-11. *Chondrite normalized REE composition of calcites of Generation 2 and 4. Chondrite data from /Evansen et al. 1978/.*

The adularia post-dating the calcite in some samples is extremely fine-grained and often mixed with quartz. Macroscopically, the adularia-quartz fillings have a greenish grey colour.

The P-T conditions for Generation 2 extend from prehnite-pumpellyite facies down to upper zeolite facies. From experimental results, the upper temperature limit of prehnite is c 380°C /Liou et al. 1983/ and the stability field of laumontite is between c 150–250°C (the upper limit decreases when Fe_2O_3 is introduced to the system) /Liou et al. 1985/. The reason for the few observations of coexisting prehnite and laumontite may be explained by dissolution/alteration of prehnite during zeolite facies. The abundance of laumontite indicates that the hydrothermal circulation during upper zeolite facies has been more intense than during prehnite-pumpellyite facies.

Chlorite and corrensite are found as a greenish black fracture coating together with the prehnite and laumontite of Generation 2. The chlorite and corrensite have in some fractures clearly grown together with the prehnite and laumontite, but most commonly represent a later reactivation (Figure 5-12). Chlorite and corrensite are amongst the most common fracture filling minerals in the Forsmark area and have most likely crystallized during several episodes.

Apophyllite has been identified in e.g. KFM05A 705.81–705.88 m where it occurs together with corrensite. From the few samples available, it has not been possible to clearly establish to which generation the apophyllite belongs. However, Generation 2 is a strong candidate.

After the hydrothermal activity responsible for the prehnite/laumontite mineralizations, there has been a period of dissolution and breakdown of earlier formed hydrothermal minerals. It is probable that this period is closely related in time to Generation 3 (see below). Many of the voids and cavities in the fractures were created during this period.

Figure 5-12. *Laumontite and calcite filled fracture which was reactivated and filled with younger chlorite/corrensite. The diameter of the drill core is c 5 cm. KFM05A 232.95–233.07 m.*

5.2.3 Generation 3

Subsequent to the dissolution phase, a period of quartz precipitation occurred (Generation 3). In addition to quartz, adularia, albite and analcime were also precipitated. Calcite may be co-precipitated with this assemblage but is usually later. This generation is abundant all over the candidate area and quartz coatings are found in open fractures in most directions but preferably in horizontal and subhorizontal ones. The quartz which is the overall dominant filling of this generation occurs as thin coatings of small euhedral quartz crystals (Figure 5-13 to 5-16). Coatings of euhedral albite have crystallized on some fracture surfaces but are far less abundant than the quartz coatings.

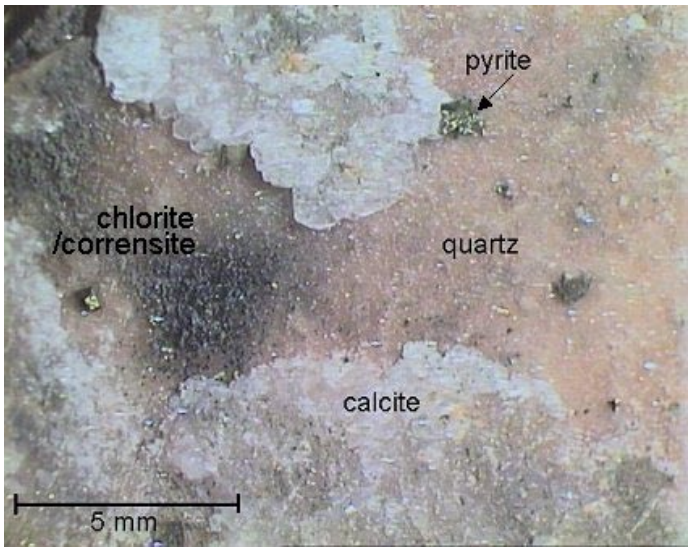

Figure 5-13. *Fracture surface with quartz coating and later calcite, pyrite and chlorite/corrensite from Generation 4. The pinkish colour of the quartz is due to laumontite underneath the transparent quartz. Photograph from stereo microscope. KFM04A 296.50–296.65 m.*

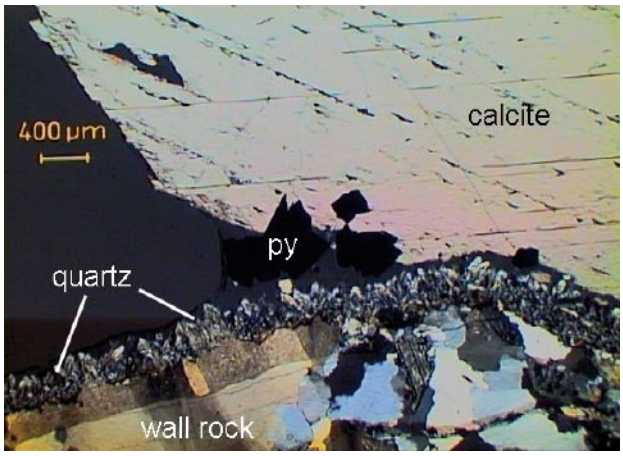

Figure 5-14. *Thin coating of small euhedral quartz crystals on fracture surface. Here overgrown by crystals of calcite with thin straight twins and pyrite (py) of Generation 4. Photomicrograph with crossed polars. KFM04A 306.40–306.55 m.*

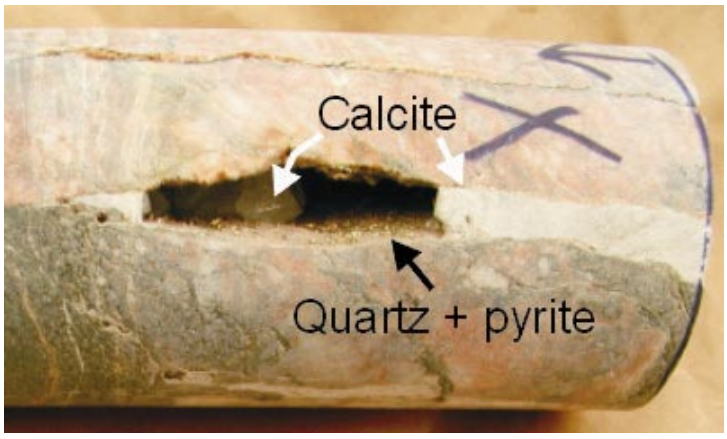

Figure 5-15. *Calcite of Generation 4 filling a fracture earlier coated with small euhedral quartz crystals. The diameter of the drill core is c 5 cm. KFM04A 306.40–306.55 m.*

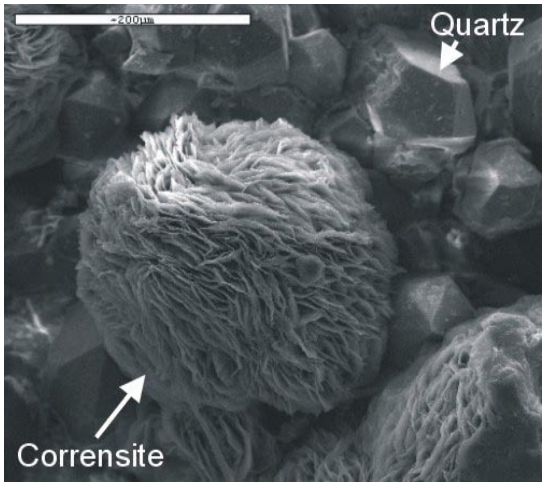

Figure 5-16. *Spherical aggregate of corrensite crystallized on euhedral quartz coating. Electron image, KFM05A 938.00–938.18 m.*

It appears as the event corresponding to Generation 3 mainly is a phase of reactivation of older fractures, although new fractures were probably also created. The preceding period of dissolution has made interpretations of cross-cutting relations difficult.

Fission track studies on apatites show that the temperature did not exceed 100°C during the Phanerozoic /Cederbom et al. 2000/ and (U-Th)/He ages in apatites show that cooling below 70–60°C occurred sometime between 630 and 250 Ma /Page et al. 2004/. The abundance of the quartz coating is a sign of intense hydrothermal circulation, probably at temperatures above 100°C. No pronounced wall rock alteration occurs adjacent to the fractures where the euhedral quartz is the first mineral to have crystallized.

5.2.4 Generation 4

A sequence of corrensite followed by calcite, pyrite and analcime has crystallized on the euhedral quartz crystals (Figure 5-13 to 5-17). This generation is closely related to Generation 3 and may be a later phase of the same event that precipitated the euhedral quartz of Generation 3. The corrensite occurs macroscopically as small black spots on open fracture surfaces. In optical and electron microscope, the corrensite can be seen as spherical aggregates of crystals with a diameter of c 0.2 mm. The calcite occurs both as a larger granular mass that fills some fractures and as smaller euhedral crystals on open fracture surfaces. This generation of calcite is the most frequent fracture calcite in the Forsmark area and also represents the largest calcite volumes. Some of the calcite fillings are in the order of ten centimeters wide.

The calcite twins of Generation 4 are thin and straight (Figure 5-14) and can easily be distinguished in thin section from the earlier thicker and more deformed twins of the Generation 2 calcites. In contrast to the isotopic composition of Generation 2, the $\delta^{13}C$ and $\delta^{18}O$ values of the Generation 4 calcites show no typical hydrothermal signature (Figure 5-9). The large variation in $\delta^{13}C$ values (in samples with similar $\delta^{18}O$ and Sr ratios) indicates various degree of interaction with biogenic carbon, at least during some phase of the Generation 4 crystallization. Extremely low $\delta^{13}C$ values (–20 to –35‰) found in some of the calcites are interpreted as the result of microbial activity in situ. The Sr isotope data of the Generation 4 calcites plot in a narrow field with $^{87}Sr/^{86}Sr$ values between 0.714 and 0.718 (Figure 5-10) which clearly separate them from Generation 2 calcites and indicate crystallization during a later, relatively well-defined event. The total Sr content of these calcites is between 21 and 54 ppm (Appendix IV and V), which is up to a factor 10 lower than the hydrothermal calcites of Generation 2. In addition, Generation 4 calcites are more enriched in the LREEs than the calcites of Generation 2 (Figure 5-11) and have also pronounced negative Eu anomalies. This may support that reducing conditions prevailed during their crystallization.

The $^{87}Sr/^{86}Sr$ ratios in the calcites of Generation 4 (Figure 5-10) indicate a significantly higher input of radiogenic Sr during this period compared with that during the period for Generation 2. This can be explained either by a relatively long separation in time or by significantly different chemistry of the hydrothermal fluids involved; a preferential leaching of K-Rb rich minerals yields solutions rich in radiogenic Sr.

LA-ICP-MS data from traverses across two calcite sealed fractures (KFM06A 142.27–142.39 m and KFM06A 324.54–324.65 m) indicate calcite precipitation during two different pulses in these fractures. Due to the similarity in e.g. LREE and Sr concentrations between the ICP-MS and LA-ICP-MS analyses (compare Figure 5-11 and 5-18), and on textural grounds, both these calcite phases in the traverses have been interpreted

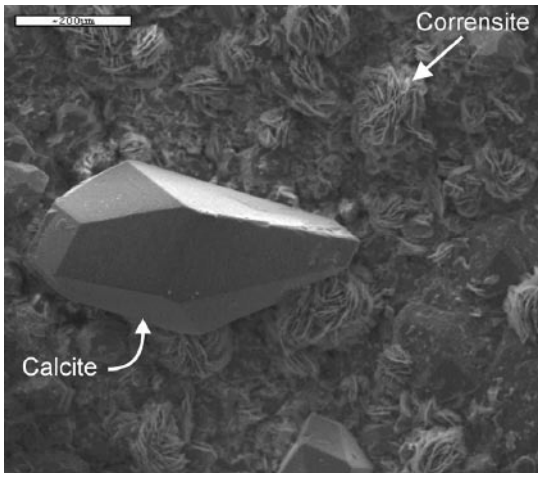

Figure 5-17. *Stubby scalenohedral crystal of calcite crystallized on spherical aggregates of corrensite. Electron image, KFM05A 146.40–146.57 m.*

as belonging to Generation 4. In comparison with the ICP-MS analyses on Generation 4 calcites leachate (Figure 5-11), the data from the traverses have more pronounced Eu anomalies, are more enriched in HREEs and have higher Y concentrations.

The older calcite phase in the traverse is mixed with quartz and cut by a younger more pure calcite even more enriched in the HREEs (Figure 5-18). This may be explained by the formation of more stable complexes between HREEs and HCO_3^- than between LREEs and HCO_3 /Möller and Moreteani 1983/. In this way, the HREEs remained in solution longer than the LREEs. Except for the enrichment in HREEs, the normalized REE curves are similar in the two different calcites. The Sc content also differs between the two calcite phases. The Sc ion is of similar size as the HREEs and therefore behaves in a similar way. Another explanation to different La/Yb ratios in these samples compared with the other Generation 4 calcite may be that some of the calcite of Generation 4 has been partly dissolved and reprecipitated during reactivation.

The pyrite occurs almost exclusively as euhedral cubic crystals. The crystals are well-preserved and show no sign of dissolution. Analyses of sulphur isotopes in the pyrite are presently carried out and will hopefully give information about the formation conditions of the pyrite.

The orientations of the Generation 3 and 4 mineral fillings are difficult to extract from SICADA due to the absence of the textural properties in SICADA that separates the quartz in Generation 1 from that of Generation 3 and the chemical characteristics that separate the different calcite generations. Pyrite, which exclusively has been found in Generation 4 and later generations, thus provides an indication of the orientation of theses fractures (Figure 5-19). It appears as these fracture fillings occur in both the NE and NW fracture orientation sets, but the most common orientation of pyrite filled fractures is horizontal or subhorizontal. This indicates that the preferred orientations for the formation of new fractures during Generation 3 and 4 mostly were horizontal or subhorizontal.

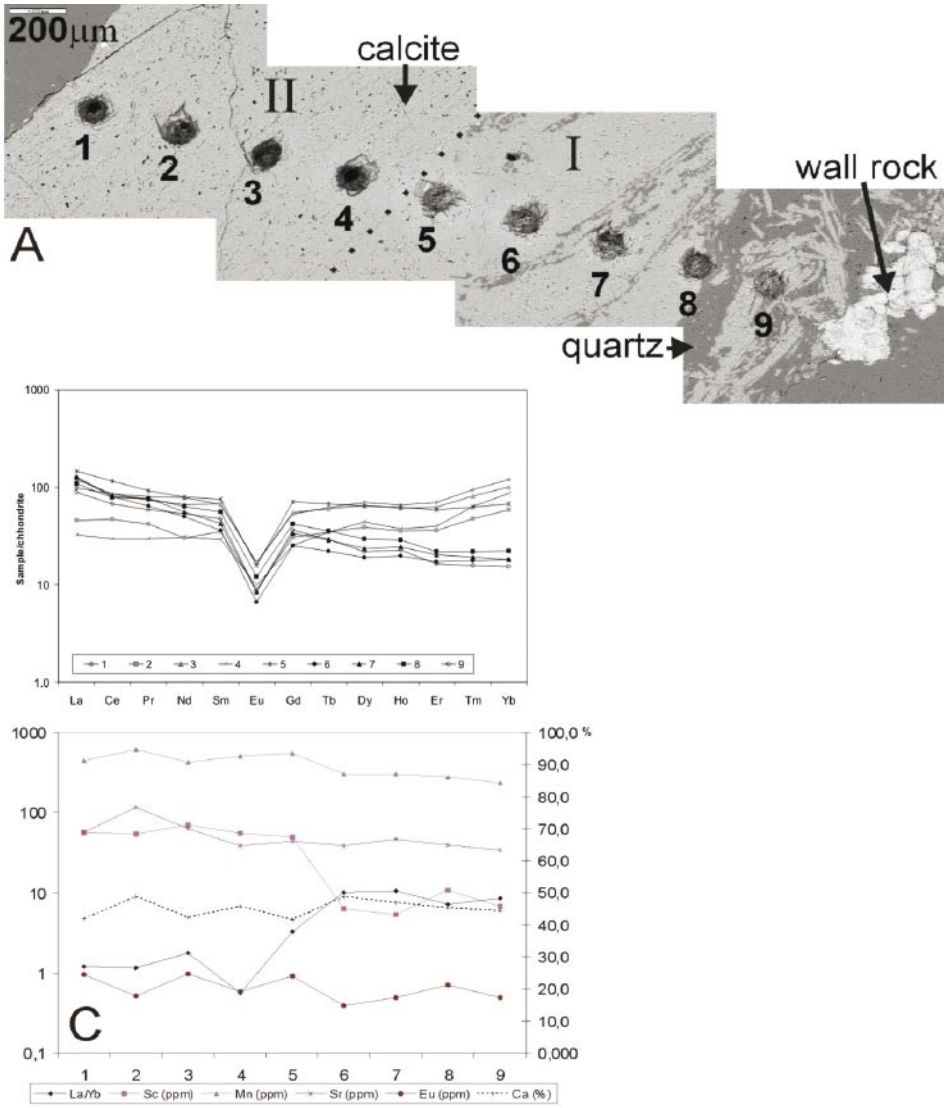

Figure 5-18. *Sample from KFM06A 142.27–142.39 m. A) Traverse across a calcite sealed fracture. The calcite consists of one older phase mixed with quartz (I) cut by a younger calcite (II). The craters represent spots analysed with LA-ICP-MS. Backscattered electron image. B) Chondrite normalized REE-curves for the sampled spots. Note the enrichment of HREEs in samples 4–9. Chondrite values from /Evansen et al. 1978/. Pm, Tb, Ho and Tm are extrapolated values and have not been analysed. C) Selected trace elements plotted along the calcite traverse, the enrichment in HREEs in the left part of the traverse can be seen in the low La/Yb ratio. The Sc concentration also differs highly between the two calcite phases while the Sr, Eu and Ca concentrations are relatively constant. The Mn content drops slightly in the left part of the traverse.*

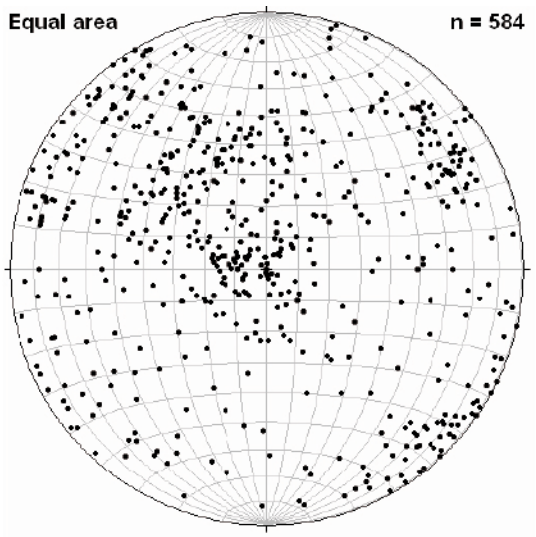

Figure 5-19. *Stereographic plot showing poles to planes of fractures with pyrite from KFM01A, KFM01B, KFM02A, KFM03A, KFM04A, KFM05A and KFM06A.*

5.2.5 Generation 5

Asphaltite has been found in samples from KFM01B, KFM05A and KFM06A (Figure 5-20). These hydrocarbons occur exclusively in the upper 150 m of the drill cores and can be seen to post-date the calcite and pyrite of Generation 4. The asphaltite occurs on open fracture surfaces and in druses in older partly dissolved quartz and calcite. In many samples the hydrocarbons have penetrated older fracture fillings, mostly the quartz and calcite of Generation 3 and 4.

ICP-MS analyses have been carried out on two samples containing asphaltite (KFM01B 25.30 and KFM01B 49.39–49.45; Appendix IX). These analyses show no elevated concentrations of U or Th which excludes that the samples contain thucholite. The high Cu and Zn content in KFM01B 25.30 m may be due to the presence of chalcopyrite and sphalerite (see below).

An organic origin is supported by $\delta^{13}C$ values between –29.5 and –30.1‰ PDB (Appendix VI). These values are consistent with previously analysed asphaltite from the Fennoscandian shield /Welin 1966, Åberg et al. 1985, Eakin 1989/. Biomarker analyses to

Figure 5-20. *Asphaltite in voids in older partly dissolved calcite. The diameter of the drill core is c 5 cm. KFM06A 106.94–107.14 m.*

further investigate the origin are currently carried out and preliminary results confirm an organic origin. A sedimentary source, rich in organic material, from which the asphaltite may originate is the middle Cambrian to lower Ordovician alum shales that covered large parts of Sweden during the Phanerozoic /Andersson et al. 1985, Thickpenny 1987/.

Galena, pyrite, sphalerite, chalcopyrite and baryte have been found in a few fractures together with asphaltite, e.g. in KFM06A 110.49–110.52 m (Figure 5-23). Although these minerals seem to slightly pre-date the asphaltite in these fractures, a close relationship is indicated. Phanerozoic galena bearing fractures younger than 500 Ma are found in the basement elsewhere, e.g. on Åland, southwestern Finland /Bergman and Lindberg 1979/, not far from Forsmark, and in the Götemar granite /Alm and Sundblad 2002/.

5.2.6 Generation 6

This generation includes the low temperature fillings of clay minerals and late calcite and dominates the hydraulically conductive zones. The clay minerals found in this late phase are dominantly corrensite (Figure 5-21), illite, smectite and some saponite.

The minerals from this generation have been the most difficult to study due to loss and disturbances during drilling of the soft and loose minerals. It is likely that lots of these minerals have been lost when flushing the borehole during drilling since soft material can be seen more abundantly in the BIPS-image than in the drill core. Based on the material sampled so far and the analyses of different late calcites, it can be suggested that low temperature alteration has occurred during a long time span (or during repeated occasions). Illite can e.g. be seen as pseudomorphs after K-feldspar in gouge material in hydraulically conductive zones. The clay minerals in Generation 6 are most frequent in the upper 200 m of the boreholes, but have also been found in hydraulically conductive zones at greater depths in e.g. KFM03A 944.30–944.50 m and in KFM06A 770.32–770.42 m and their abundance are probably more dependent on the presence of hydraulically conductive zones than on the depth itself.

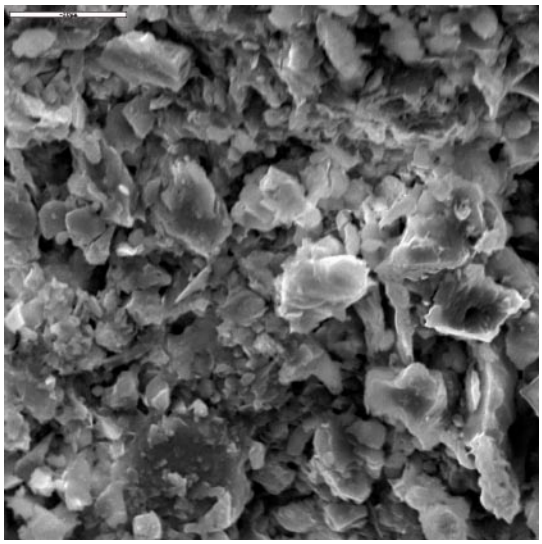

Figure 5-21. *Electron image of a surface covered with clay minerals (corrensite) in a hydraulically conductive zone. The white bar is 20 µm. KFM06A 622.31–622.36 m.*

A few samples of Generation 6 calcite, mostly in KFM02A, have been found /Sandström et al. 2004/. Based on stable isotope values (Figure 5-9), the calcites in the upper part of KFM02A (110–118 m) seem to have precipitated from a groundwater with higher $\delta^{18}O$ values than the present meteoric (–12‰), although a water of Baltic Sea type can not be ruled out. Another possibility is a groundwater similar to the Littorina/glacial mixtures found at depth in Forsmark /SKB 2005a/. The population of late calcites found at approximately 111 to 118 m in KFM02A has high $\delta^{13}C$ values (–6 to +8‰). The crystal morphology is elongated to equant.

Other late calcites occur as thin precipitates on open fracture surfaces and show crystals with short C-axis (nailhead or coin shaped platy crystals) (Figure 5-22). These crystal shapes have been interpreted as precipitated from fresh groundwaters in Äspö and Laxemar

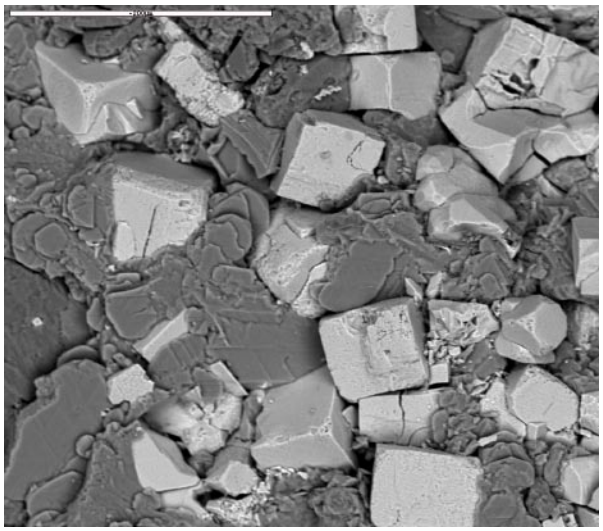

Figure 5-22. *Platy calcite crystals partly covering cubic pyrite crystals of Generation 4. The white bar is 200 µm, backscattered electron image. KFM06A 794.78–794.88 m.*

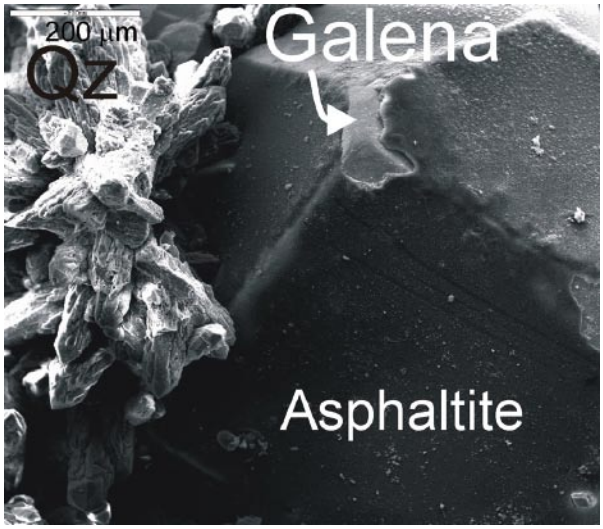

Figure 5-23. *Euhedral porous quartz crystals have crystallized over galena and asphaltite. Backscattered electron image (KFM06A 110.49–110.52 m).*

in southern Sweden and also in Sellafield, England /Milodowski et al. 1998/. It is probable that the continued sampling of late stages calcites will make it possible to recognise low temperature precipitates from different groundwater types.

Euhedral quartz crystals have precipitated after the galena and asphaltite of Generation 5 in samples from KFM06A (Figure 5-23). This quartz post-dates the quartz of Generation 3 and has a white colour and is more porous.

5.3 Fracture minerals in individual zones

ZFMNE00A2 is the only zone with sufficient information to present a sequence of events. Too few samples have been studied to get sufficient information from the other zones. During future sampling, emphasis will be put on sampling the different zones.

5.3.1 Zone ZFMNE00A2

Based on the results from the microscopy of 7 samples presented in this report (Table 5-1) and 5 in /Sandström et al. 2004/ a description of the mineralogy in fractures belonging to the gently SE-S dipping deformation zone has been compiled. Epidote and quartz of Generation 1 occur in mylonites and cataclasites as the oldest minerals. These fracture fillings are cut by fractures filled with chlorite/corrensite. Prehnite and laumontite of Generation 2 have not been found in any of the examined samples from ZFMNE00A2 or by /Sandström et al. 2004/ although data from the drill core mapping extracted from SICADA show some occurrences of laumontite within the zone. However, those fractures cut the zone steeply. The samples selected for the detailed fracture mineral study are often chosen from hydraulically conductive sections of the borehole. It is thus possible that prehnite and laumontite did exist in some of the fractures but have been dissolved and replaced by lower-T minerals. Euhedral quartz of Generation 3 which occurs as thin coatings of euhedral crystals in open fractures are found abundantly in the zone. Calcite and pyrite from Generation 4 are also common as well as clay minerals of Generation 6. Asphaltite occurs in the zone in KFM01B, KFM05A and KFM06A down to depths of 124 m.

5.4 Minerals in the individual fracture orientation sets

The relative sequence of fracture minerals in the different fracture orientation sets are based on the microscopy results (Table 5-1) and data from SICADA. The fracture orientation sets are those defined by /La Pointe et al. 2005/. The number of samples from the different sets varies. Samples from the NE set are in majority while only a few samples from the minor EW (L4) fracture orientation set have been examined. The later orientation set is therefore not accounted for below. Samples from KFM01A, KFM02A, KFM03A and KFM03B presented in /Sandström et al. 2004/ have been re-examined with focus on their belonging to the different fracture orientation sets and are included in the compilation below.

5.4.1 Minerals in the NS fracture orientation set (L1)

The few samples examined from the NS fracture orientation set suggest that the sequence of fracture filling minerals is similar to that in the NE fracture orientation set (see below). Although no laumontite filled fractures belonging to the NS fracture orientation set have been found in the samples examined in this study, fracture orientation data from SICADA show that laumontite occurs in many NS orientated fractures.

5.4.2 Minerals in the NE fracture orientation set (L2)

The abundance of Generation 2 laumontite and calcite is typical for the NE fracture orientation set. These fractures cut the older epidote filled fractures of Generation 1. Some of the fractures have been reactivated with associated precipitation of chlorite and corrensite. The euhedral quartz coating and the calcite and pyrite of Generation 3 and 4 are also found in the NE fracture orientation set and they represent a younger reacti-vation. Most of the fractures in which minerals from Generation 3 and 4 are present are open or partly open. Late clay minerals also occur in open fractures.

5.4.3 Minerals in the NW fracture orientation set (L3)

The NW fracture orientation set mainly contains the epidote, quartz and Fe-chlorite fillings of Generation 1. The examined samples are mostly sealed fractures and the wall rock is highly altered up to a few centimetres adjacent to the fractures. Some fractures are filled with the brick-red adularia and hematite which are interpreted as an early phase of Generation 2. A few prehnite and laumontite fillings have also been found in fractures belonging to the NW fracture orientation set, were they have crystallized on epidote (e.g. KFM03A 451.85–451.90 m /Sandström et al. 2004/).

5.4.4 Minerals in Horizontal fracture orientation set (HZ)

Only a few of these fractures have been examined. However, mineral data together with boremap data from SICADA suggest that many of the sealed fractures in the HZ fracture orientation set are filled with epidote of Generation 1. Further, the open fractures contain mainly euhedral quartz, calcite and pyrite of Generation 3 and 4 as well as later clay minerals.

5.5 Wall rock alteration

The wall rock alteration is most intense adjacent to the fractures of Generation 1 and 2. The dominant alteration is saussuritization of the plagioclase, chloritization of the biotite and sericitization of the K-feldspar. The alteration of the K-feldspar is far less intense than that of the plagioclase. The saussuritized plagioclase is often completely altered into albite, adularia and epidote. The altered wall rock is red-coloured due to micro-grains of hematite mainly in the plagioclase (Figure 5-24). The extent of the alteration rim is highly variable from < 1 cm to tens of centimetres. The biotite is replaced by pseudomorphs of chlorite with lenses of titanite, prehnite (Figure 5-25) and less commonly laumontite. Quartz dissolution is obvious in some samples and especially in samples from borehole KFM02A at 100 to 300 m. This alteration has increased the porosity along some of the fracture pathways considerably.

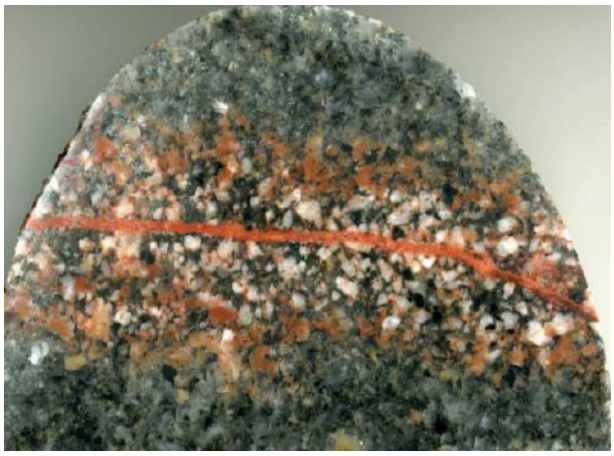

Figure 5-24. *Wall rock alteration around a fracture filled with hematite-stained adularia of Generation 2. The width of the altered area is c 2 cm. KFM05A 692.00–692.15 m.*

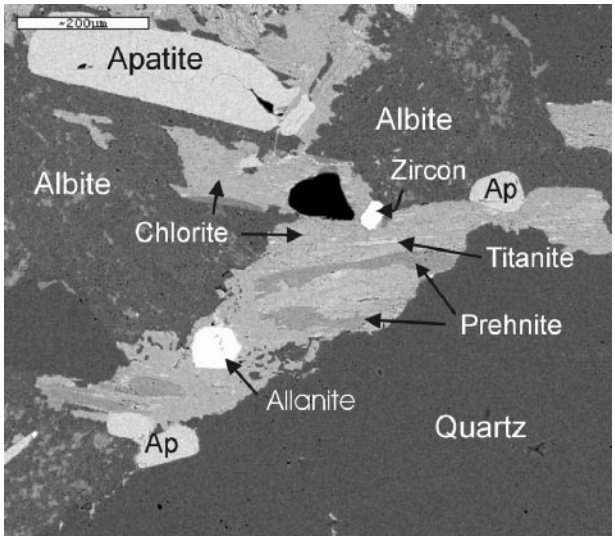

Figure 5-25. *Biotite completely replaced by pseudomorphus chlorite with lenses of titanite and prehnite together with apatite, zircon and allanite, of which the three later probably existed before the chloritization. The black spot is a hole created during the thin section preparation. Ap = apatite, backscattered electron image.KFM05A 692.00–692.15 m.*

5.6 Fracture reactivation

Many of the older fractures have been reactivated with associated crystallization of younger minerals during different events. The epidote filled fractures of Generation 1 have been reactivated during both ductile and brittle conditions. The oldest reactivations are associated with recrystallization of larger epidote crystals and appear to be closely related in time with the first formation of the fractures. Occurrences of prehnite and laumontite in epidote sealed fractures indicate a later reactivation.

The laumontite filled fractures of Generation 2 are the most commonly reactivated fractures. The reactivation has mostly resulted in crystallization of chlorite/corrensite but also later crystallization of euhedral quartz coatings of Generation 3. Based on the well-preserved euhedral crystals of quartz, calcite and pyrite of Generation 3 and 4, no major reactivations of fractures appear to have occurred after the formation of Generation 4.

5.7 Redox conditions

The presence of pyrite (Fe(II)) and hematite (Fe(III)) provides indications of redox conditions during the periods of fracture mineral precipitations. Many of the fracture coatings are red-stained due to presence of micro-grains of hematite. This is e.g. the case for the early adularia/albite sealings and the laumontite of Generation 2. Ce-anomalies are also found in calcite samples from Generation 2 indicating oxidation conditions. The epidote filled fractures of Generation 1 is also closely related to oxidation of the wall rock. Pyrite formation is indicated as a late phase that starts with Generation 4 in many, mostly open, fractures. The preservation of these euhedral pyrites is a strong indication that reducing conditions have prevailed from this period until present (valid at least for this set of samples representing depths deeper than 100 m). Uranium series analyses on fracture filling material are at present carried out as part of the fracture filling studies and will add information about the redox conditions during the last 1 Ma. The present redox conditions (late Generation 6) probably varies with depth, showing oxidizing conditions close to the surface whilst reduction prevails at depth (Figure 5-26) based on mineralogical observations but also ground water chemistry /SKB 2005a/.

Mössbauer analyses on preferentially chlorite have been carried out on a few samples collected from KFM02A, KFM03A and KFM04A (Appendix VIII). The oxidation factor ($Fe^{3+}/(Fe^{3+}+Fe^{2+})$) in most of the silicates is between 0.28–0.42 which means that there is more Fe^{2+} in the chlorite than Fe^{3+}. The oxides in the samples were mainly hematite, although traces of magnetite were also found. Traces of FeOOH were found in the drillcore sample KFM03A 803.85–804.05 m, which has a low oxidation factor in the silicates (0.12). It is important to note that although hematite is present in the sample, reduced Fe^{2+} is still present to a high degree in the chlorite.

A summary of the redox conditions in the fractures can be seen in Figure 5-26.

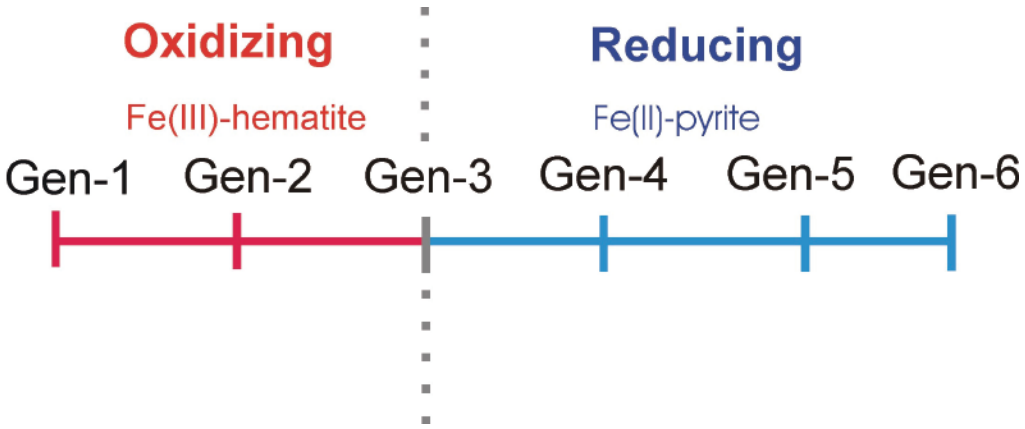

Figure 5-26. *Schematic picture of the redox conditions during crystallization of different fracture generations in the Forsmark area at repository depth (not to scale).*

5.8 Chemical analyses of fracture fillings

The purpose of the fracture mineral study has been to identify minerals and provide interpretations of the low temperature evolution in the Forsmark area. For this purpose mainly XRD, microscopy (including electron microscopy) and chemical analyses of single minerals have been carried out. For the general description of the fracture filling minerals present along important groundwater path ways it is, however, important to ensure that no minor phases, rich in certain trace elements have been overlooked. Therefore chemical analyses (ICP-MS) on bulk samples from fracture coatings have been carried out. Totally 25 samples have been analysed including two asphaltite rich fillings (Appendix IX). Furthermore, XRD diffractometry has been carried on corresponding samples (Appendix VII and IX). It is shown that the chemical composition generally corresponds to the major mineral phases identified, although two samples with high U content were identified by the chemical analyses.

The chemical composition of the samples is briefly discussed below:

K, Rb, Ba, Cs

These elements are mainly hosted in K-feldspar, mica and clay minerals. From the chemical analyses it is obvious that K correlates with Ba (Figure 5-27), which indicates that most K is hosted in K-feldspar which preferably contains Ba and to lesser degree Rb and Cs. The latter elements are instead hosted together with K in clay minerals. Especially illite and mixed layer clays of illite/smectite type tend to enrich Rb and even more Cs. However, the sample showing the highest Rb content (439 ppm) is low in Cs (< 1 ppm). This is a sample containing almost solely apophyllite (KFM02A 893.45 m). The highest Cs/Rb ratios (3 to 4.2 ppm) are shown by the samples containing the Na-zeolite analcime (KFM01A 127.4 m, KFM01A 148.8 m and KFM01A 269.9 m) which selectively exchange Cs.

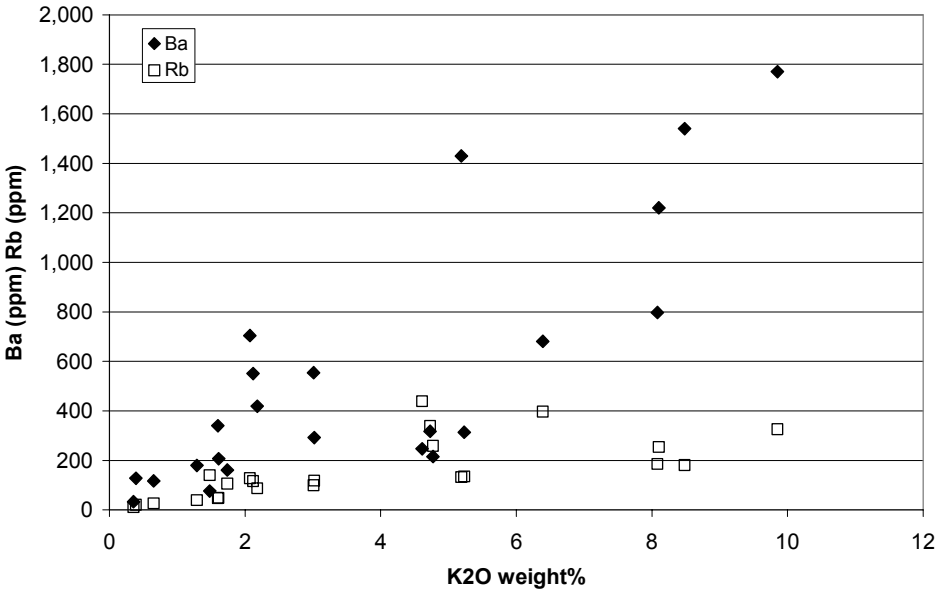

Figure 5-27. *Ba and Rb plotted versus K_2O for bulk samples of fracture fillings (Appendix IX).*

The most common zeolite in the area, laumontite, which is represented in e.g. sample KFM01A 188.10–188.20 m, does not show any significant enrichment of Rb or Cs.

The Cs content in the host rock is generally < 1 ppm /Petersson et al. 2004b/, whereas the values in the fracture coatings are significantly higher (2.5 to 32.7 ppm in 17 of the 23 samples analysed for Cs).

Na, Ca, Sr

The Sr content in the analysed fracture fillings varies between 16 and 490 ppm. A positive correlation between Sr and Ca is observed for the samples with CaO contents < 5 weight % (Figure 5-28) whereas the samples with the highest CaO contents (15 to 25 weight %) show relatively low Sr contents. The latter samples consist dominantly of prehnite, analcime and calcite, but also the apophyllite sample is amongst these. From calcite analyses (Appendix IV and V) it is known that the Sr/CaO ratio in the calcites is very low. The minerals hosting most Sr seem to be laumontite and plagioclase (including albite). Another possible candidate is epidote although this has not yet been confirmed.

Na shows a positive correlation with Sr in the samples with albite, whereas the analcime samples do not follow this trend.

Fe, Mg, Mn, Ti, V, Sc

Fe correlates with Mg in most samples (Figure 5-29), which is explained by the presence of chlorite and corrensite in the fracture fillings. As has been shown by SEM-EDS analyses, the Fe/Mg ratio in the chlorites of different generations varies (See Section 5.2), which partly explains the variation in Fe/Mg ratio in the entire bulk samples. Additional contents of minerals containing Fe but no Mg are another explanation. The two samples with the highest Fe_2O_3 content also have high Cr and Ni content, indicating that part of the Fe in these samples can result from iron-rich debris produced during the drilling which may have soaked into the split-tube and penetrated the fractured drill core.

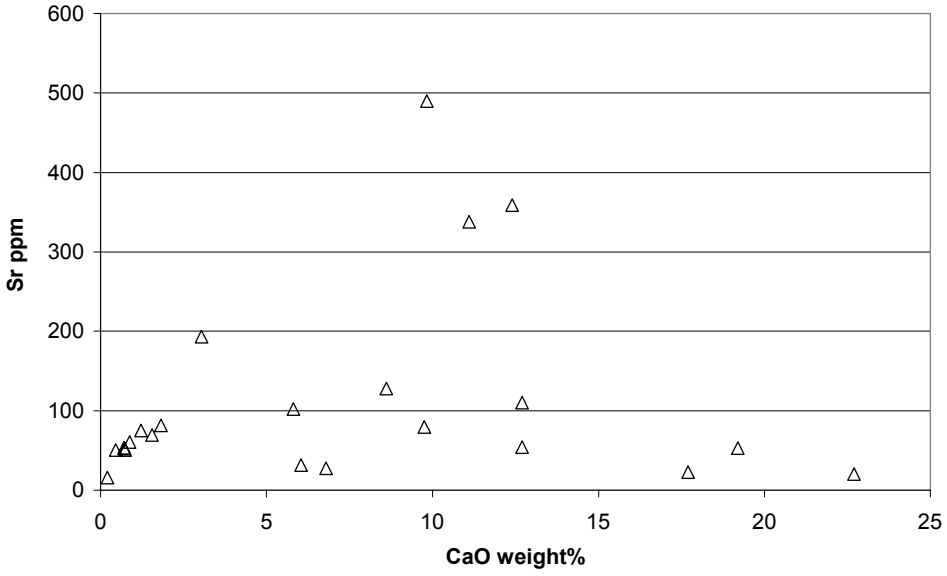

Figure 5-28. *Sr plotted versus CaO for bulk samples of fracture fillings (Appendix IX).*

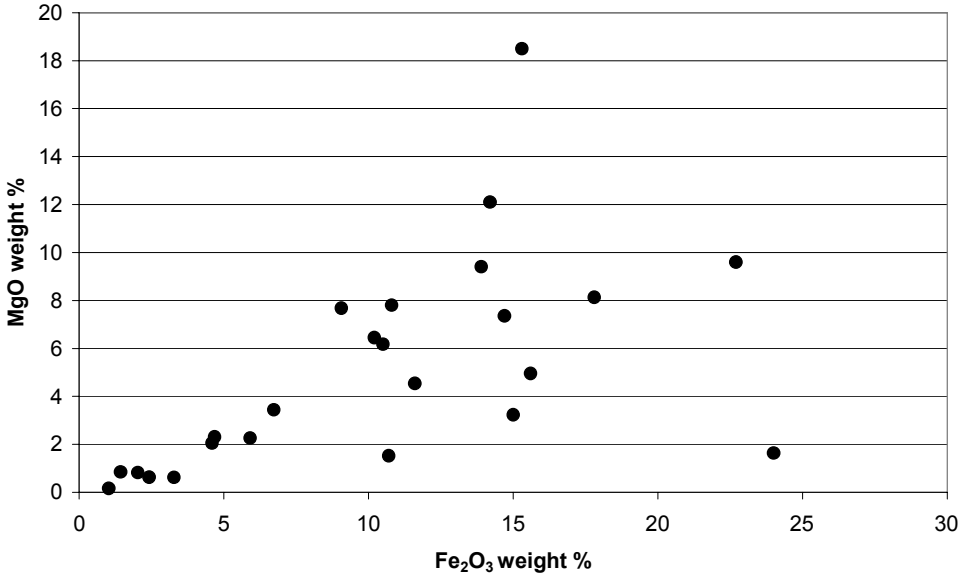

Figure 5-29. *MgO versus Fe_2O_3 for bulk samples of fracture fillings (Appendix IX).*

Mn shows a significant positive correlation with Fe indicating its presence in chlorite and clay minerals. Ti, V and Sc generally show a positive correlation with Fe except for some prehnite and pyrite rich samples that show very low Ti, Sc and V contents.

U and Th

The U content varies between 0.46 and 40 ppm except in two samples from KFM03A 643.8–644.12 m and KFM03A 644.17 m which show U values of 2,200 and 2,310 ppm.

The Th values, in contrast, are all within the interval 0.2 to 14.7 ppm. The Th/U ratios are < 1 for all except three samples, indicating an enrichment of U in the fracture coatings compared to the fresh rock (Th/U usually > 2) /Petersson et al. 2004b/. A thin section from one of the fractures showing the high U value has been studied in detail, in order to identify the U–rich phase which turned out to be pitchblende (See Section 5.11).

The asphaltite samples (KFM01B 25.3 m and KFM01B 49.4 m) show low U and Th contents (< 8 ppm).

REEs

Chondrite normalised REE curves are shown in Figure 5-30. The La/Yb ratios vary between 2 and 28 with one exception of 128. The latter is found in the apophyllite sample (KFM02A 893.45 m) which also shows the highest contents of LREEs (La = 815 ppm) of the samples analysed. The laumontite sample (KFM01A 188.10–188.20 m), in contrast, shows very low REE values (La = 6.6 ppm and Yb below detection limit). The two U-rich samples show the highest HREE content (Y = 30 and 28.7 ppm). A negative Ce-anomaly is indicated in sample KFM03B 65.20 m, which may be due to groundwater/mineral interaction close to the (past or present) redox front. Sample KFM01A 185.35 m shows a positive Ce anomaly, which is probably related to the (hydrothermal?) oxidation and breakdown of prehnite observed in this sample /Sandström et al. 2004/.

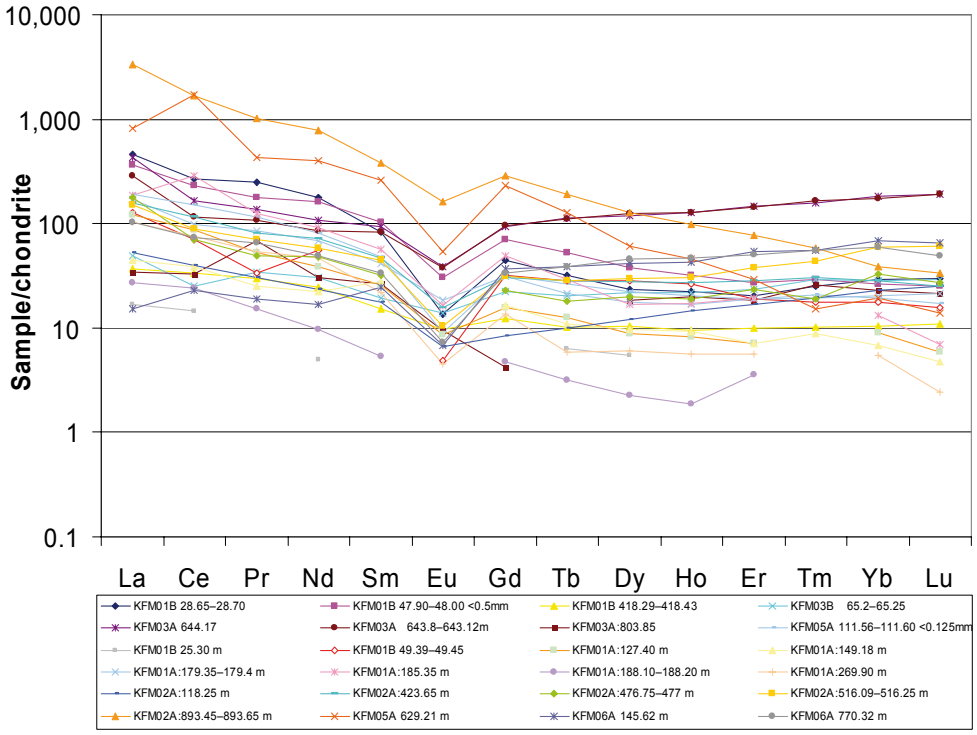

Figure 5-30. *Chondrite normalized REE curve for bulk samples of fracture fillings. Chondrite data from /Evansen et al. 1978/.*

5.9 Palaeohydrogeological information based on fracture calcites

In order to sort out different calcite generations and to provide palaeohydrogeological information, 81 samples have been analysed for $\delta^{13}C$/ $\delta^{18}O$, of which 31 have been analysed for $^{87}Sr/^{86}Sr$ and 20 for chemical composition. This is the total of the analyses carried out on fracture calcites from Forsmark and includes previously reported values in /Sandström et al. 2004/.

The majority of the samples belongs to Generation 2 or 4 and has already been discussed in Sections 5.2.2 and 5.2.4. Of larger importance for the palaeohydro-geological interpretations are the late calcites present as euhedral crystals or thin, usually flaky, coatings. Figure 5-31 shows the variation in $\delta^{18}O$ for all the analysed calcites versus depth. The samples marked as belonging to Generation 6 are the possible low temperature precipitates. The separation between the $\delta^{18}O$ intervals for the different generations is not perfect but some major differences can be seen; generation 2 generally shows the lowest $\delta^{18}O$ (down to 19‰ PDB), all except one of these calcites also show $\delta^{13}C$ values between –6 and –2‰ (Figure 5-32). As discussed in Section 5.2.2, all evidences like stable isotopes, chemical composition and paragenesis support a hydrothermal origin for these calcites.

The majority of the Generation 4 calcites show $\delta^{18}O$ values between –14 and –11‰ but show large variation in carbon isotope composition (values ranging from –35 to –3‰). Very low $\delta^{13}C$ values are usually interpreted as a result of biogenic activity in situ. This is not expected to take place at temperatures much above 100°C. Relatively low temperatures are therefore suggested for most of the Generation 4 calcites. The variation in $\delta^{13}C$ versus depth (Figure 5-32) shows that the extremely low $\delta^{13}C$ values in the Generation 4 calcites are found in the depth interval 150 to 300 m, whereas the samples from larger depth show

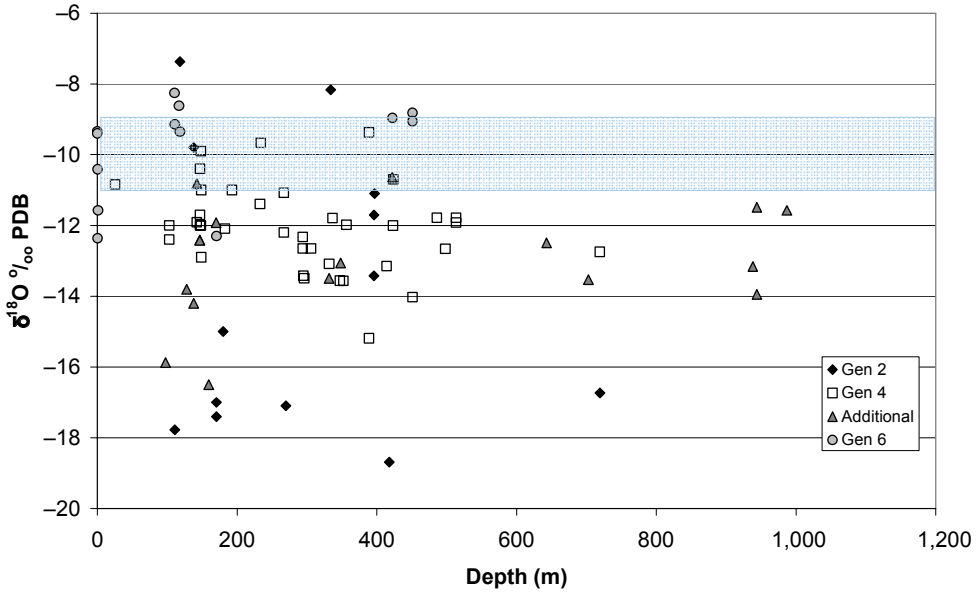

Figure 5-31. *$\delta^{18}O$ values for fracture calcites from KFM01A, KFM01B, KFM02A, KFM03A, KFM03B, KFM04A, KFM05A and DS5 (bedrock surface) versus depth. The blue interval represents the $\delta^{18}O$ interval for calcite precipitated at ambient temperatures from meteoric groundwater similar to the present at Forsmark site. For the samples marked additional, it has not been possible to confirm to which generation they belong.*

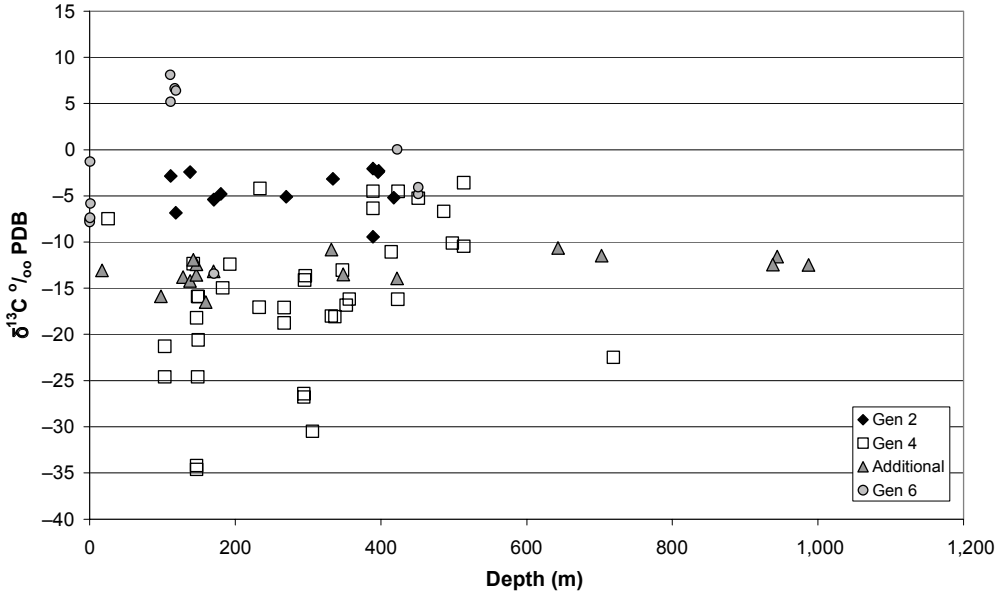

Figure 5-32. *$\delta^{13}C$ values for fracture calcites from KFM01A, KFM01B, KFM02A, KFM03A, KFM03B, KFM04A, KFM05A and DS5 versus depth. For the samples marked additional, it has not been possible to confirm to which generation they belong.*

less negative values and the three samples from below 800 m show no significant biogenic modification. One possible interpretation is that organic material has been contributed from the surface (or overlaying sediments) and that breakdown of this material in the bedrock have produced HCO_3^- with very low $\delta^{13}C$ signatures. One problem with the present set of analyses is that most of the samples analysed represent the upper 500 m and only a minority is from larger depth. The distribution reflects the fracture frequencies in the boreholes but introduces a larger uncertainty in the interpretation of conditions at depth.

The generation 6 calcites are not a distinct group. It is more probable that these calcites represent different groundwater regimes. The $\delta^{18}O$ values vary between –13 and –8‰. If precipitation at ambient temperature is the case, the highest values (close to –8‰) represent precipitates from water similar to the present Baltic Sea water. Some of these calcites also show extremely high $\delta^{13}C$ values (+5 to +8‰), indicating biogenic modification in situ which resulted in carbon isotope exchange between CH_4 and CO_2 which in turn may have produced very high $\delta^{13}C$ values in the resulting HCO_3. These $\delta^{13}C$ values have later been transferred into the calcites.

The Generation 6 calcites with $\delta^{18}O$ values between –13 to –9‰ can be precipitated from waters similar to present day meteoric groundwater and in a slightly colder climate. These calcites are found close to the surface but also in samples from e.g. the ZFMNE00A2 zone in KFM02A (422 m). It is not possible to confirm a postglacial age of these calcites; instead they may represent older events of similar conditions as the present. No samples of a low temperature origin showing precipitation from glacial melt water have been found in the present set of data.

Very few Generation 6 calcites have been possible to sample so far, probably due to the fact that the amount of these calcites is small compared to e.g. Generation 4 calcites but also that the tiny crystals on the outermost fracture surfaces are easily destroyed during drilling. Due to the small sample volumes of the Generation 6 calcites, neither Sr isotope nor trace element analyses have been performed.

The $\delta^{13}C/\delta^{18}O$ plot (Figure 5-9) shows that there is no complete separation between the calcite generations. This is probably due to zonation, younger calcite generations grown on top of older crystals, e.g. Generation 6 calcites may be present as thin rims on Generation 4 calcites. Detailed studies of zoning can provide useful information about changes in the hydrogeochemical conditions and more detailed studies within this field are planned.

5.10 Sediment-like fracture fillings in KFM01B and KFM05A

During the drill core mapping of KFM01B and KFM05A, fractures filled with what looked like sediments or fault gouge were found in the upper 120 m of the drill cores. In order to study the composition of these fillings, four fractures were sampled. The samples selected were: KFM01B 28.65–28.70 m, KFM05A 105.41–105.46 m, KFM05A 109.75–109.90 m and KFM05A 111.56–111.60 m (Appendix I).

The fracture fillings in KFM05A 105.41–105.46 m and KFM05A 109.75–109.90 m both show euhedral quartz very similar to the coatings of small euhedral quartz crystals belonging to Generation 3. It is therefore suggested that some of the fracture fillings (that can be mistaken for sediment filled fractures) are just a variety of this quartz generation. In two other fractures, KFM01B 28.65–38.70 and KFM05A 111.56–111.60, the filling appears to be more of a fault gouge material with mainly wall rock fragments together with some clay minerals (mostly illite) and asphaltite.

Macroscopically, the two kinds of fracture filling materials can be distinguished since the gouge material is more porous and consists of particles of different sizes. The quartz-adularia filling is more of a hard mineral coating on the fracture surface. The quartz and adularia occur as small euhedral crystals, but are often too small to be recognised macroscopically.

5.11 Fracture with increased U content

High U contents in groundwater have been observed in samples from 110 m to 640 m depth /Wacker et al. 2004/. Chemical analyses carried out on bulk fracture fillings for more than twenty samples showed enrichment of U in two samples from one fracture (2,200 to 2,310 ppm in KFM03A 643.80–644.17 m) whereas the other samples all showed values below 22 ppm. Th was below 14 ppm for all samples. To explain this enrichment in U, a thin section of the sample was made (KFM03A 643.80–644.17 m) and analysed with SEM-EDS. A small grain of a U-oxide was found, probably altered Pitchblende (Figure 5-33) together with chlorite and hematite. This is probably the main source of the high U content in the fracture filling and most likely also in the groundwater.

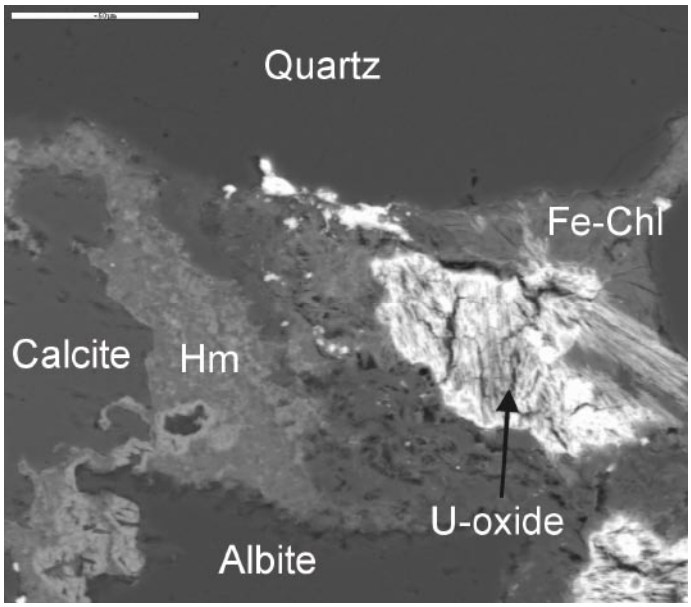

Figure 5-33. *Altered U-oxide (Pitchblende) together with chlorite (Fe-Chl), hematite (Hm) and calcite. Backscattered electron image, the bar is 50 µm. KFM03A 643.80–644.17 m.*

6 Conclusions

The present fracture filling mineral study comprises results from the boreholes KFM01B, KFM03A, KFM04A, KFM05A and KFM06A which are compared with earlier obtained results from KFM01A, KFM02A, KFM03A and KFM03B /Sandström et al. 2004/.

Most of the mineral identification carried out supports previous studies, and many of the fillings with unknown phases are in fact fine grained material of the common minerals of the area, sometimes showing a different colour. Asphaltite is more common in fractures in the upper 150 m of the bedrock and envisaged from the earlier fracture filling study, its organic origin is supported by carbon isotopes determinations. The few chemical analyses of the asphaltite show low U and Th contents. Some new mineral findings can be noted in connection with the asphaltite such as baryte, galena, chalcopyrite and sphalerite.

High U content in groundwater has been observed in samples from 110 m to 640 m depth /Wacker et al. 2004/. Chemical analyses carried out on bulk fracture fillings for more than twenty samples showed enrichment of U in two samples (2,200 to 2,300 ppm) from one fracture, whereas the other samples all showed values below 22 ppm. Th was below 14 ppm for all samples. Minor grains of altered Pitchblende were later found in the U enriched fracture.

The horizontal and sub-horizontal fracture zones in the upper part of the bedrock show presence of material that could be fault gouge or potential sediments. Detailed SEM-EDS studies were carried out on four such samples showing that some of the samples consist of gouge material while some samples contain euhedral quartz and adularia from Generation 3 (see below). No sediment fillings were identified.

The sequence of fracture mineralogy earlier described in /Sandström et al. 2004/ is strengthened although minor revisions are suggested. The Boremap database together with the detailed mineralogy also allows interpretations of orientations of fractures active during different phases of the geological evolution.

The sequence of events based on the first six boreholes (with addition of KFM01B and KFM03B) in Forsmark starts with epidote, quartz and chlorite formation during greenschist facies and semi-ductile to brittle condition **(Generation 1)**. Only very thin mylonites are present whereas cataclasites are more frequent. Biotite $^{40}Ar/^{39}Ar$ data show that cooling below 300°C occurred between 1704 and 1635 Ma /Page et al. 2004/ which therefore is suggested as a minimum age of Generation 1. These fractures mainly have NW-SE strike (steeply dipping) or are subhorizontal based on the drill core mapping data extracted from SICADA.

The next phase of fracture mineralization is a hydrothermal event responsible for the crystallization of prehnite and laumontite **(Generation 2)**. In addition, calcite as well as chlorite/corrensite, adularia and hematite have been precipitated during this event. The stable isotope ratios of O, C and Sr for the calcites support a close relationship between the prehnite and laumontite formation. The results show typical hydrothermal signatures for the carbon isotopes, a narrow interval in $^{87}Sr/^{86}Sr$ supporting a common origin, and increasing trend in the oxygen isotope values, indicative of precipitation during decreasing temperatures. This information supports the interpretation of fracture mineralization during brittle conditions and P-T conditions changing from prehnite-pumpellyite phases over to upper zeolite phases.

Generation 2 represents a distinct stress regime separated from Generation 1 and seems to represent an event of new fracturing characterized by laumontite as the oldest coating, mainly in steep NE-orientated fractures. The age of this hydrothermal event is so far unclear, but according to the $^{40}Ar/^{39}Ar$ data from biotite /Page et al. 2004/ they are younger than 1,704–1,635 Ma. The frequent brick-red thin, sealed fractures (hematite stained adularia ± albite ± quartz) commonly found in the area belong to an early phase of this generation.

The following phase starts with dissolution along older laumontite/prehnite sealed fractures causing cavities in fractures and to a lesser extent in the adjacent host rock. Subsequent temperature decrease has caused precipitation of euhedral quartz covering fracture surfaces and coating voids. Adularia, chlorite/corrensite and calcite are also precipitated during this period **(Generation 3)**, and in a later phase calcite, pyrite and analcime **(Generation 4)**. The difference between Generation 3 and 4 is probably only a gradual decrease in temperature. The $^{87}Sr/^{86}Sr$ ratios indicate a significantly higher input of radiogenic Sr during this period compared with that during the period for Generation 2 and 3. This can be explained either by a relatively long separation in time or by significantly different chemistry of the hydrothermal fluids involved; a preferential leaching of K-Rb rich minerals yields solutions rich in radiogenic Sr. The carbon isotopes in calcites are depleted in ^{13}C. Such values are usually caused by microbial activity along the fractures in the bedrock. However, microbial activity is not expected above 110–115°C. This is in contrast to the extensive quartz and adularia formation which is not believed to have taken place at such low temperatures. This contradiction may be explained by microbiologically modified HCO_3^- that was transported into higher temperature domains where it precipitated together with quartz and adularia. The event during which Generation 4 was formed seems to have affected large parts of the fracture systems at Forsmark. However, it has not been possible to recognize any preferred directions of fractures in which this mineral assemblage was precipitated. Reactivation of fractures is obviously common during this period although new fractures were probably also formed. No age information is available, but based on the indicated formation temperatures, a Precambrian age is suggested.

Based on stable carbon isotopes, asphaltite **(Generation 5)** found in the upper 170 m of the drill cores (c 124 m below the surface) has been interpreted as migrated hydrocarbons from an organic, probably Phanerozoic source. **Generation 6** includes the precipitates found as a top-layer on the fractures and represents calcite, clay minerals like illite, mixed-layer clays and smectite. Generation 6 is mostly found in hydraulically conductive fractures. The timing for the precipitation of the Generation 6 minerals probably extends from the Precambrian until the Neogene.

Stable isotopes have been used for the identification of calcites belonging to Generation 2 and 4 but also younger calcites (Generation 6), grown as the outermost phase (partly as minor euhedral grains) in fractures, have been sampled when possible. A number of calcite fillings sampled very close to the surface from drill site 5 and from the upper metres in KFM03B show $\delta^{13}C$ and $\delta^{18}O$ values in accordance with the present meteoric water. A few late calcites also showed values within the same interval (111–118 m in KFM02A, 422–423 m in KFM02A (Zone ZFMNE00A2) and 389 m in KFM03A). This does not invoke a recent origin for these calcites although a low temperature meteoric water origin is possible. Calcites precipitated from a Baltic Sea water should have values around –8‰ $\delta^{18}O$ PDB or higher. Such values have so far only been recorded for samples in the 110–118 m zone in KFM02. Calcite is a very common fracture mineral in the Forsmark area and the majority of these belong to Generation 2 and Generation 4. It is however expected that especially Generation 4 calcites, which are found in hydraulically conductive fractures, are partly zoned and that younger calcites (Generation 6) may have grown as a thin layer over some of the older calcites.

7 Acknowledgment

We would like to thank Jesper Petersson, Johan Berglund, Anders Wängnerud and Peter Danielsson (Swedpower AB) for their help during the drill core sampling and the interpretation of the Boremap data, Michael Stephens (SGU) and Assen Simeonov (SKB) for support and constructive discussions, Allan Stråhle (Geosigma AB) for help with e.g. the BIPS-images, Owe Gustavsson and Cees-Jan de Hoog (Göteborg University) for their help with the stable C and O isotopes, ICP-MS and LA-ICP-MS analyses, Ulf Brising (Sweco) for the geological map and Henrik Drake (Göteborg University) for rewarding discussions concerning fracture mineralogy. Kjell Helge (Minoprep AB) and Ali Firoozan (Göteborgs University) are thanked for the thin section preparations. We also thank Sven Åke Larson (Göteborg University) for reviewing the report.

8 References

Alm E, Sundblad K, 2002. Flourite-calcite-galena-bearing fractures in the counties of Kalmar and Blekinge, Sweden, SKB R-02-42, Svensk Kärnbränslehantering AB, 116 pp.

Andersson A, Dahlman B, Gee D G, Snäll S, 1985. The Scandinavian Alum Shales. Sveriges Geologiska Undersökning, Ser. Ca 56: p 50 pp.

Berglund J, Petersson J, Wängnerud A, Danielsson P, 2004. Boremap mapping of cored drilled borehole KFM01B, Forsmark site investigation, SKB P-04-114, Svensk Kärnbränslehantering AB, 71 pp.

Bergman L, Lindberg B, 1979. Phanerozoic veins of galena in the Åland rapakivi area, southwestern Finland. Bulletin of the Geological Society of Finland, 51: p 55–62.

Burkhard M, 1993. Calcite twins, their geometry, appearance and significance as stress-strain markers and indicators of tectonic regime: a review. Journal of Structural Geology, 15: p 351–368.

Carlsten S, Petersson J, Stephens M B, Mattsson H, Gustafsson J, 2004. Geological single-hole interpretation of KFM02A and HFM04-05 (DS2), Forsmark site investigation, SKB P-04-117, Svensk Kärnbränslehantering AB, 32 pp.

Cederbom C, Larson S Å, Tullborg E-L, Stiberg J-P, 2000. Fission track thermo-chronology applied to Phanerozoic themotectonic events in central and southern Sweden. Tectonophysics, 316: p 153–167.

Eakin P A, 1989. The origin of uranium-niobium-tantalum mineralised hydrocarbons at Narestø, Arendal, southern Norway. Norsk Geologisk Tidsskrift, 69: p 29–37.

Evansen N M, Hamilton P J, O'Nions R K, 1978. Rare Earth Abundances in Chondritic Meteorites. Geochimica et Cosmochimica Acta, 42: p 1199–1212.

Ferrill D A, 1991. Calcite twin widths and intensities as metamorphic indicators in natural low-temperature deformation of limestone. Journal of Structural Geology, 13: p 667–675.

Hoefs J, 2004. Stable isotope geochemistry. 5., rev. and updated ed. Berlin. Springer-Verlag. pp 244.

La Pointe P R, Olofsson I, Hermansson J, 2005. Statistical model of fractures and deformations zones for Forsmark, preliminary site description Forsmark area – version 1.2, SKB R-05-26, Svensk Kärnbränslehantering AB, 134 pp.

Liou J G, 1971. Analcime equilibria. Lithos, 4: p 389–402.

Liou J G, Kim H S, Maruyama S, 1983. Prehnite – epidote equilibria and their petrologic applications. Journal of Petrology, 24: p 321–342.

Liou J G, Maruyama S, Cho M, 1985. Phase equilibria and mineral paragenesis of metabasites in low-grade metamorphism. Mineralogical Magazine, 49: p 321–333.

Milodowski A E, Gillespie M R, Pearce J M, Metcalfe R, 1998. Collaboration with the SKB EQUIP programme; Petrographic characterisation of calcites from Äspö and Laxemar deep boreholes by scanning electron microscopy, electron microprobe and cathodoluminescence petrography, WG/98/45C. British Geological Survey, Keyworth, Nottingham, (1998).

Möller P, Moreteani G, 1983. On the geochemical fractionation of rare earth elements during the formation of Ca-minerals and its application to problems of the genesis of ore deposits, *In* S.S. Augustithis (ed.): The significance of trace elements in solving petrogenic problems and controversies. Theophrastus Publications S.A.: Athens. p 747–791.

Page L, Hermansson T, Söderlund P, Andersson J, Stephens M B, 2004. Bedrock mapping U-Pb, $^{40}Ar/^{39}Ar$ and (U-Th)/He geochronology. Forsmark site investigation, SKB P-04-126, Svensk Kärnbränslehantering AB, 64 pp.

Petersson J, Berglund J, Wängerud A, Danielsson P, 2004a. Boremap mapping of telescopic drilled borehole KFM05A. Forsmark site investigation, SKB P-04-295, Svensk Kärnbränslehantering AB, 45 pp.

Petersson J, Skogmo G, Berglund J, Wängerud A, 2005. Boremap mapping of telescopic drilled borehole KFM06A and core drilled borehole KFM06B. Forsmark site investigation, SKB P-05-xx, Svensk Kärnbränslehantering AB, pp.

Petersson J, Tullborg E-L, Mattsson H, Thunehed H, Isaksson H, Berglund J, Lindroos H, Danielsson P, Wängnerud A, 2004b. Petrography, geochemistry, petrophysics and fracture mineralogy of boreholes KFM01A, KFM02A and KFM03A+B, SKB P-04-103, Svensk Kärnbränslehantering AB, 69 pp.

Petersson J, Wängerud A, Berglund J, Danielsson P, 2004c. Boremap mapping of telescopic drilled borehole KFM04A. Forsmark site investigation, SKB P-04-115, Svensk Kärnbränslehantering AB, 55 pp.

Sandström B, Savolainen M, Tullborg E-L, 2004. Fracture Mineralogy. Results from fracture minerals and wall rock alteration in boreholes KFM01A, KFM02A, KFM03A and KFM03B, Forsmark site investigation, P-04-149, Svensk Kärnbränslehantering AB, 93 pp.

SKB, 2005a. Hydrogeochemical evaluation for Forsmark model version 1.2. Preliminary site description of the Forsmark area, SKB R-05-17, Svensk Kärnbränslehantering AB, xx pp.

SKB, 2005b. Preliminary site description. Forsmark – version 1.2, SKB R-05-18, Svensk Kärnbränslehantering AB, 752 pp.

Thickpenny A, 1987. Paleo-oceanography and depositional environment of the Scandinavian alum shales; sedimentological and geochemical evidence, *In* J.K. Leggett and G.G. Zuffa (ed.): Marine clastic sedimentology; concepts and case studies. Graham and Trotman: London, United Kingdom. p 156–171.

Tullborg E-L, 1997. Recognition of low-temperature processes in the Fennoscandian shield. Ph.D Thesis, Earth Sciences Centre, Göteborg University. A17: p 35.

Wacker P, Bergelin A, Berg C, Nilsson A-C, 2004. Hydrochemical characterisation in KFM03A. Results from six investigated borehole sections: 386.0–391.0 m, 448.0–453.0 m, 448.5–455.6 m, 639.0–646.1 m, 939.5–946.6 m, 980.0–1001.2 m. Forsmark site investigation, SKB P-04-108, Svensk Kärnbränslehantering AB, 125 pp.

Welin E, 1966. The occurence of asphaltite and thucholite in the Precambrian bedrock of Sweden. Geologiska Föreningens i Stockholm Förhandlingar, 87: p 509–526.

Åberg G, Löfvendal R, Nord A G, Holm E, 1985. Radionuclide mobility in thucholitic hydrocarbons in fractured quartzite. Canadian Journal of Earth Sciences, 22: p 959–967.

Appendix 1

Results from microscopy – including order of mineralizations

Sample: **KFM01B 28.65–28.70 m**
Rock type: Metagranite
Fracture: Crushed zone
Orientation: 074/16°
Deformation zone: ZFMNE00A2
Fracture orientation set: HZ
Fracture minerals: Adularia

The sample consists of a material from a crushed zone. The surfaces are coated with a sediment-like layer of greyish material. The thin section was made on material scraped of the fracture surface. The grains consist of angular fragments of wall rock in different sizes, mainly quartz and microcline. The plagioclase is extremely saussuritized and is difficult to recognize as plagioclase in thin section. The fragments are surrounded by a fine-grained matrix consisting of adularia. The sample gives the impression as being the remnants of a crushed cataclasite.

Figure A-1. *Crushed zone with wall rock fragments in an adularia matrix. The diameter of the drill core is c 5 cm.*

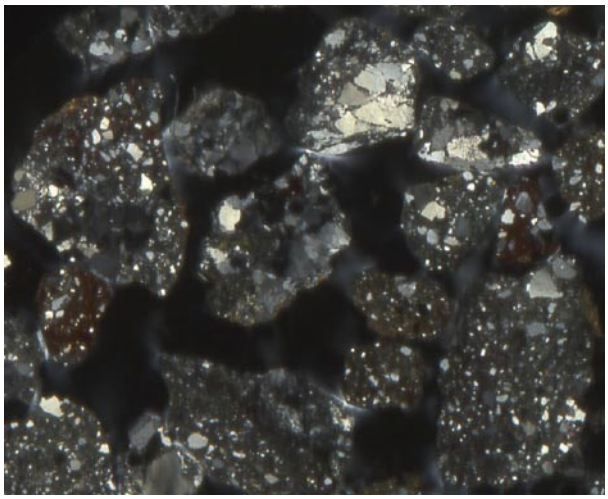

Figure A-2. *Fragments from the crushed zone, the dark matrix consists of adularia. Photomicrograph with crossed polars.*

Sample: **KFM01B 417.53–417.63 m**
Rock type: Metagranite
Fracture: Closed fracture
Orientation: Not in BIPS
Deformation zone: ZFMNS0404
Fracture orientation set: n.a.
Fracture minerals: Epidote, calcite

Sequence of mineralizations:

1. Epidote
2. Calcite and chlorite

Epidote sealed fracture that later has been penetrated by calcite which has split the epidote into thin bands. Chlorite is interlayered with the calcite

Figure A-3. *Epidote and calcite filled fracture. The diameter of the drill core is approximately 5 cm.*

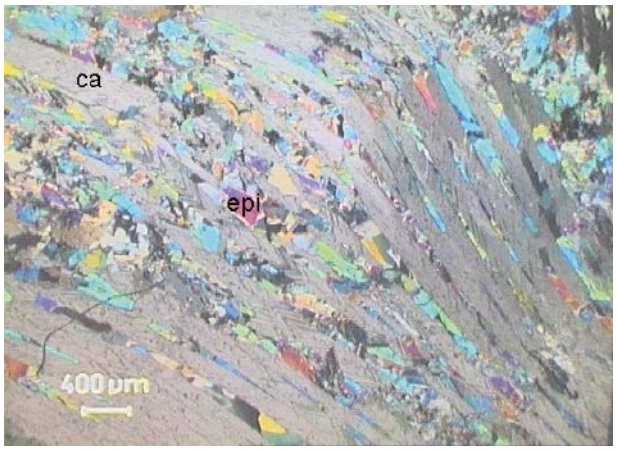

Figure A-4. *Thin bands of alternating calcite and epidote. Photomicrograph with crossed polars.*

Sample: **KFM04A 171.62–171.72 m**
Rock type: Metabasite and metagranite, highly foliated
Fracture: Closed fracture
Orientation: 324/85°
Deformation zone: ZFMNE00A2
Fracture orientation set: NW
Fracture minerals: Calcite, adularia, hematite, quartz

Sequence of mineralizations

1. Calcite, fine-grained adularia and quartz
2. Euhedral quartz crystals
3. Calcite

The highly altered wall rock is cut by a fracture sealed with extremely fine-grained adularia together with calcite, quartz, titanite plus some hematite. The titanite probably origins from the wall rock. This fracture has later been cut by a small open fracture on which surface euhedral quartz has crystallized. The open fracture has later been sealed with a younger generation of calcite with thin, well-developed twins.

Wall rock alteration: Saussuritized plagioclase and partly chloritized amphiboles.

Figure A-5. *Pale greenish mineral filling with fine-grained adularia, calcite, quartz and hematite. Penetrated by a pure calcite. The diameter of the drill core is c 5 cm.*

Figure A-6. *Fine grained adularia with calcite, quartz and hematite, later cut by a calcite sealed fracture. Photomicrograph with crosser polars.*

Sample: **KFM04A 179.70–179.85 m**
Rock type: Metagranitoid, highly foliated
Fracture: Closed fracture
Orientation: 234/72°
Deformation zone: –
Fracture orientation set: NE
Fracture minerals: Calcite, quartz, chlorite

Sequence of mineralizations:

1. Calcite
2. Euhedral quartz
3. Fe-Chlorite
4. Calcite

Small nail-like calcite crystals have grown in an open fracture. Small euhedral quartz crystals have grown on the calcite. The fracture has later been filled with a green porous Fe-chlorite (FeO~18%, MgO~15%). This mineral filling has later been fractured and new fractures have been filled with large prismatic calcite crystals. The wall rock contains chlorite and epidote, some of the quartz have recrystallized as subgrains. The plagioclase is saussuritized and the amphiboles chloritized. The wall rock also contains small grains of hematite.

Figure A-7. *Metagranite cut by a fracture with two mineral fillings, the green consist of chlorite and calcite with some quartz and the white is a second generation of calcite. The diameter of the drill core is c 5 cm.*

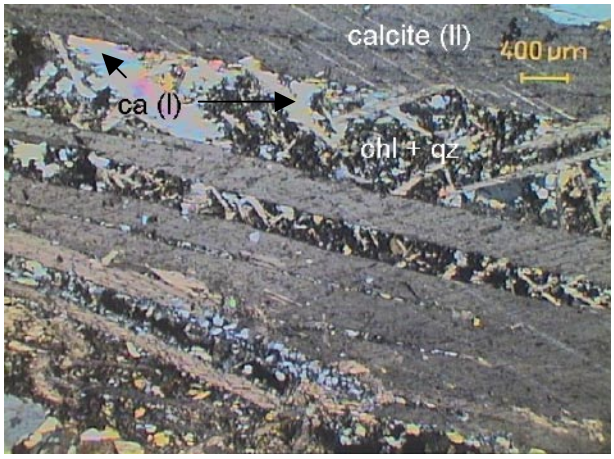

Figure A-8. *Calcite nails (I) and quartz in matrix of Fe-chlorite later cut by a second generation of larger calcite grains (II). Photomicrograph with crossed polars.*

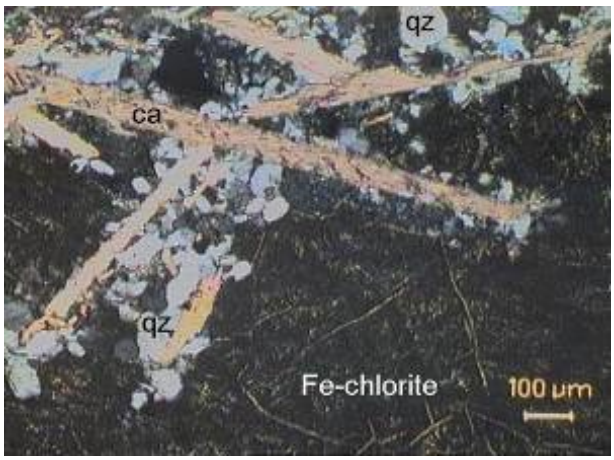

Figure A-9. *Small euhedral quartz grains have grown on the calcite nails. Later the Fe-chlorite has filled the void. Photomicrograph with crossed polars.*

Sample: **KFM04A 197.95–198.10 m**
Rock type: Highly hydrothermal altered tonalite and pegmatite
Fracture: Two closed fractures
Orientation: 269/46°
Deformation zone: –
Fracture orientation set: NW
Fracture minerals: K-feldspar, albite, epidote, quartz, feldspar, calcite, hematite

Sequence of mineralizations:

1. Cataclasite with fragments of K-feldspar, albite and quartz sealed by epidote and with micro-grains of hematite.
2. Younger fracture filled with pure epidote and euhedral epidote crystals
3. Quartz
4. Calcite

The pegmatite in the sample has faulted along an epidote cataclasite. The tonalite is red-coloured near the fracture. The epidote cataclasite is cut by a younger fracture with larger epidote crystals. The larger epidote crystals have later been deformed. In connection to this later fracture filling, euhedral epidote crystals have crystallized in voids in small new fractures or along the margins of the cataclasite. The voids in which the epidote grew have later been filled with quartz that shows no signs of deformation. Some of the quartz crystals are euhedral. The last stage is a calcite that has penetrated both the cataclasite and the epidote sealed fracture.

Wall rock alteration: The plagioclase has been highly saussuritized and epidote exists abundantly in the wall rock.

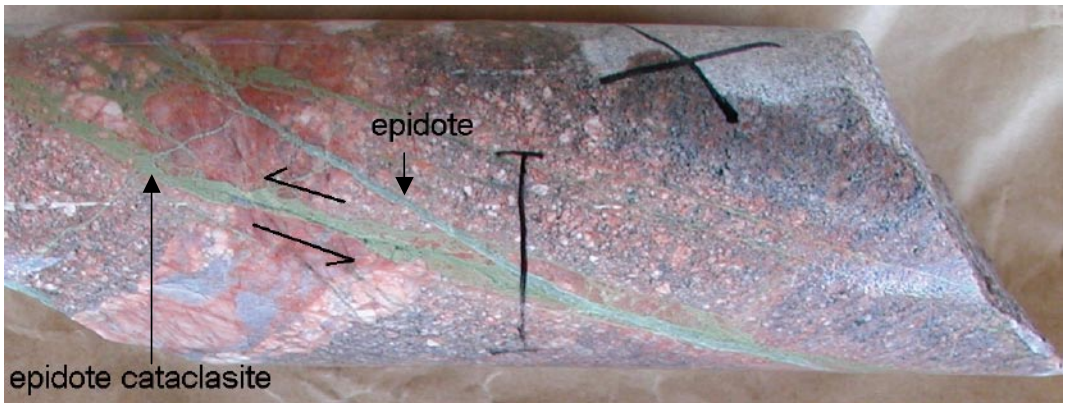

Figure A-10. *Red-coloured tonalite and pegmatite cut by epidote-quartz-feldspar cataclasite that later has been cut by a younger fracture filled with pure epidote. Observe the faulting along the cataclasite. The diameter of the drill core is c 5 cm.*

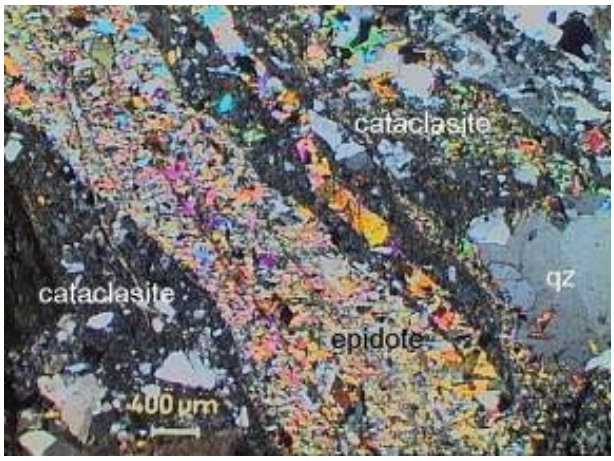

Figure A-11. *Cataclasite with fragments of K-feldspar, albite and quartz sealed by epidote, cut by a fracture filled with pure epidote. Photomicrograph with crossed polars.*

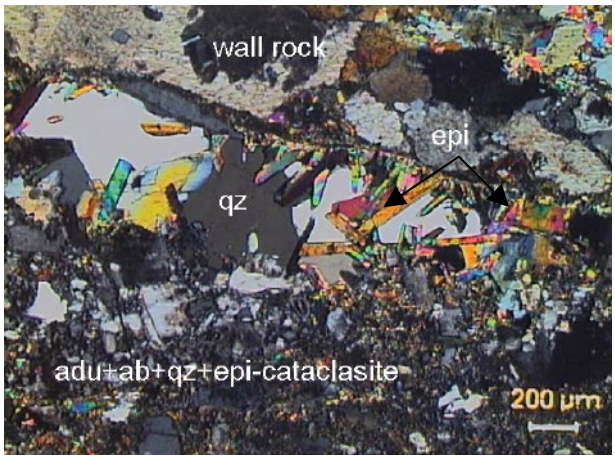

Figure A-12. *Euhedral epidote crystals have grown in a void between the wall rock and the cataclasite. The void has later been filled with quartz. Photomicrograph with crossed polars.*

Sample: **KFM04A 212.77–212.79 m**
Rock type: Mylonite
Fracture: Sealed fracture parallel to two open fractures
Orientation: 148/83°
Deformation zone: ZFMNE00A2
Fracture orientation set: NW
Fracture minerals: Mg-chlorite, K-feldspar, quartz, epidote, apatite, calcite, yttrium calcium silicate

Sequence of mineralization:

1. Mylonite (Mg-chlorite, K-feldspar, quartz, epidote, hematite, apatite).
2. Cut by fine-grained mix of adularia and quartz with some fragments of epidote and calcite and small crystals of an yttrium calcium silicate.
3. Euhedral quartz
4. Calcite

Extremely fine grained fracture filling, c1.5 cm between two parallel open fractures covered with black chlorite and clay minerals. The wall rock is a mylonite that consists of chlorite, K-feldspar, quartz, epidote, hematite and apatite. The chlorite in the mylonite is Mg-rich, although in some of the chlorites, bands of Fe-rich chlorite are interlayered. An extremely fine-grained mixture of quartz and adularia with some larger grains of calcite and epidote cuts the mylonite. In this matrix, small crystals of an unknown mineral (yttrium-calcium silicate) have crystallized. (SiO_2~36%, Ca~18%, Y_2O_3~30%). In voids in this matrix euhedral crystals of quartz have grown. The voids have later been filled with calcite.

Figure A-13. *Grey extremely fine-grained filling. The diameter of the drill core is c 5 cm.*

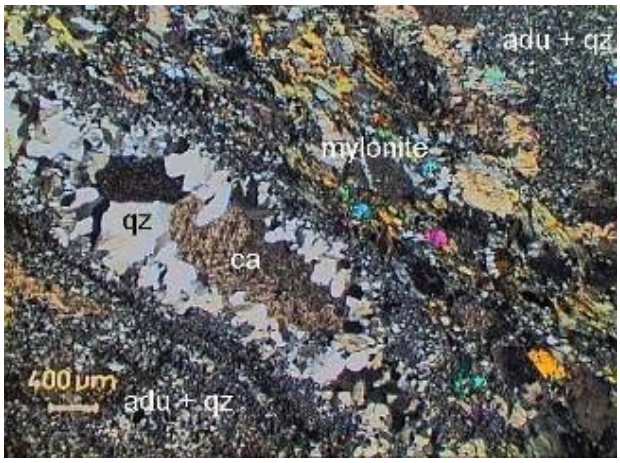

Figure A-14. *Mylonite parallel to fine-grained matrix of adularia and quartz. Euhedral quartz crystals have crystallized in a void in the matrix. The void has later been filled with calcite. Photomicrograph with crossed polars.*

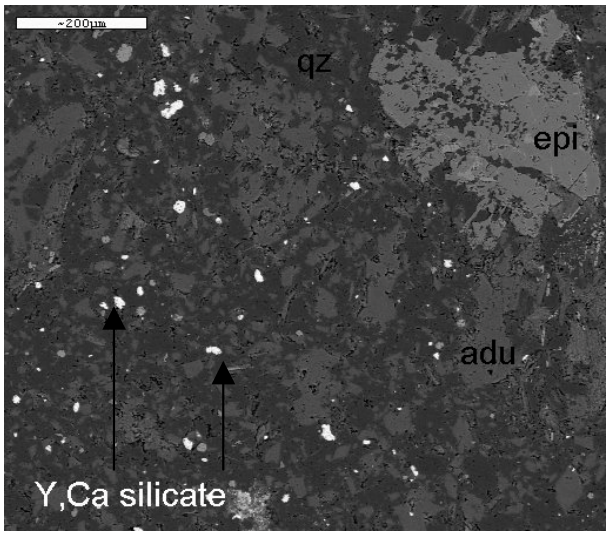

Figure A-15. *Close-up of the fine-grained matrix. It consists of adularia, quartz, fragments of epidote and an yttrium-calcium silicate. Back-scattered electron image.*

Sample: **KFM04A 226.20–226.40 m**
Rock type: Metagranite
Fracture: Sealed fracture parallel to foliation, cut by sealed fracture
Orientation: 298/42°
Deformation zone: –
Fracture orientation set: NW
Fracture minerals: Epidote, albite, chlorite, quartz, adularia, laumontite, calcite, hematite.

Sequence of mineralization:

1. Cataclasite with quartz, adularia, albite, epidote and Fe-chlorite.
2. Laumontite and Fe-chlorite
3. Euhedral quartz
4. Calcite

A thin green epidote bearing cataclasite cuts the rock parallel to the foliation. The wall rock is red-coloured c 0.5 cm on each side of the fracture. The cataclasite consists of small, often angular grains of quartz, adularia, albite (An_{09}), epidote and Fe-chlorite (FeO~25%, MgO~12%). The cataclasite is cut by a fracture sealed with laumontite and chlorite. At a later phase, small euhedral quartz crystals have grown in the fracture that then has been sealed again with calcite.

Wall rock alteration: The wall rock is highly red-coloured around the epidote bearing fracture but not around the laumontite sealed fracture. The alteration consists of saussuritized plagioclase, sericitized K-feldspar and crystallization of subgrains of quartz. The wall rock also contains epidote.

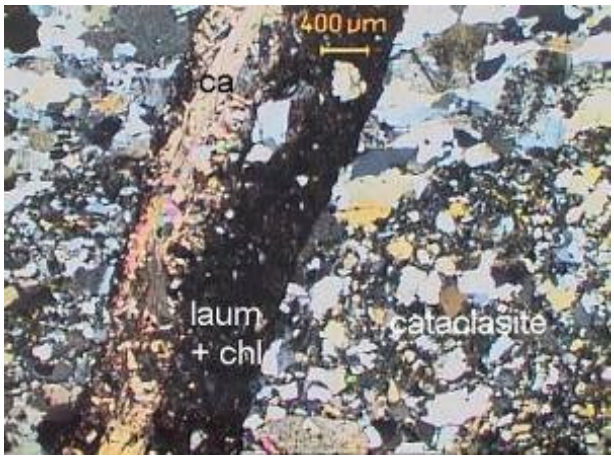

Figure A-16. *Cataclasite cut by sealed fracture with laumontite, chlorite and calcite. Photomicrograph with crossed polars.*

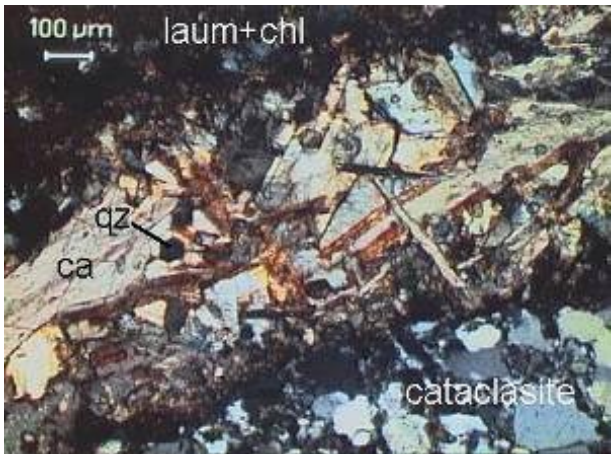

Figure A-17. *Laumontite, chlorite and calcite filling with some euhedral quartz crystals. Micro-grains of hematite give the calcite and the laumontite a brown-red colour. Photomicrograph with crossed polars.*

Sample: **KFM04A 226.98–227.10 m**
Rock type: Contact between metabasite and metagranite
Fracture: Breccia and closed fracture
Orientation: Not in BIPS
Deformation zone: –
Fracture orientation set: –
Fracture minerals: Epidote, quartz, chlorite, laumontite, hematite

Sequence of mineralizations:

1. Mylonite with epidote, quartz and chlorite
2. Breccia sealed with laumontite and hematite

A c 0.3 cm thick mylonite that consists of mainly epidote, quartz and chlorite parallel to the foliation of the wall rock is cut by a breccia with large fragments of the wall rock and fragmented quartz grains. The breccia is sealed with laumontite and hematite.

Wall rock alteration: The plagioclase is highly saussuritized and red stained of hematite.

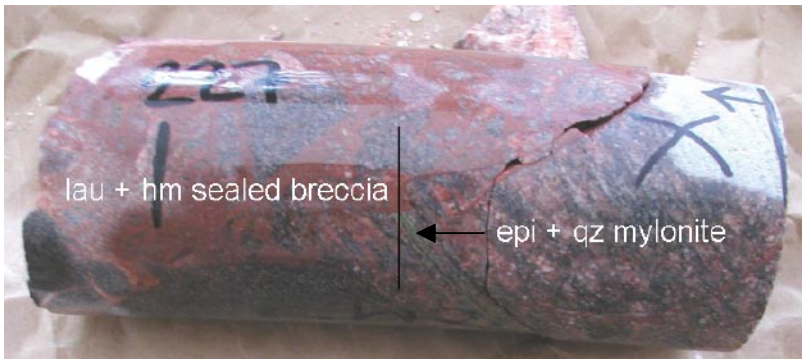

Figure A-18. *Epidote-quartz mylonite with chlorite cut by a laumontite and hematite sealed breccia. The diameter of the drill core is c 5 cm.*

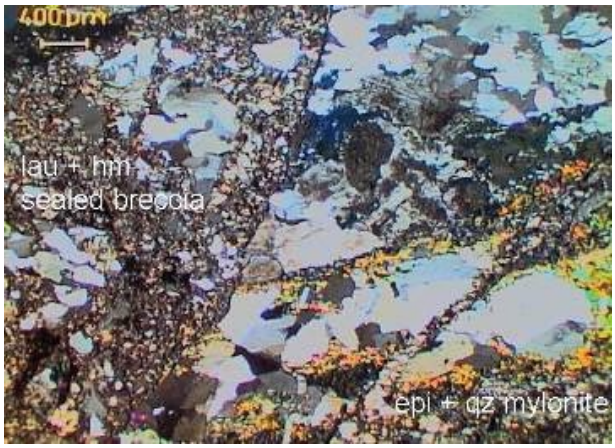

Figure A-19. *Epidote-quartz mylonite with chlorite cut by laumontite and hematite sealed breccia. Photomicrograph with crossed polars.*

Sample: **KFM04A 244.46–244.58 m**
Rock type: Contact between metabasite and metagranite
Fracture: Breccia and closed fracture
Orientation: 222/80° (qz, ab, adu, hm)
Deformation zone: –
Fracture orientation set: NE
Fracture minerals: Laumontite, hematite, chlorite, quartz, calcite, adularia, albite.

Sequence of mineralization:

1. Laumontite, hematite, quartz
2. Calcite, hematite, adularia, albite

The breccia contains fragments of the wall rock that has been chloritized and partly rounded. The breccia is sealed with laumontite and hematite. The quartz from the wall rock in the breccia has been exposed to subgrain formation. The breccia is closely related to a brick-red, smaller fracture filled with adularia, albite, quartz, hematite and calcite.

Figure A-20. *Laumontite sealed breccia and smaller fracture filled with adularia, quartz, albite, hematite and calcite. The diameter of the drill core is c 5 cm.*

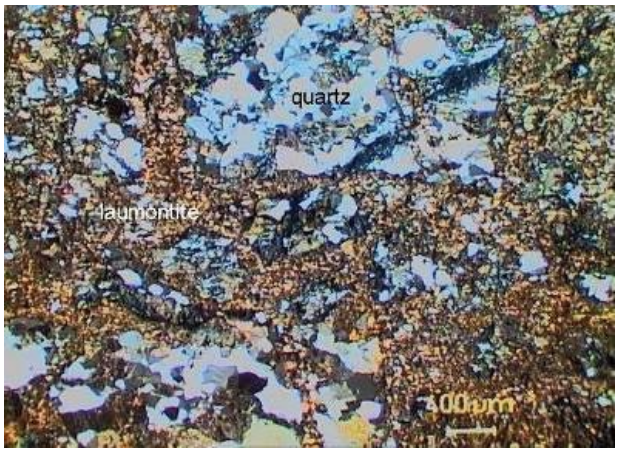

Figure A-21. *Breccia with fragments of the wall rock, here mainly quartz, sealed with laumontite. Photomicrograph with crossed polars.*

Sample: **KFM04A 247.00–247.07 m**
Rock type: Metagranite
Fracture: Breccia and closed fracture
Orientation: 037/78° (calcite)
Deformation zone: –
Fracture orientation set: NE
Fracture minerals: Laumontite, hematite, adularia, quartz, calcite

Sequence of mineralizations:

1. Laumontite and hematite sealed breccia
2. Adularia, quartz, chlorite, hematite
3. Calcite

The breccia is sealed with laumontite and hematite. The breccia is cut by a fracture filled with adularia, quartz, Fe-chlorite (FeO~14%, MgO~9%) and hematite. Both these structures are cut by an extremely deformed and twinned calcite.

Wall rock alteration: The plagioclase is saussuritized, the K-feldspar sericitized and contains epidote and chlorite.

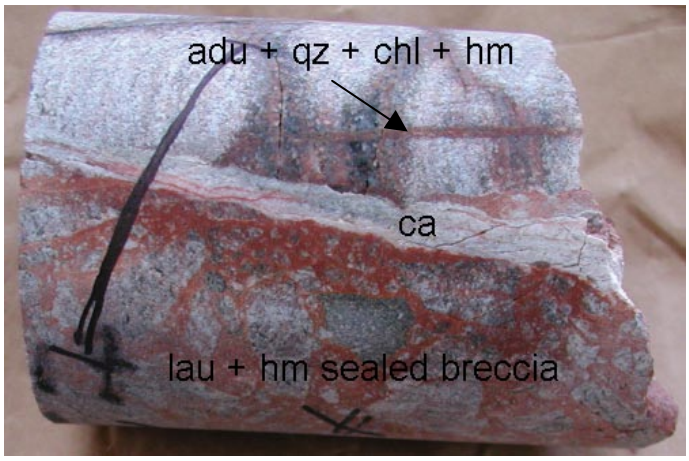

Figure A-22. *Laumontite and hematite sealed breccia cut by small fracture filled with adularia, quartz, chlorite and hematite. Cutting these structures is a later calcite. The diameter of the drill core is c 5 cm.*

Sample: **KFM04A 263.25–263.50 m**
Rock type: Metagranite
Fracture: Open fracture
Orientation: 221/81°
Deformation zone: –
Fracture orientation set: NE
Fracture minerals: Quartz, analcime, Fe-chlorite/corrensite

Sequence of mineralizations:

1. Euhedral quartz
2. Analcime
3. Chlorite/corrensite

The surface is covered with a coating of small euhedral quartz crystals on which euhedral analcime has crystallized. Between the analcime crystals and on the quartz coating, spherical aggregates of chlorite/corrensite have crystallized. The FeO content in the chlorite/corrensite is c 16%. However, the absence of plane surfaces makes the analyses imprecise.

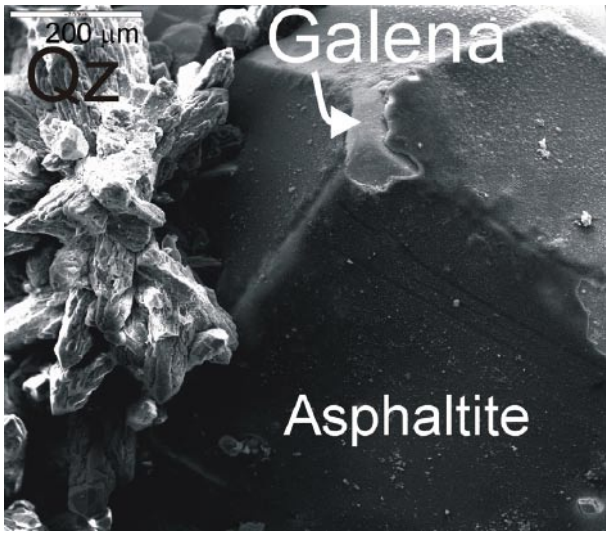

Figure A-23. *Corrensite and analcime crystallized on a quartz coating. The base of the picture is c 1 cm. Photo from stereomicroscope.*

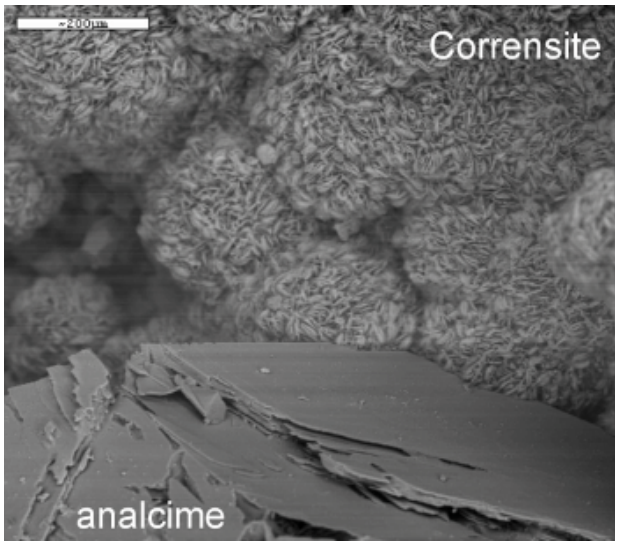

Figure A-24. *Analcime crystal surrounded by spherical aggregates of corrensite. Electron image.*

Sample: **KFM04A 294.50–294.65 m**
Rock type: Metagranite
Fracture: Open and sealed fractures
Orientation: Fracture network
Deformation zone: –
Fracture orientation set: –
Fracture minerals: Quartz, calcite

Sequence of mineralizations:

1. Quartz
2. Calcite

The rock is very fine-grained and is cut by numerous sealed, open and partly open fractures. The fractures are coated with a rim of small euhedral quartz crystals. The quartz has many small inclusions. The fractures have later been partly or completely filled with calcite, which shows thin straight twins.

Wall rock alteration: The plagioclase is saussuritized and the biotite is chloritized. Some of the microcline has also been altered, but to a much lesser degree.

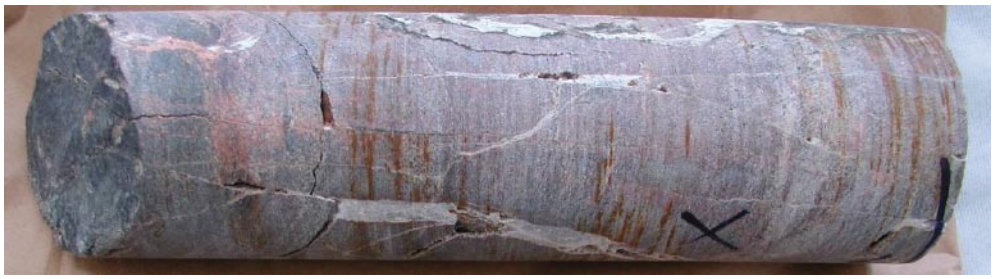

Figure A-25. *Network of quart and calcite filled fractures. The diameter of the drill core is c 5 cm.*

Sample: **KFM04A 296.50–296.65 m**
Rock type: Metagranite
Fracture: Open fracture
Orientation: 232/78°
Deformation zone: –
Fracture orientation set: NE
Fracture minerals: Laumontite, calcite, quartz, pyrite, Fe-chlorite

Sequence of mineralizations:

1. Laumontite
2. Euhedral quartz
3. Calcite
4. Fe-chlorite/corrensite + pyrite

Laumontite has filled the fracture, which later has been reactivated and covered with a coating of small euhedral quartz crystals. Later than this coating is a generation of calcite, pyrite and spherical aggregates of chlorite/corrensite.

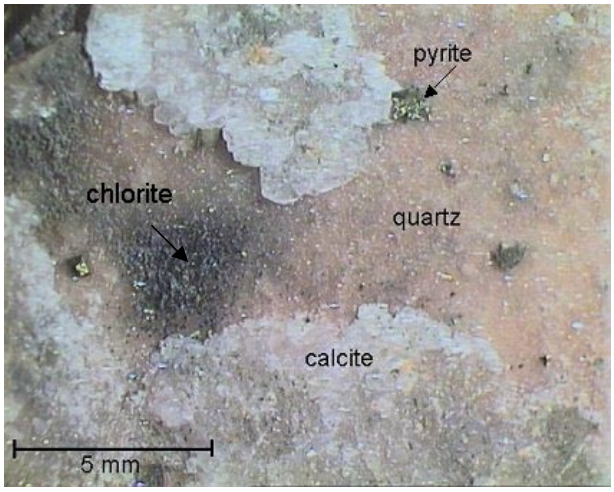

Figure A-26*. Calcite, pyrite and chlorite/corrensite on a quartz coating. The laumontite can be seen through the quartz coating. Photo from stereomicroscope.*

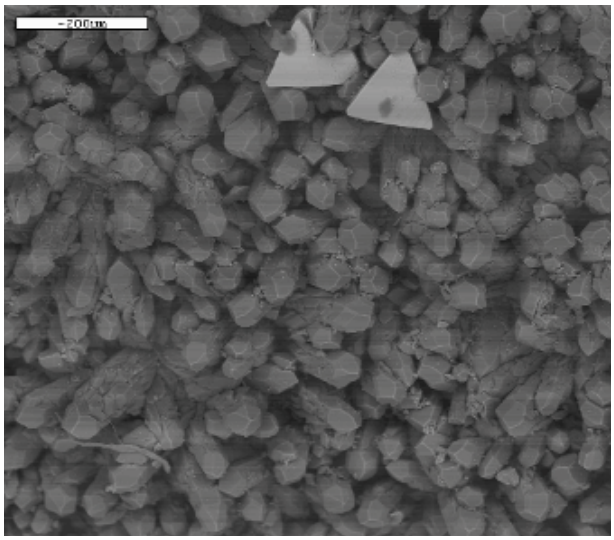

Figure A-27. *Coating with euhedral quartz crystals on which pyrite has crystallized (white crystals). Back-scattered electron image.*

Sample: **KFM04A 306.40–306.55 m**
Rock type: Contact between pegmatite and metabasite
Fracture: Partly open fracture
Orientation: 011/79°
Deformation zone: –
Fracture orientation set: NE
Minerals: Laumontite, quartz, pyrite, calcite

Sequence of mineralizations:

1. Laumontite
2. Calcite
3. Euhedral quartz crystals
4. Pyrite and euhedral calcite

The fracture surface is coated with laumontite on which euhedral quartz has crystallized. Euhedral pyrite and both euhedral and massive calcite have crystallized on the quartz coating. The calcite shows thin straight twins.

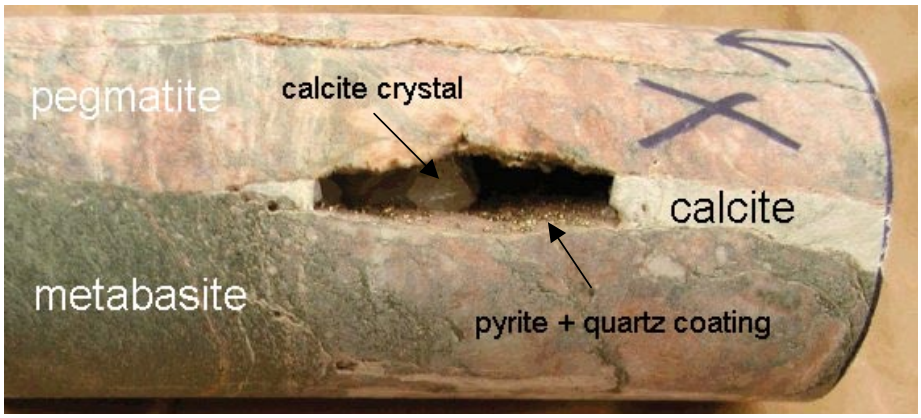

Figure A-28. *Large calcite crystal and massive calcite filling together with pyrite on a surface coated with euhedral quartz. Laumontite occurs as a thin coating between the calcite and the wall rock. The diameter of the drill core is c 5 cm.*

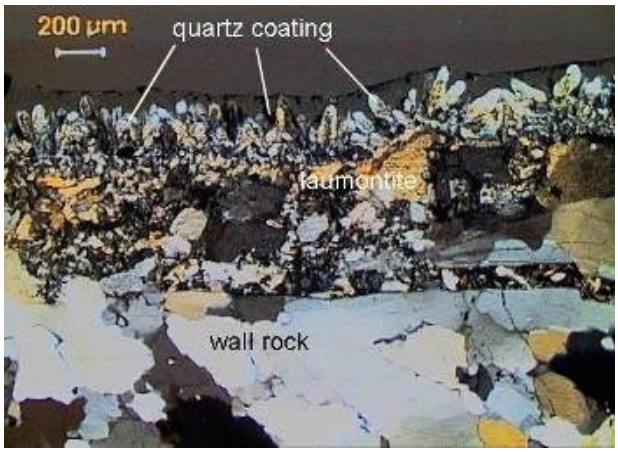

Figure A-29. *Coating of euhedral quartz crystals that have crystallized on laumontite. Photomicrograph with crossed polars.*

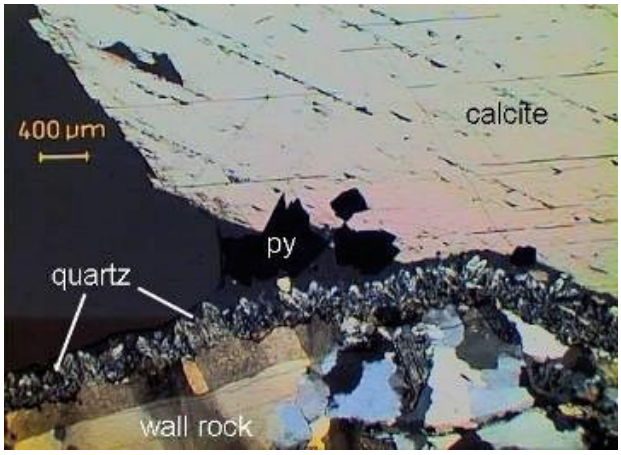

Figure A-30. *A large euhedral calcite crystal with pyrite on a coating of euhedral quartz crystals. Photomicrograph with crossed polars.*

Sample: **KFM04A 347.32–347.50 m**
Rock type: Metagranite
Fracture: Breccia and closed fracture
Orientation: 230/74° (calcite)
Deformation zone: –
Fracture orientation set: NE
Fracture minerals: Laumontite, calcite, hematite

Sequence of mineralizations:

1. Breccia sealed with calcite, laumontite and hematite
2. Laumontite
3. Calcite

The breccia contains fragments of highly altered wall rock and fragments of the laumontite sealed breccia itself. The breccia is sealed with extremely deformed calcite, laumontite and hematite. The boundary between the breccia and the wall rock consists of a fracture filled with laumontite, which later has been reactivated and filled with calcite.

Wall rock alteration: The plagioclase has been saussuritized and partly albitized.

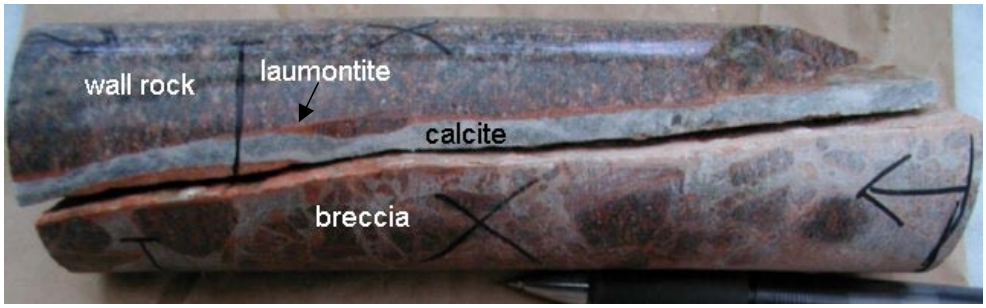

Figure A-31. *Calcite, laumontite and hematite sealed breccia cut by laumontite and calcite filled fracture. The diameter of the drill core is c 5 cm.*

Figure A-32. *Breccia sealed with extremely deformed calcite. Photomicrograph with crossed polars.*

Sample: **KFM04A 414.10–414.12 m**
Rock type: Hydrothermal altered zone
Fracture: Open fracture
Orientation: 237/69°
Deformation zone: ZFMNE1188
Fracture orientation set: NE
Fracture minerals: Laumontite, hematite, quartz, calcite, analcime, albite, adularia, epidote

Sequence of mineralizations:

1. Laumontite, calcite, hematite and aggregates of fine-grained adularia and quartz with some fragments of epidote.
2. Euhedral quartz
3. Analcime
4. Calcite

The sample is highly hydrothermally altered and consists of laumontite, hematite and greenish aggregates of fine-grained adularia and quartz with some fragments of epidote. Around these mineral assemblages, a coating of euhedral quartz crystals has precipitated. On this coating euhedral analcime has crystallized followed by euhedral calcite.

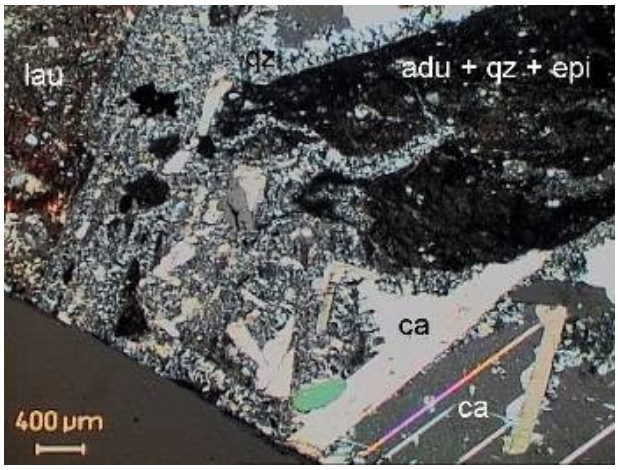

Figure A-33. *Laumontite, calcite and aggregates of fine-grained adularia quartz and epidote. Later, small euhedral quartz crystals have crystallized on the calcite. Photomicrograph with crossed polars.*

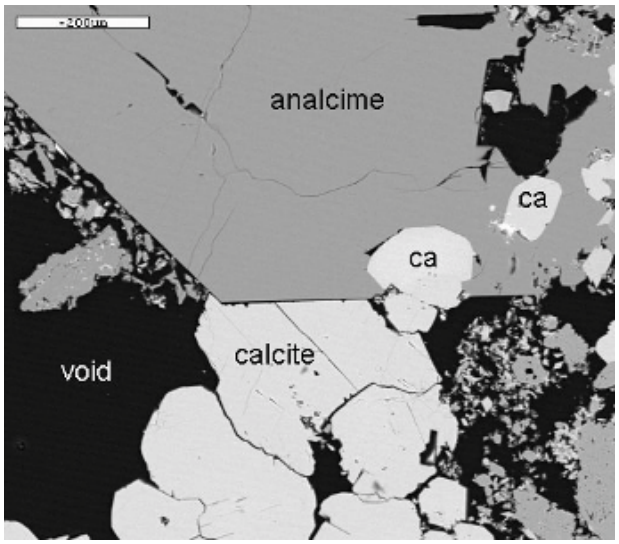

Figure A-34. *Euhedral analcime crystal on which smaller calcite crystals have crystallized. Back-scattered electron image.*

Sample: **KFM04A 415.30–415.35 m**
Rock type: Metatonalite
Fracture: Open fracture
Orientation: 230/76°
Deformation zone: ZFMNE1188
Fracture orientation set: NE
Fracture minerals: Laumontite, quartz, analcime, pyrite, calcite.

Sequence of mineralizations:

1. Laumontite
2. Euhedral quartz
3. Analcime
4. Pyrite
5. Calcite

Laumontite sealed fracture cut by an open fracture covered with a coating of small euhedral quartz crystals. Fibrous crystals of analcime have crystallized on this surface followed by pyrite and calcite.

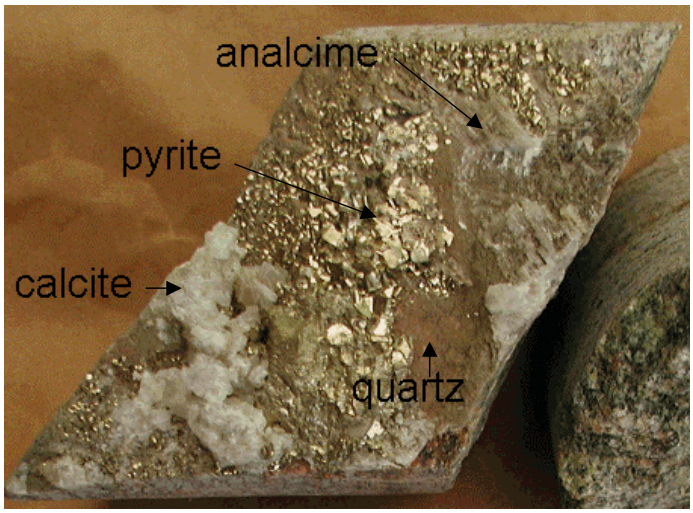

Figure A-35. *Quartz coating covered with analcime, calcite and pyrite. The diameter of the drill core is c 5 cm.*

Sample: **KFM05A 105.41–105.46 m**
Rock type: Metagranite
Fracture: Open fracture
Orientation: Not in BIPS
Deformation zone: ZFMNE00A2
Fracture orientation set: n.a.
Fracture minerals: Calcite, quartz, adularia, asphaltite

Sequence of mineralizations:

1. Quartz + adularia
2. Calcite + asphaltite

The thick mineral coating consists of a fine grained mass with small crystals of quartz and adularia. Some of the adularia crystals are euhedral. The asphaltite appears as small brownish irregular bodies spread evenly between the quartz crystals. Closest to the wall rock can small amounts of calcite can be found that has penetrated between the wall rock and the other fracture minerals. Small grains of pyrite are also found in voids in the quartz and adularia coating. The fracture coating appears to have been partly dissolved which has led to a high porosity.

Figure A-36. *Drill core covered with quartz, adularia and asphaltite (black). The diameter of the drill core is c 5 cm.*

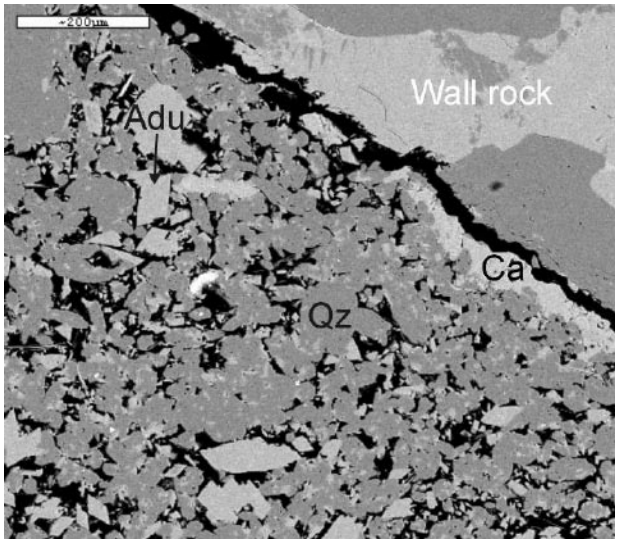

Figure A-37. *Subhedral quartz grains and euhedral adularia. Observe the high porosity. Between the wall rock and the fracture filling calcite has precipitated. Back-scattered electron image.*

Sample: **KFM05A 109.75–109.90 m**
Rock type: Metagranite
Fracture: Open fracture
Orientation: 324/14°
Deformation zone: ZFMNE00A2
Fracture orientation set: HZ
Fracture minerals: Quartz, calcite, pyrite, asphaltite, corrensite

Sequence of mineralizations:

1. Quartz + calcite + pyrite
2. Corrensite + chlorite + asphaltite

The fracture is covered with a sediment-like grey layer together with black hydrocarbons (asphaltite).The sediment-like fracture fillings consist of quartz and adularia together with some calcite and asphaltite. The quartz makes up the largest part of the fracture filling and occurs as a fine-grained matrix. Into voids, the quartz has grown as subhedral to euhedral crystals and has the same shapes and inclusions as the commonly occurring euhedral quartz generation found as coatings along many fractures. The adularia occurs as small euhedral monoclinic crystals in the quartz matrix. The asphaltite is found inside the matrix and seems to have penetrated the porous fracture filling.

Wall rock alteration: The wall rock is relatively unaltered with intact K-feldspar and many unaltered biotites. The plagioclase shows only moderate saussuritization. The quartz shows intense subgrain formation.

Figure A-38. *(Upper left). Drill core with black asphaltite on grey quartz coated surface. The diameter of the drill core is c 5 cm.*

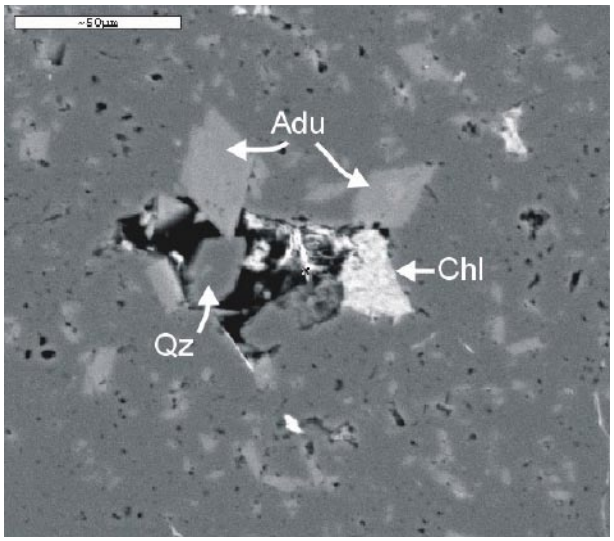

Figure A-39. *(Upper right). Small void with euhedral quartz and adularia crystals and later chlorite. The surrounding matrix consists of quartz (dark grey) and adularia (light grey). Back-scattered electron image.*

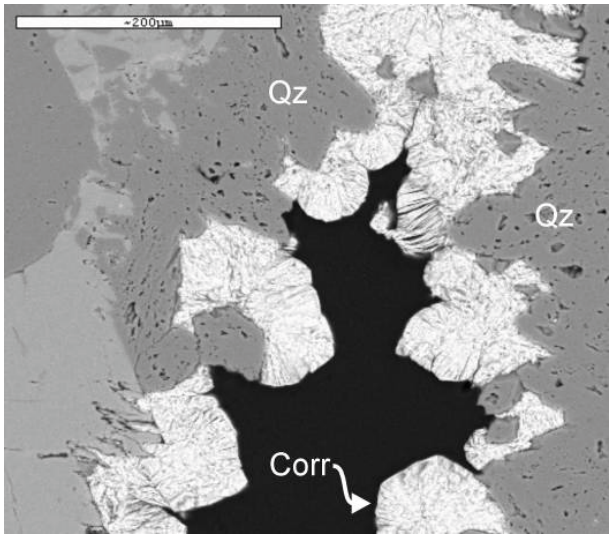

Figure A-40. *(Left). Open fracture with euhedral quartz crystals on which corrensite has crystallized. Back-scattered electron image.*

Sample: **KFM05A 111.56–111.60 m**
Rock type: Metagranite
Fracture: Open fracture
Orientation: 317/08°
Deformation zone: –
Fracture orientation set: HZ
Fracture minerals: Quartz, adularia, asphaltite, illite

Macroscopic description: The fracture is coated with a sediment-like layer of small grains together with black asphaltite.

The fracture filling material in KFM05A 111.56–111.60 m consists of wall rock fragments with additional illite and asphaltite. The minerals are more fine-grained along the margins of the fragments. The illite is incorporated in the wall rock fragments and may have crystallized before the fracturing, although, more likely it is a product of post-fracturing alteration of feldspars. Asphaltite occurs both as separate grains and in larger grains together with other minerals.

Figure A-41. *Drill core with gauge material. The diameter of the drill core is c 5 cm.*

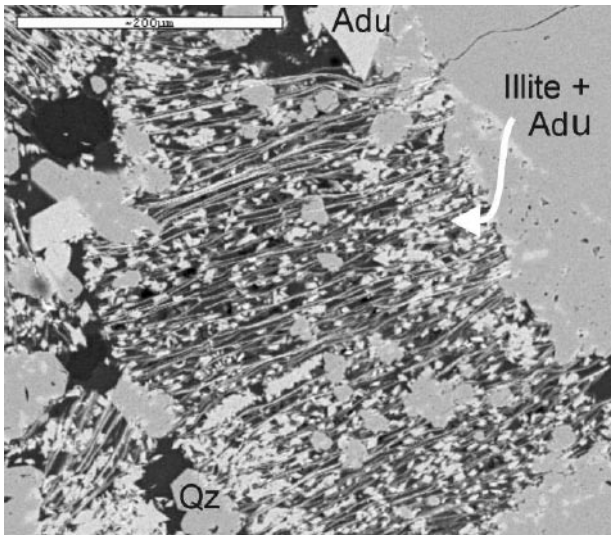

Figure A-42. *Illite with small euhedral adularia crystals between the thin layers. Some larger euhedral quartz and adularia crystals can also be seen around and inside the illite. Back-scattered electron image.*

Sample: **KFM05A 146.40–146.57 m**
Rock type: Metagranite
Fracture: Open fracture
Orientation: 045/65°
Deformation zone: –
Fracture orientation set: NE
Fracture minerals: Quartz, corrensite, calcite, pyrite

Sequence of mineralizations:

1. Quartz
2. Corrensite
3. Pyrite + calcite

The fracture is coated with a thin layer of small euhedral quartz crystals. Spread over this surface small clusters of spherical aggregates of corrensite occur. Small euhedral crystals of calcite and pyrite have crystallized on the corrensite. Many of the calcites have scalenohedral crystals.

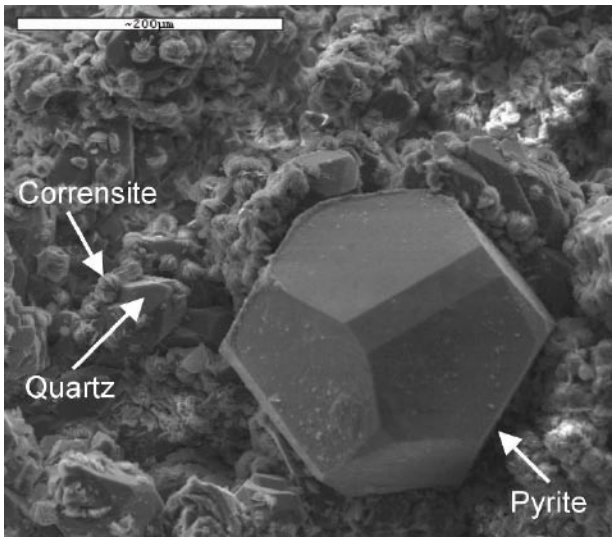

Figure A-43. *Euhedral quartz coating overgrown by corrensite and later euhedral pyrite. Electron image.*

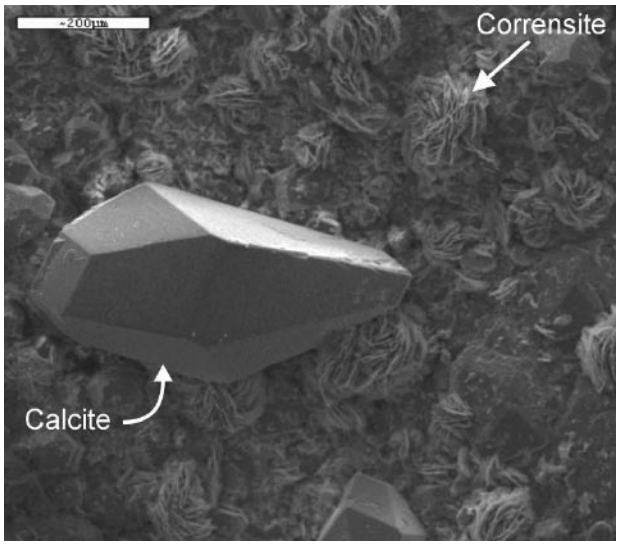

Figure A-44. *Corrensite crystals on which scalenohedral calcite has crystallized. Electron image.*

Sample: **KFM05A 232.95–233.07 m**
Rock type: Metagranite
Fracture: Open fracture
Orientation: 227/80°
Deformation zone: –
Fracture orientation set: NE
Fracture minerals: Adularia, hematite, laumontite, calcite, corrensite.

Sequence of mineralizations:

1. Adularia + quartz + hematite
2. Laumontite
3. Calcite
4. Corrensite

Macroscopic description:

Open fracture with thin (c 1 mm) laumontite coating with a red colour. The laumontite is covered with a green-black clay mineral.

Hematite stained laumontite cuts a thin vein of adularia and quartz with micro-grains of hematite. On the laumontite surface, small calcite crystals have grown. Some of the crystals show thin straight twins. Corrensite has later grown into the laumontite and calcite, often along the crystal planes. Microveins filled with adularia cut the corrensite in a few places in the thin section.

Wall rock alteration:

Close to the fracture (< 1 cm), the plagioclase is highly saussuritized and the biotite is completely chloritized. The K-feldspar is mostly unaltered. Further away from the fracture, the wall rock is relatively unaltered with only a few saussuritized plagioclases. The biotite is unaltered and crystals of titanite and euhedral epidote are present.

Figure A-45. *Drill core with red laumontite and green-black corrensite seen on the surface. The diameter of the drill core is c 5 cm.*

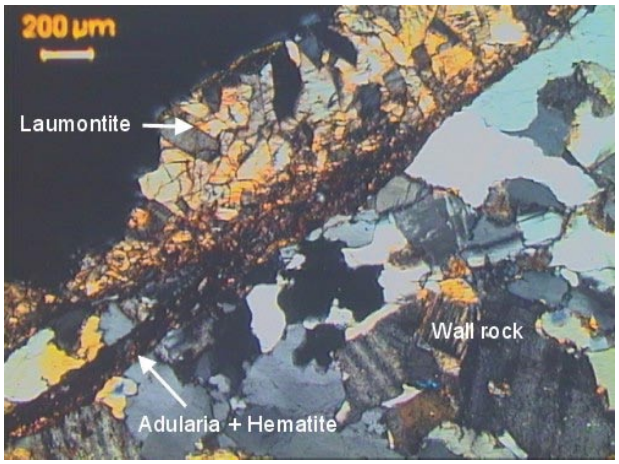

Figure A-46. *Hematite stained laumontite cutting a thin vein filled with adularia and hematite and some quartz. Photomicrograph with crossed polars.*

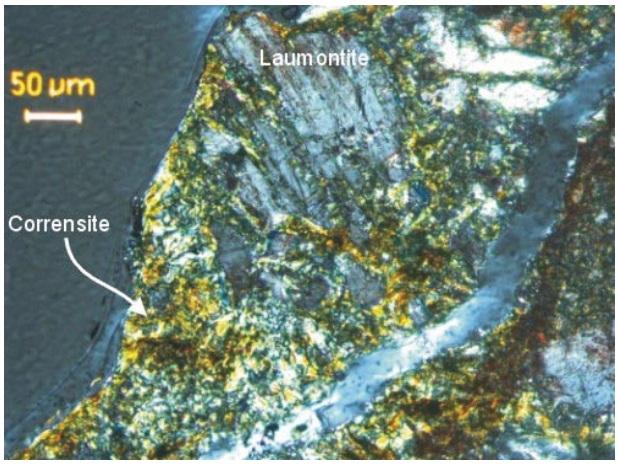

Figure A-47. *Corrensite penetrating older laumontite crystal. Photomicrograph with crossed polars.*

Sample: **KFM05A 395.75–395.85 m**
Rock type: Metagranite
Fracture: Sealed fracture
Orientation: 057/68°
Deformation zone: –
Fracture orientation set: NE
Fracture minerals: Prehnite, adularia, hematite, calcite, corrensite

Sequence of mineralizations:

1. Prehnite
2. Calcite
3. Adularia + hematite
4. Calcite
5. Corrensite

Macroscopic description:

The drill core is cut by a c 3 cm wide sealed fracture. The filling is a mixture of red, white and pale greenish minerals.

Large fan-like prehnite crystals are cut and broken into fragments by calcite. The calcite has a heavily deformed and curved twin structure. The calcite is broken by adularia that is red-stained by micro-grains of hematite. In some parts of the thin section, the adularia has euhedral crystals. A later generation of calcite cuts both the older calcite and the adularia. All these minerals are probably closely related in time. Corrensite has later grown along micro fractures that cut the older minerals.

The MgO and FeO contents in the corrensite differ highly over small distances. MgO contents between 7 and 21% and FeO between 8 and 28% have been found in adjacent parts of the mineral. Some parts of the corrensite contain up to 10% Ce_2O_3.

Wall rock alteration:

The plagioclase has been somewhat saussuritized and the biotite totally chloritized. The microcline is unaltered. Small epidote crystals are found in the wall rock, often inside or adjacent to the altered plagioclase.

Figure A-48. *Greenish prehnite together with white calcite and red hematite stained adularia. The diameter of the drill core is c 5 cm.*

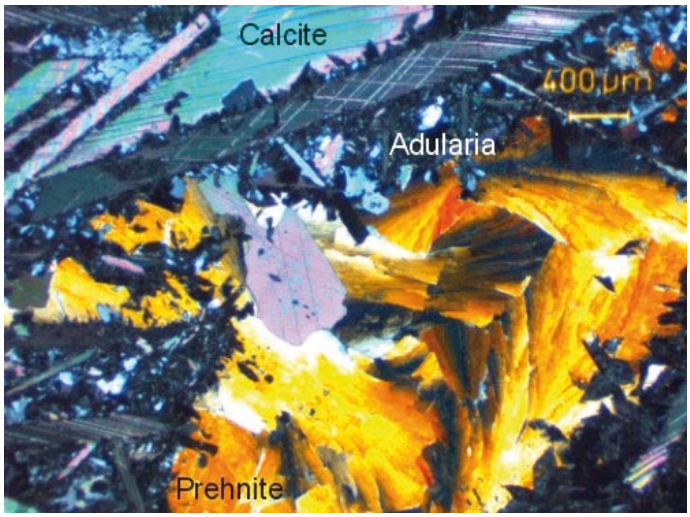

Figure A-49. *Fan-like prehnite crystals together with prismatic calcite crystals on which small adularia crystals have grown. Photomicrograph with crossed polars.*

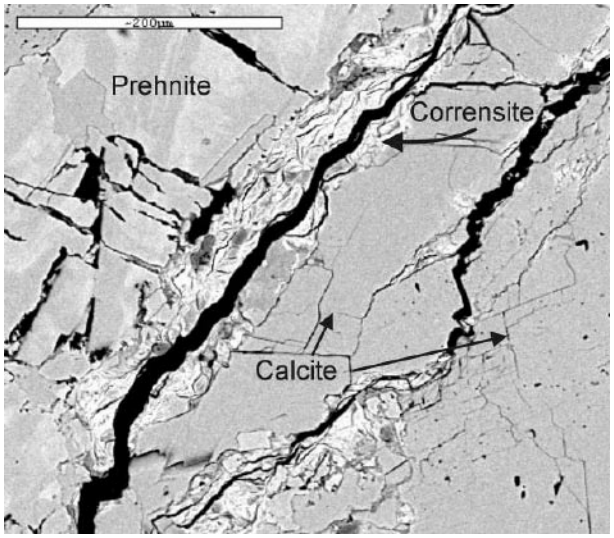

Figure A-50. *Prehnite and calcite penetrated by corrensite. Back-scattered electron image.*

Sample: **KFM05A 428.00–428.13 m**
Rock type: Metagranite
Fracture: Two open fractures
Orientation: 228/89°
Deformation zone: ZFMNE0401
Fracture orientation set: NE
Fracture minerals: Epidote, quartz, adularia, calcite, corrensite

Sequence of mineralizations:

1. Quartz cataclasite + epidote + adularia
2. Calcite
3. Euhedral quartz
4. Calcite
5. Corrensite

The drill core is penetrated by a cataclasite with mainly quartz fragments. Parts of the cataclasite consist of small veins filled with epidote crystals. The epidote crystals are euhedral and some have a well developed zoning. The quartz in the wall rock has been exposed to subgrain formation and some of the subgrains have recrystallized into crystals with euhedral surfaces into an open fracture. The fracture has then been filled with calcite. On these quartz and calcite crystals, small euhedral quartz crystals have grown. These crystals contain more fluid inclusions than the older quartz crystals. A younger generation of calcite with thin straight twins has later filled the fracture. The MnO content in the calcite is below detection limit. Parts of the calcite have been partly dissolved. The fracture then appears to have been reactivated and the smaller quartz crystals have been unattached from the wall rock. Corrensite has penetrated in the space between the wall rock and the quartz. Some of the voids in the partly dissolved calcite have also been filled with corrensite. The corrensite contains between 17 and 21% MgO and around 18% FeO (one analyse gave a FeO content of only 11%).

Wall rock alteration:

The plagioclase has only been partly saussuritized and the biotite has been chloritized. The K-feldspar is unaltered.

Figure A-51. *Two fractures filled with mainly calcite and corrensite. The diameter of the drill core is c 5 cm.*

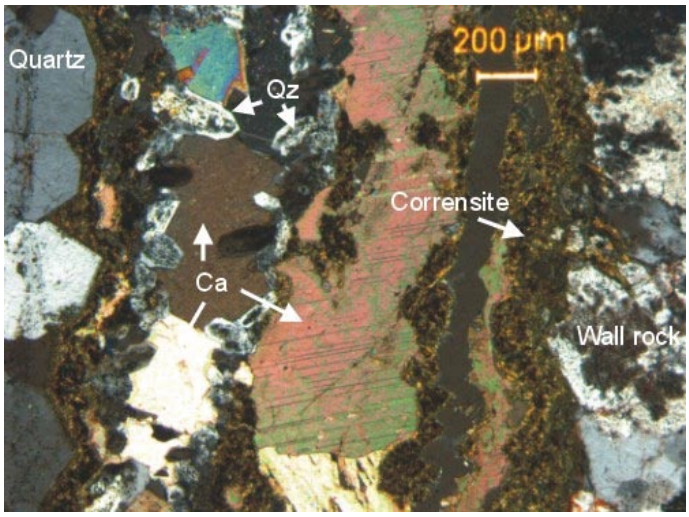

Figure A-52. *A first generation of calcite, the one which is partly dissolved and has visible twins to the right in the figure, on which euhedral quartz crystals have grown. A second generation of calcite has later filled the space between the quartz crystals. This generation has no visible twins. The latest event is the crystallization of corrensite along the open veins in the fracture. Photomicrograph with crossed polars.*

Sample: **KFM05A 689.33–689.61 m**
Rock type: Metatonalite
Fracture: Two sealed fractures
Orientation: 020/84° cut by 323/79°
Deformation zone: –
Fracture orientation set: NE cut by NW
Fracture minerals: Adularia, hematite, prehnite

Sequence of mineralizations:

1. Adularia + hematite + prehnite
2. Prehnite

The brick-red sealed fracture is filled with adularia and hematite together with small amounts of prehnite. The adularia is an almost pure K-feldspar. This fracture is cut by a fracture filled with small fan-like prehnite crystals. The prehnite-sealed fracture has many voids, and the prehnite appears to have grown as nails in an open fracture. The prehnite can also be found inside the wall rock, most abundantly a few millimetres from the prehnite filled fracture. The FeO is concentrated in parts of the prehnite where the content may be up to 7%, while adjacent crystals have values as low as 1%. The Fe content in the prehnite in the adularia sealed fracture does not differ from the Fe content in the prehnite sealed fracture. A hematite stained adularia has penetrated along the border between the prehnite-filled fracture and the wall rock and into some voids between prehnite crystals.

Wall rock alteration:

The wall rock is highly altered with completely saussuritized plagioclase and chloritized biotite. The pseudomorphs of biotite are replaced by chlorite, adularia and titanite. The quartz grains have shown subgrain formation. The wall rock alteration extends through the entire thin section, although the plagioclase is a bit more unaltered furthest away from the fracture (c 4 cm).

Figure A-53. *Brick-red adularia and hematite filled fracture cut by a prehnite filled fracture. Both fractures are surrounded by altered wall rock. The diameter of the drill core is c 5 cm.*

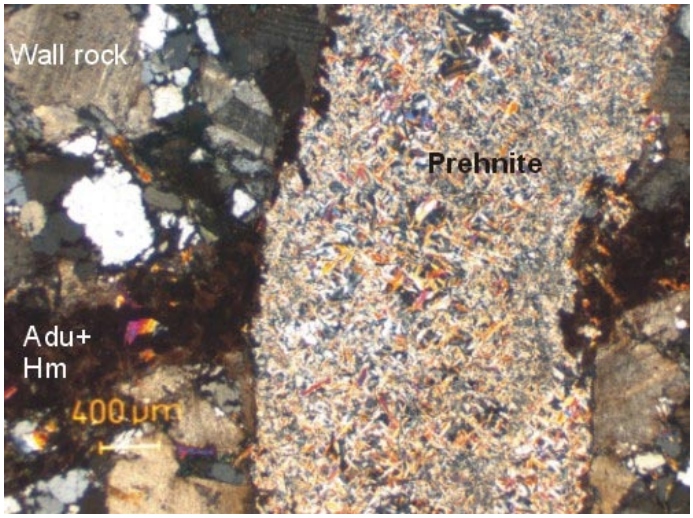

Figure A-54. *Adularia and hematite filled fracture cut by prehnite filled fracture. Photomicrograph with crossed polars.*

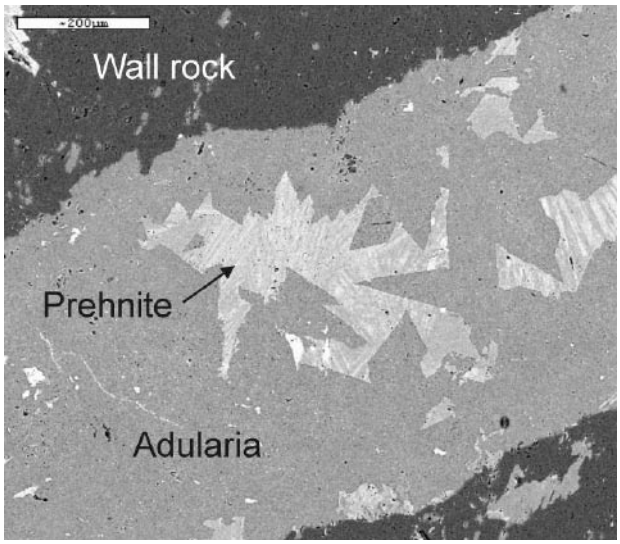

Figure A-55. *Adularia together with prehnite. Back-scattered electron image.*

Sample: **KFM05A 692.00–692.15 m**
Rock type: Metatonalite
Fracture: Two sealed fractures
Orientation: 128/07° cut by 032/89°
Deformation zone: –
Fracture orientation set: NW cut by NE
Fracture minerals: Epidote, prehnite, chlorite, allanite, adularia, titanite, apatite

Sequence of mineralizations:

1. Epidote + chlorite + allanite + quartz + adularia + titanite + apatite
2. Adularia + hematite
3. Prehnite
4. Calcite

Macroscopic description:

One thin sealed fracture with a green mineral filling is cut by a sealed fracture with a brick-red filling. Both fractures are surrounded by c 1 cm of red-coloured wall rock on both sides of the fracture.

The thin green fracture contains epidote crystals together with Fe-chlorite, quartz, and adularia. The FeO content in the chlorite is c 34% and the MgO content c 11%. Accessory minerals like allanite, titanite and apatite are also found together with the epidote, but they probably origin from the wall rock and have not crystallized in the fracture. The cutting fracture is filled with adularia with small micro-grains of hematite together with prehnite. Later calcite has filled the fracture.

Wall rock alteration:

The wall rock is highly altered around much of the sealed fractures. The plagioclase is almost entirely saussuritized and the biotite chloritized. The pseudomorphs after biotite contain chlorite, prehnite, epidote, allanite, titanite, and apatite. The chlorite is deep blue under crossed polars and has approximately the same chemistry as the chlorite in the fracture; a FeO content of c 34% and MgO content of c 13%.

Figure A-56. *Epidote filled fracture cut by a brick-red adularia and hematite filled fracture. Both fractures are surrounded by wall rock alteration. The diameter of the drill core is c 5 cm.*

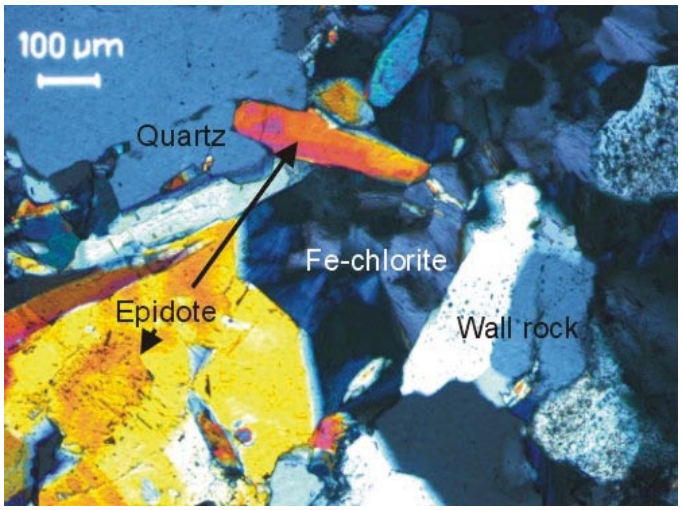

Figure A-57. *Epidote together with Fe-rich chlorite. Photomicrograph with crossed polars.*

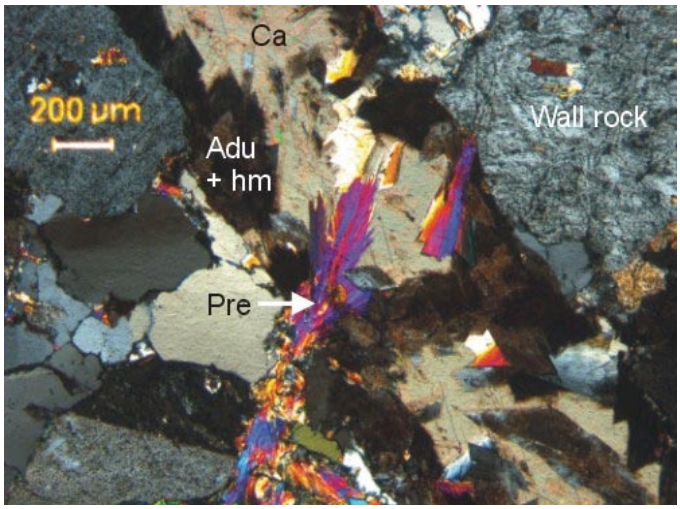

Figure A-58. *Adularia and hematite together with prehnite and later calcite. Photomicrograph with crossed polars.*

Sample: **KFM05A 702.42–702-56 m**
Rock type: Metagranite
Fracture: Open fracture
Orientation: 214/88°
Deformation zone: –
Fracture orientation set: NE
Fracture minerals: Laumontite, analcime, adularia, quartz, chalcopyrite, chlorite

Sequence of mineralizations:

1. Laumontite
2. Adularia + quartz
3. Chalcopyrite
4. Mg/Fe-chlorite/corrensite + calcite
5. Fe-chlorite

On the fracture surface, laumontite has first crystallized together with analcime. On these minerals then a mixture of adularia and quartz has grown. These two generations of minerals have then partly dissolved and chalcopyrites can be found in some of the voids. On the adularia chlorite (FeO ≈ 20%, MgO ≈ 21%) has crystallized. Calcite has also penetrated the adularia, but no clear relation between the chlorite/corrensite and the calcite can be seen in the sample. On these minerals, and in small fractures inside it, a more Fe-rich chlorite/corrensite has crystallized.

Wall rock alteration: Saussuritization of the plagioclase and chloritization of the biotite. The pseudomorphs after the biotite now contain chlorite, adularia, titanite and zircons. Parts of the chlorite had been altered into clay minerals.

Figure A-59. *Fracture with red laumontite and greenish chlorite/corrensite. The diameter of the drill core is c 5 cm.*

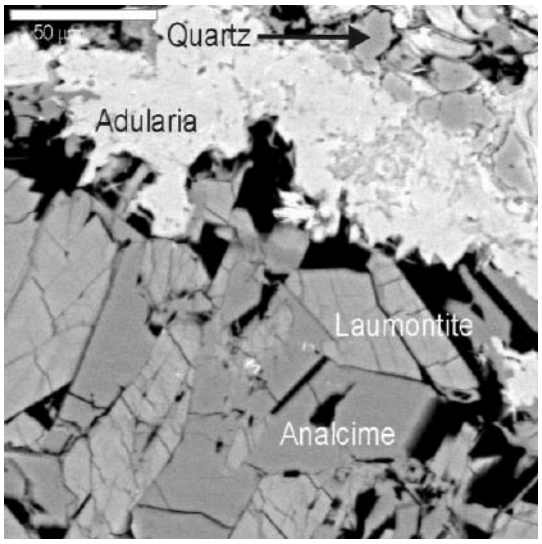

Figure A-60. *Laumontite and analcime with later adularia and quartz. Back-scattered electron image.*

Sample: **KFM05A 737.78–737.89 m**
Rock type: Metagranite
Fracture: Sealed fracture
Orientation: 031/22°
Deformation zone: –
Fracture orientation set: HZ
Fracture minerals: Epidote, prehnite, quartz

Sequence of mineralizations:

1. Epidote + chlorite
2. Prehnite + quartz + adularia

Epidote filled fracture with some fragments of wall rock, mainly quartz. The epidote contains c 12% FeO and can be seen as elongated crystals on a surface sample.

This c 1.5 mm wide fracture is cut by a micro-vein filled with prehnite with small amounts of quartz and adularia. The prehnite contains c 3% FeO.

Wall rock alteration:

The wall rock is highly altered and contains saussuritized plagioclase, large quantities of small epidote crystals and Fe-chlorite, of which the latter under crossed polars has a deep blue colour. The FeO in the chlorite is very high, c 30% and the MgO c 10%. The quartz is highly undulatory and the subgrain formation has been intense.

Figure A-61. *Epidote and chlorite filled fracture. The diameter of the drill core is c 5 cm.*

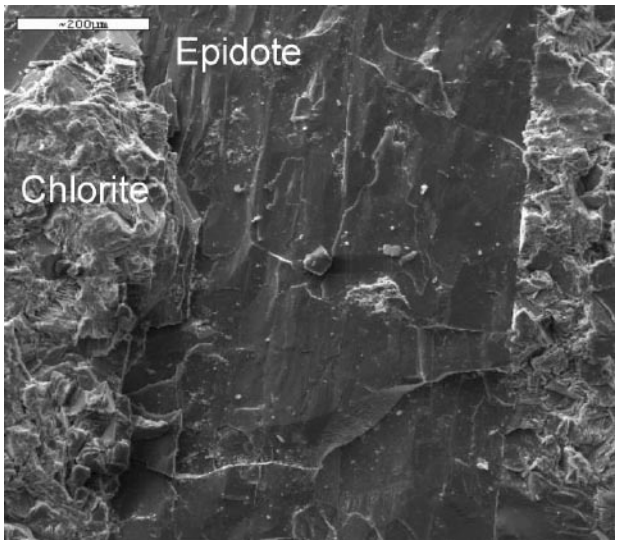

Figure A-62. *Epidote and chlorite crystals on fracture surface. Electron image.*

Sample: **KFM05A 938.00–938.18 m**
Rock type: Metagranite
Fracture: Open fracture cutting sealed network
Orientation: 042/80°
Deformation zone: ZFMNE062A
Fracture orientation set: NE
Fracture minerals: Hematite, prehnite, laumontite, quartz, corrensite

Sequence of mineralizations:

1. Cataclasite with fragments of quartz, plagioclase, K-feldspar, hematite, prehnite, laumontite in a matrix of adularia, hematite, albite and some corrensite
2. Laumontite
3. Euhedral quartz + pyrite
4. Corrensite

Cutting the sample is a sealed network that consists of a cataclasite with fragments of the wall rock, mainly quartz, plagioclase and K-feldspar and larger hematite grains together with prehnite. The matrix is made up of adularia, albite and hematite plus some corrensite. In an open fracture has hematite stained laumontite grown over the cataclasite. On this laumontite small euhedral quartz crystals have grown together with small pyrite crystals. The latest mineral is a spherical aggregate of corrensite that appears as fan-like aggregates on the quartz crystals.

Wall rock alteration:

The wall rock alteration consists of a subgrain formation of the quartz, saussuritization of plagioclase and chloritization of biotite. The K-feldspar is mostly unaltered. The pseudomorphs after the biotite contain chlorite, titanite and laumontite.

Figure A-63. *Older fracture network of mainly laumontite and hematite cut by open fracture with quartz, pyrite and corrensite.*

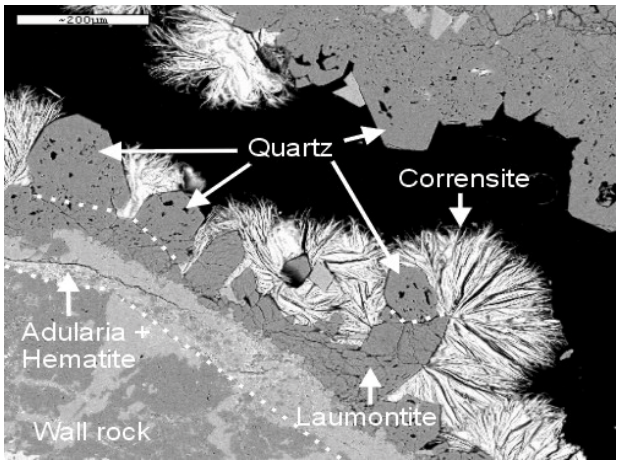

Figure A-64. *Sequence of mineralizations starting with adularia and hematite on which laumontite, euhedral quartz and spherical aggregates of corrensite have grown. Back-scattered electron image.*

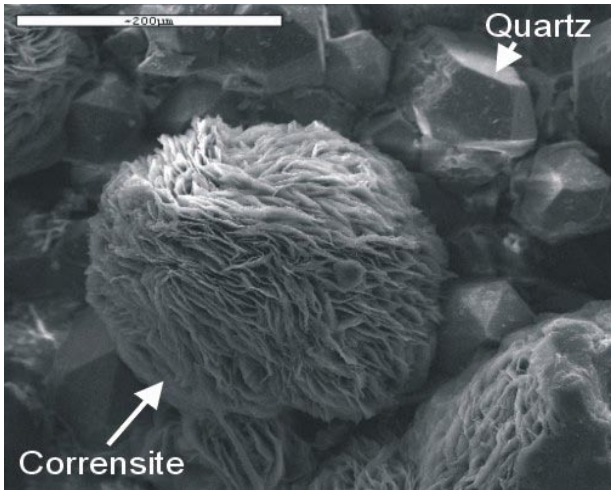

Figure A-65. *Spherical aggregate of corrensite on a coating of euhedral quartz crystals. Electron image.*

Sample: **KFM06A 102.62–102.82 m**
Rock type: Metagranite
Fracture: Open fracture
Orientation: 008/84°
Deformation zone: Not defined
Fracture orientation set: NS
Fracture minerals: Calcite, asphaltite, clay mineral

Sequence of mineralizations:

1. Calcite
2. Clay mineral
3. Asphaltite

Figure A-66. *Open fracture with calcite, clay mineral and asphaltite. The diameter of the drill core is c 5 cm.*

Sample: **KFM06A 106.18–106.36 m**
Rock type: Metagranite
Fracture: Open fracture
Orientation: 190/86°
Deformation zone: Not defined
Fracture orientation set: NS
Fracture minerals: Quartz, calcite, pyrite, asphaltite

Sequence of mineralizations:

1. Quartz
2. Calcite + pyrite
3. Asphaltite

Figure A-67. *Quartz covered fracture surface on which calcite, pyrite and asphaltite have precipitated. The diameter of the drill core is c 5 cm.*

Sample: **KFM06A 106.94–107.14 m**
Rock type: Metagranite
Fracture: Open fracture
Orientation: 189/85°
Deformation zone: Not defined
Fracture orientation set: NS
Fracture minerals: Quartz, calcite, galena, sphalerite, chalcopyrite, baryte, asphaltite

Sequence of mineralizations:

1. Quartz + pyrite + galena + chalcopyrite + baryte + adularia
2. Asphaltite

Large calcite crystals with thin straight thin twins have crystallized together with pyrite, galena, sphalerite, chalcopyrite, baryte and adularia in a porous quartz matrix. The galena contains small inclusions of baryte. The FeO and MnO contents in the calcite are below detection limit in the SEM-EDS. Asphaltite has penetrated the fracture fillings as the latest event.

Figure A-68. *Fracture filled with calcite, pyrite, galena, chalcopyrite, baryte, adularia and asphaltite. The diameter of the drill core is c 5 cm.*

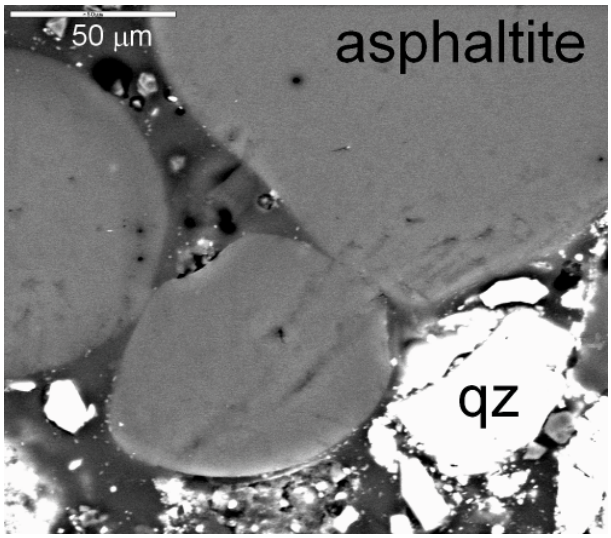

Figure A-69. *Dropplets of asphaltite in thin section together with quartz. Back-scattered electron image.*

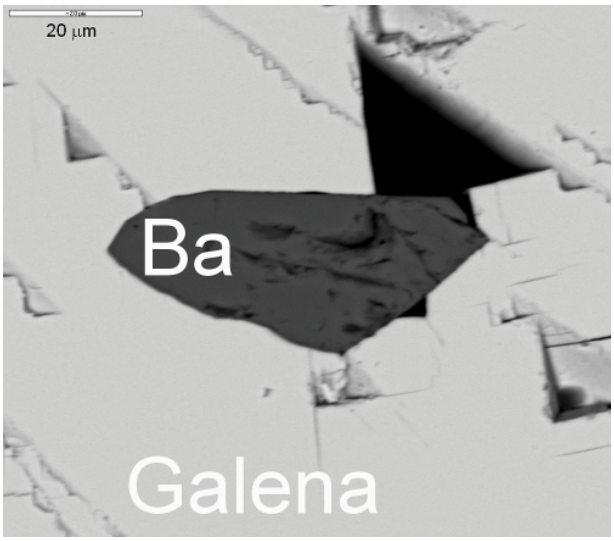

Figure A-70. *Larger galena crystal with small inclusion of baryte (Ba). Back-scattered electron image.*

Sample: **KFM06A 110.49–110.52 m**
Rock type: Metagranite
Fracture: Sealed fracture
Orientation: 007/84°
Deformation zone: Not defined
Fracture orientation set: NS
Fracture minerals: Quartz, calcite, pyrite, galena, asphaltite

Sequence of mineralizations:

1. Quartz
2. Calcite + pyrite + galena
3. Asphaltite
4. Quartz

Open fracture with a thin coating of euhedral quartz. On this coating calcite, pyrite and galena have crystallized as subhedral to euhedral crystals. Asphaltite has then covered many of the crystals as a thin coating or as small grains. As a latest phase, aggregates of euhedral quartz crystals with a porous character have grown over the asphaltite.

Figure A-71. *Open fracture with two generations of quartz, calcite, pyrite, galena and asphaltite. The diameter of the drill core is c 5 cm.*

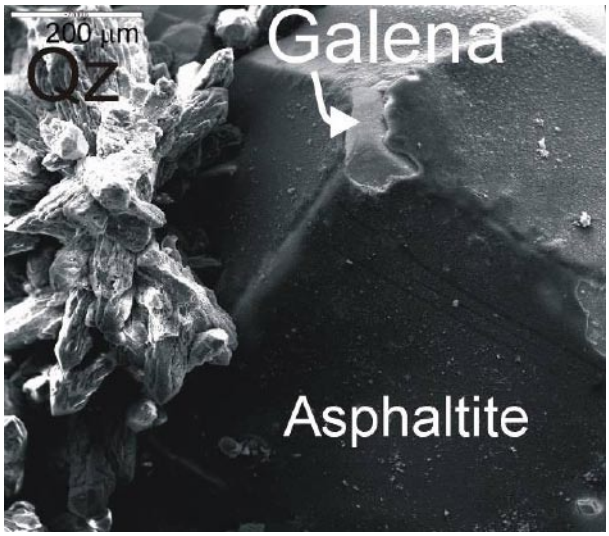

Figure A-72. *Euhedral galena crystal covered with a thin film of asphaltite. Porous euhedral quartz crystals have then crystallized over the older minerals. Back-scattered electron image.*

Sample: **KFM06A 110.53–110.59 m**
Rock type: Metagranite
Fracture: Open fracture
Orientation: 019/74°
Deformation zone: Not defined
Fracture orientation set: NS
Fracture minerals: Quartz, calcite, asphaltite

Sequence of mineralizations:

1. Quartz
2. Calcite
3. Quartz
4. Asphaltite

Figure A-73. *Open fracture with quartz, calcite and asphaltite. The diameter of the drill core is c 5 cm.*

Sample: **KFM06A 110.72–110.83 m**
Rock type: Metagranite
Fracture: Open fracture
Orientation: 005/82°
Deformation zone: Not defined
Fracture orientation set: NS
Fracture minerals: Quartz, calcite, pyrite, galena, asphaltite

Sequence of mineralizations:

1. Quartz
2. Calcite + galena + pyrite
3. Asphaltite

Figure A-74. *Fracture with quartz coating, calcite, galena, pyrite and asphaltite. The diameter of the drill core is c 5 cm.*

Sample: **KFM06A 111.40–111.52 m**
Rock type: Metagranite
Fracture: Open fracture
Orientation: 018/82°
Deformation zone: Not defined
Fracture orientation set: NS
Fracture minerals: Quartz, calcite, galena, asphaltite

Sequence of mineralizations:

1. Galena + pyrite + calcite
2. Asphaltite
3. Quartz

Euhedral crystals of galena and pyrite are covered with a thin film of asphaltite. Small elongated euhedral quartz crystals have precipitated on the asphaltite.

Figure A-75. *Fracture with galena, pyrite, calcite, quartz. The diameter of the drill core is c 5 cm.*

Sample: **KFM06A 142.27–142.93 m**
Rock type: Metagranite
Fracture: Sealed fracture
Orientation: 046/85°
Deformation zone: Not defined
Fracture orientation set: NE
Fracture minerals: Quartz, calcite, pyrite

Sequence of mineralization:

1. Quartz + calcite
2. Calcite + pyrite

Small subhedral to euhedral quartz crystals have crystallized together with small lenses of calcite. The fracture has later been reactivated and a younger calcite has penetrated the fracture.

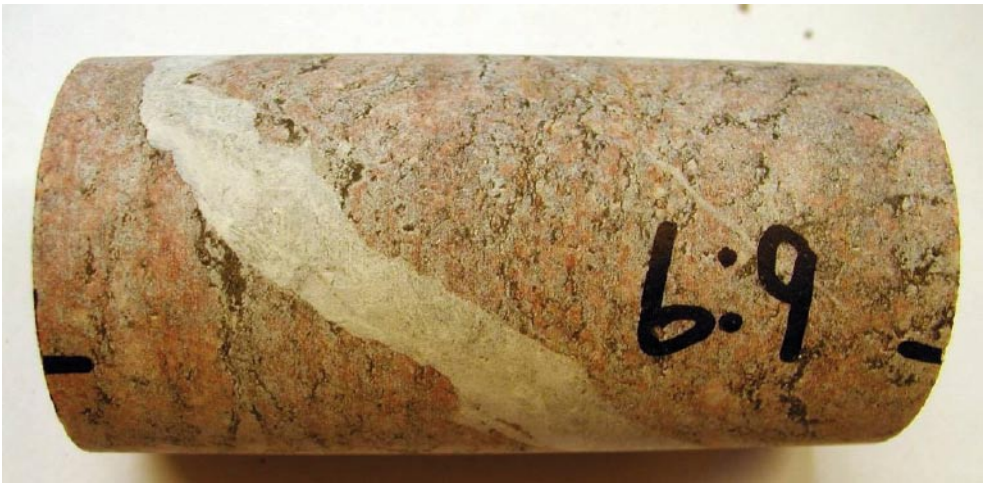

Figure A-76. *Calcite sealed fracture. The diameter of the drill core is c 5 cm.*

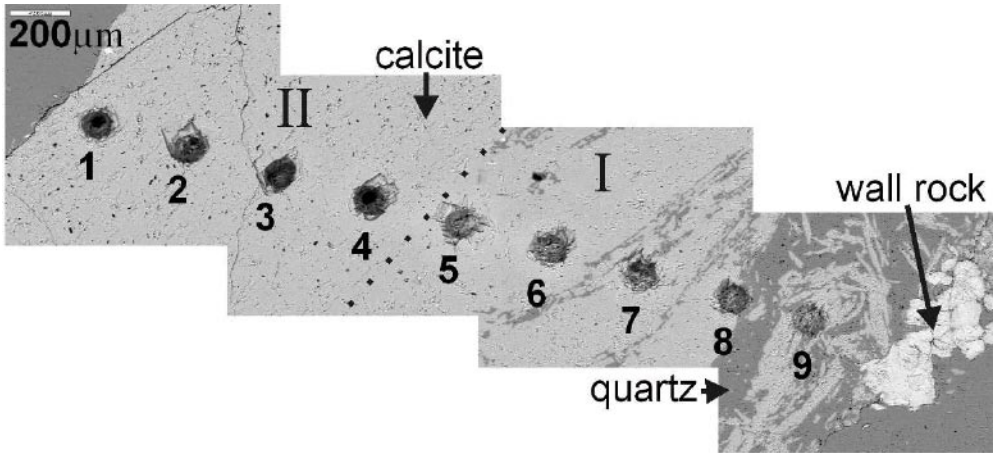

Figure A-77. *Fracture filled with two different calcites (I and II) where the older is mixed with quartz. The black craters are spots from laser ablation. Back-scattered electron image.*

Sample: **KFM06A 142.93–143.03 m**
Rock type: Metagranite
Fracture: Open fracture
Orientation: 023/74°
Deformation zone: Not defined
Fracture orientation set: NE
Fracture minerals: Quartz, calcite, asphaltite

Sequence of mineralizations:

1. Quartz
2. Calcite
3. Pyrite + sphalerite
4. Asphaltite

The fracture surface is covered with small euhedral quartz crystals on which euhedral crystals of calcite, pyrite and sphalerite have crystallized. As the latest phase, asphaltite has precipitated on the surface.

Figure A-78. *Open fracture with quartz, calcite, pyrite, sphalerite and asphaltite. The diameter of the drill core is c 5 cm.*

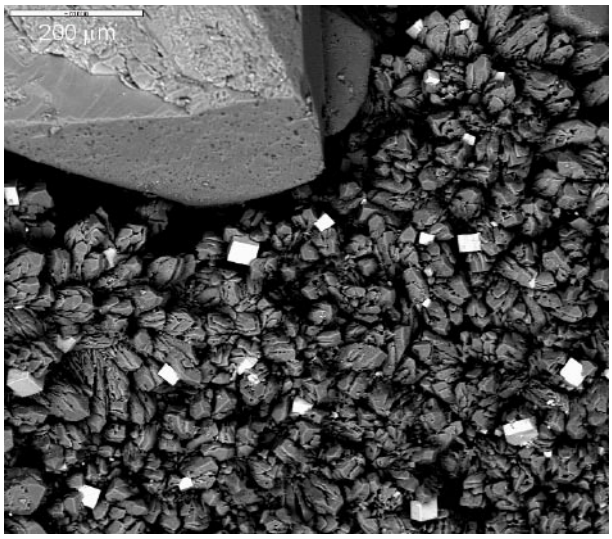

Figure A-79. *Cubic pyrite (white in picture) and a larger calcite crystal have crystallized over a coating of small euhedral quartz crystals. Back-scattered electron image.*

Sample: **KFM06A 145.62–145.73 m**
Rock type: Pegmatite
Fracture: Open fracture
Orientation: 018/76°
Deformation zone: Not defined
Fracture orientation set: NS
Fracture minerals: Quartz, albite, adularia, smectite, chlorite/corrensite, pyrite, illite

Figure A-80. *Clay mineral filling. A white band of older calcite can be seen under the clay minerals. The diameter of the drill core is c 5 cm.*

Sample: **KFM06A 170.06–170.13 m**
Rock type: Quartz vein
Fracture: Open fracture
Orientation: 016/86°
Deformation zone: Not defined
Fracture orientation set: NS
Fracture minerals: Calcite, corrensite, pyrite
Sequence of mineralizations:

1. Calcite + corrensite + pyrite

Figure A-81. *Granular calcite that occurs euhedral in the voids. Spherical aggregates of corrensite appear to have crystallized during approximately the same period. The diameter of the drill core is c 5 cm.*

Sample: **KFM06A 187.68–187.78 m**
Rock type: Metagranite
Fracture: Sealed fracture
Orientation: 239/79°
Deformation zone: Not defined
Fracture orientation set: NE
Fracture minerals: Adularia, hematite, prehnite, calcite

Sequence of mineralizations:

1. Adularia + albite + quartz + hematite
2. Prehnite + calcite
3. Calcite
4. Calcite

Thin brick-red fracture is cut by prehnite. The prehnite has then been cut by a calcite with thick twins. This filling has later been reactivated while a younger calcite with thin straight twins has crystallized.

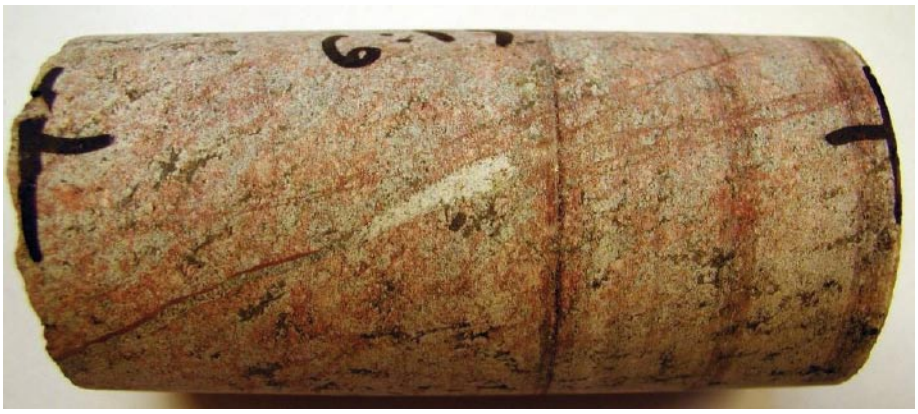

Figure A-82. *Thin brick-red sealing with later white prehnite. The diameter of the drill core is c 5 cm.*

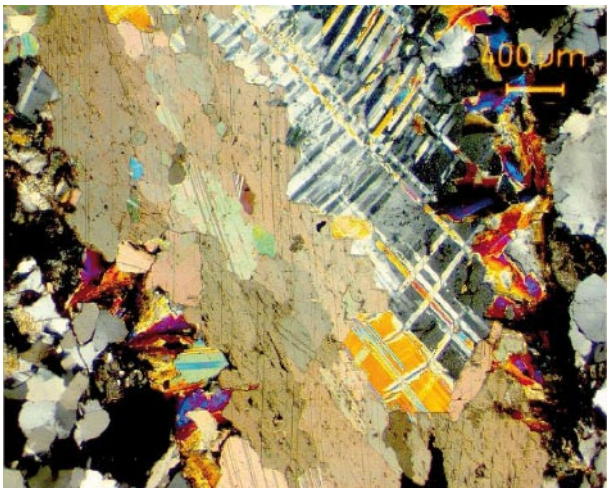

Figure A-83. *Prehnite along the margins of the fracture has been cut by a calcite with thick twins which later has been cut by a younger calcite with thin twins.*

Sample: **KFM06A 199.66–199.80 m**
Rock type: Metagranite
Fracture: Open fracture
Orientation: 359/84°
Deformation zone: Not defined
Fracture orientation set: NS
Fracture minerals: Quartz, calcite, pyrite

Sequence of mineralizations:

1. Quartz
2. Calcite + pyrite

Figure A-84. *Open fracture with coating of euhedral quartz crystals on which calcite has precipitated. The diameter of the drill core is c 5 cm.*

Sample: **KFM06A 201.94–202.07 m**
Rock type: Metagranite
Fracture: Open fracture
Orientation: 017/80°
Deformation zone: Not defined
Fracture orientation set: NS
Fracture minerals: Quartz, adularia, chlorite/corrensite, illite

Figure A-85. *Open fracture covered with quartz, adularia, chlorite/corrensite and illite. The diameter of the drill core is c 5 cm.*

Sample: **KFM06A 220.22–220.39 m**
Rock type: Metagranite
Fracture: Sealed fracture
Orientation: 224/81°
Deformation zone: Not defined
Fracture orientation set: NE
Fracture minerals: Adularia, albite, hematite, quartz, Fe-chlorite

Sequence of mineralizations:

1. Adularia + albite + hematite
2. Quartz
3. Chlorite/corrensite

Older filling with hematite stained adularia and albite and wall rock fragments are cut by thin bands of subhedral to euhedral quartz crystals. In one part of the fracture, the quartz has grown as large crystals with zonation and incorporated chlorite/corrensite. The latter has also crystallized in voids between quartz crystals.

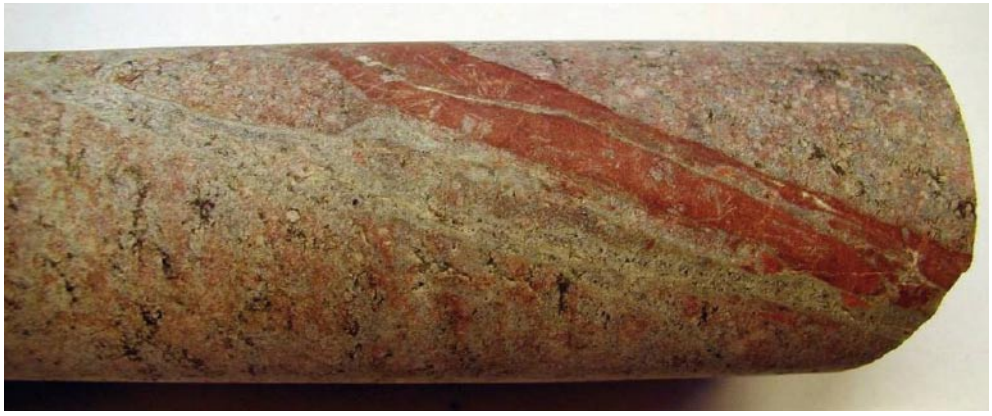

Figure A-86. *Brick-red filling of adularia, albite and hematite cut by younger quartz filling. The diameter of the drill core is c 5 cm.*

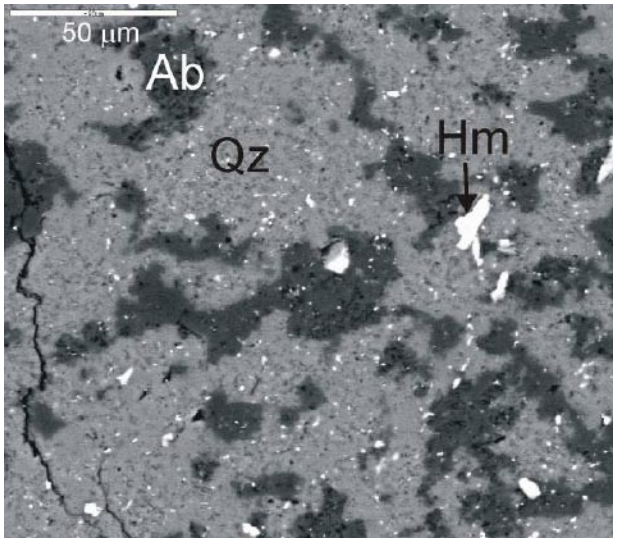

Figure A-87. *Back-scattered electron image of adularia, albite and hematite filled fracture.*

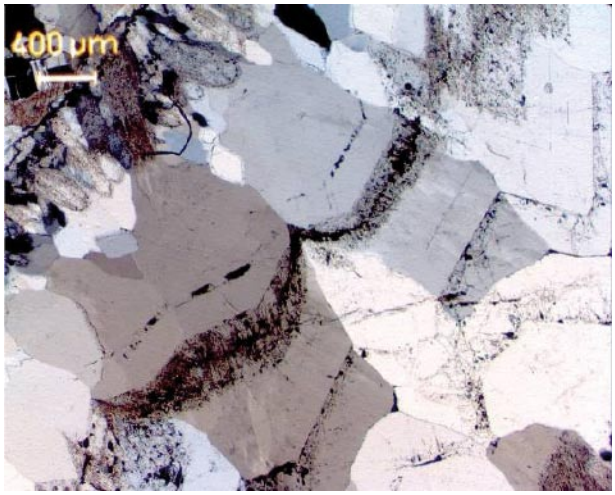

Figure A-88. *Quartz crystals with zonation and incorporated black chlorite/corrensite. Photomicrograph with crossed polars.*

Sample: **KFM06A 223.33–223.40 m**
Rock type: Metagranite
Fracture: Sealed fracture
Orientation: 241/79°
Deformation zone: Not defined
Fracture orientation set: NE
Fracture minerals: Epidote, chlorite, clay minerals, adularia, quartz, hematite

Sequence of mineralizations:

1. Epidote
2. Chlorite + Clay minerals
3. Adularia + quartz + hematite

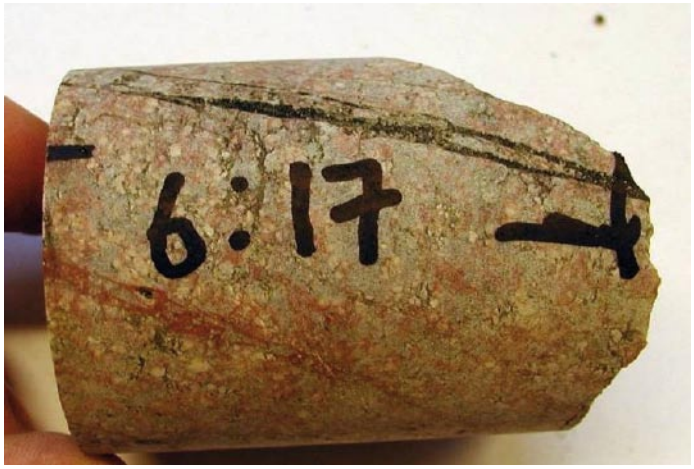

Figure A-89. *The black fracture sealing consists of small fragments of epidote in a matrix of chlorite and clay minerals. The brick-red filling consists of adularia, albite and hematite.*

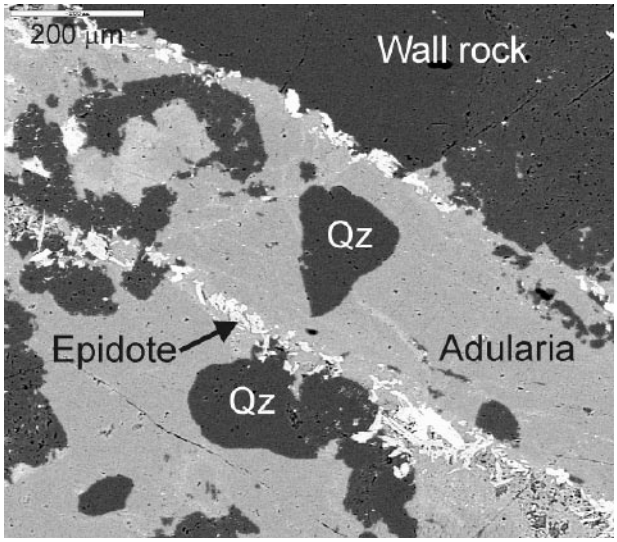

Figure A-90. *Back-scattered electron image of the brick-red fracture sealing.*

Sample: **KFM06A 260.81–260.86 m**
Rock type: Metagranite
Fracture: Sealed fracture
Orientation: 136/26°
Deformation zone: Not defined
Fracture orientation set: HZ
Fracture minerals: Epidote

Figure A-91. *Sealed network with epidote filled fractures. The diameter of the drill core is c 5 cm.*

Sample: **KFM06A 268.48–268.71 m**
Rock type: Metagranite
Fracture: Crushed zone
Orientation: 294/18°–105/02°
Deformation zone: Not defined
Fracture orientation set: HZ
Fracture minerals: Quartz, calcite

Figure A-92. *Conductive zone with surfaces covered with quartz and calcite. The diameter of the intact drill core seen in the middle is c 5 cm.*

Sample: **KFM06A 268.77–268.82 m**
Rock type: Metagranite
Fracture: Sealed fracture
Orientation: 305/18°
Deformation zone: Not defined
Fracture orientation set: HZ
Fracture minerals: Epidote

Figure A-93. *Cataclasite sealed with epidote. The diameter of the drill core is c 5 cm.*

Sample: **KFM06A 317.43–317.48 m**
Rock type: Metagranite
Fracture: Sealed fracture
Orientation: 245/85°
Deformation zone: Not defined
Fracture orientation set: NE
Fracture minerals: Laumontite, calcite

Sequence of mineralizations:

1. Laumontite
2. Calcite

Figure A-94. *Laumontite and calcite sealed fracture. The diameter of the drill core is c 5 cm.*

Sample: **KFM06A 324.54–324.65 m**
Rock type: Metagranite
Fracture: Sealed fracture
Orientation: 216/88°
Deformation zone: Not defined
Fracture orientation set: NE
Fracture minerals: Adularia, albite, hematite, quartz, calcite

Sequence of mineralizations:

1. Adularia + albite + hematite
2. Quartz
3. Calcite
4. Calcite

Brick-red sealing of adularia, albite and hematite is cut by a fracture with subhedral to euhedral quartz crystals. This quartz has been penetrated by small nails of calcite. This mixture of quartz and calcite has then been cut by a younger calcite.

Figure A-95. *Older brick-red fracture with adularia, albite and hematite with white later filling, consisting of quartz and two phases of calcite crystallizations. The diameter if the drill core is c 5 cm.*

Sample: **KFM06A 331.88–332.06 m**
Rock type: Metagranite
Fracture: Sealed and open fracture
Orientation: 217/82°
Deformation zone: Not defined
Fracture orientation set: NE
Fracture minerals: Calcite, quartz, pyrite

Sequence of mineralizations:

1. Calcite + quartz + pyrite
2. Calcite

Figure A-96. *Fracture filled with calcite, quartz and pyrite. The diameter of the drill core is c 5 cm.*

Sample: **KFM06A 332.62–332.87 m**
Rock type: Metagranite (fine-grained)
Fracture: Sealed fracture
Orientation: 215/80°
Deformation zone: Not defined
Fracture orientation set: NE
Fracture minerals: Adularia, albite, hematite, quartz, calcite

Sequence of mineralizations:

1. Adularia + albite + hematite
2. Quartz
3. Calcite + pyrite

Thin brick-red sealed fractures with adularia, albite and hematite cut by partly open fractures with quartz, calcite and pyrite.

Figure A-97. *Open fracture with quartz, calcite and pyrite. The diameter of the drill core is c 5 cm.*

Sample: **KFM06A 336.68–336.83 m**
Rock type: Metagranite
Fracture: Sealed fracture
Orientation: 230/77°
Deformation zone: Not defined
Fracture orientation set: NE
Fracture minerals: Adularia, hematite, calcite, pyrite, chlorite/corrensite

Sequence of mineralizations:

1. Adularia + hematite
2. Quartz + adularia
3. Chlorite/corrensite + pyrite
4. Calcite

A brick-red sealing with hematite stained adularia has been cut by a matrix of subhedral to euhedral quartz and adularia. Chlorite/corrensite and pyrite have crystallized in voids in the matrix. This matrix has also penetrated a hematite stained adularia that appears to be of approximately the same age as the corrensite. Closely related to the euhedral quartz has a prismatic calcite crystallized. This calcite has well developed twins and is deformed. In small voids inside the matrix calcite has precipitated which shows no or a very diffuse twin structure. A c 0.7 cm wide calcite filled fracture cuts the older sealing. Highly altered wall rock with saussuritized plagioclase and chloritized biotite.

Figure A-98. *Brick-red fracture filling with adularia and hematite cut by greenish filling of quartz and adularia which later has been cut by calcite. The diameter of the drill core is c 5 cm.*

Figure A-99. *Matrix of subhedral to euhedral quartz and adularia crystals with chlorite/ corrensite and pyrite. Calcite has crystallized in the void. Photomicrograph with crossed polars.*

Sample: **KFM06A 348.06–348.19 m**
Rock type: Metagranite
Fracture: Sealed fracture (breccia)
Orientation: 228/80°
Deformation zone: Not defined
Fracture orientation set: NE
Fracture minerals: Quartz, calcite

Sequence of mineralizations:

1. Quartz
2. Calcite

Figure A-100. *Calcite sealed breccia. The rock near the breccia is penetrated with a network with older quartz filled fractures.*

Sample: **KFM06A 352.27–352.37 m**
Rock type: Metagranite
Fracture: Sealed fracture
Orientation: 188/80°
Deformation zone: Not defined
Fracture orientation set: NS
Fracture minerals: Quartz, calcite, pyrite

Sequence of mineralizations:

1. Quartz
2. Calcite + pyrite

The c 1.2 cm thick fracture is sealed with quartz, calcite and pyrite. The quartz has crystallized prior to the calcite which later has penetrated the quartz with prismatic crystals. Vugs in the partly dissolved quartz are also filled with calcite and pyrite.

Figure A-101. *Thick fracture sealing with quartz, calcite and some pyrite. The diameter of the drill core is c 5 cm.*

Sample: **KFM06A 356.53–356.71m**
Rock type: Metagranite
Fracture: Sealed and open fracture
Orientation: 200/87°
Deformation zone: Not defined
Fracture orientation set: NS
Fracture minerals: Calcite, quartz, pyrite

Thick fracture filling with quartz, calcite and pyrite that have crystallized during the same period.

Figure A-102. *Quartz, calcite and pyrite filling. The diameter of the drill core is c 5 cm.*

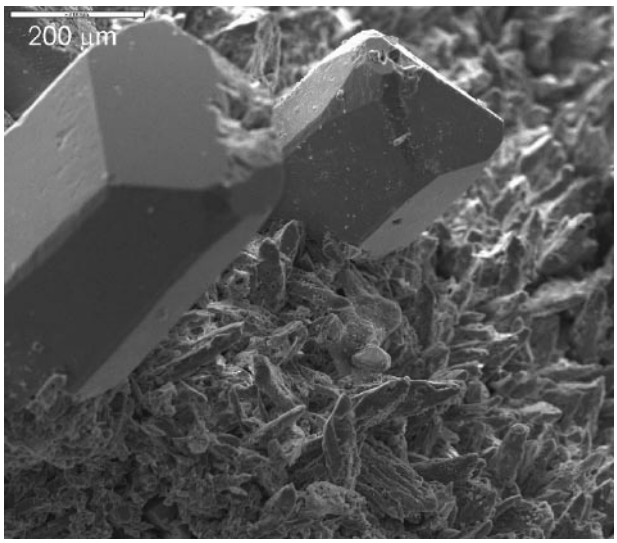

Figure A-103. *Larger euhedral calcite crystals together with small porous euhedral quartz crystals. Electron image.*

Sample: **KFM06A 404.99–405.06 m**
Rock type: Metagranite
Fracture: Open fracture
Orientation: 100/89°
Deformation zone: Not defined
Fracture orientation set: EW
Fracture minerals: Corrensite, pyrite

Sequence of mineralizations:

1. Corrensite
2. Pyrite + calcite

The fracture surface is covered with spherical aggregates of corrensite crystals on which a few pyrite and calcite crystals have grown.

Figure A-104. *Fracture surface with small black spherical aggregates of corrensite. The diameter of the drill core is c 5 cm.*

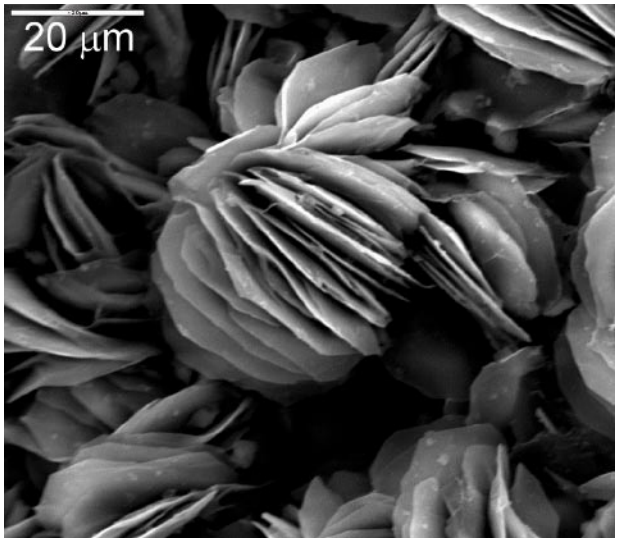

Figure A-105. *Electron image of small spherical aggregate of corrensite.*

Sample: **KFM06A 503.44–503.49 m**
Rock type: Metagranite
Fracture: Open fracture
Orientation: 036/73°
Deformation zone: Not defined
Fracture orientation set: NE
Fracture minerals: Calcite, albite, adularia, quartz, biotite

Figure A-106. *Open fracture with calcite, albite, adularia, quartz and biotite. The diameter of the drill core is c 5 cm.*

Sample: **KFM06A 568.94–569.04 m**
Rock type: Metagranite
Fracture: Open fracture
Orientation: 212/89°
Deformation zone: Not defined
Fracture orientation set: NE
Fracture minerals: Adularia, hematite, chlorite/corrensite, calcite

Sequence of mineralizations:

1. Adularia + hematite
2. Chlorite/corrensite
3. Calcite

Figure A-107. *Open fracture with calcite, albite, adularia, quartz and biotite. The diameter of the drill core is c 5 cm.*

Sample: **KFM06A 620.14–620.23 m**
Rock type: Metagranite
Fracture: Sealed and open fractures
Orientation: 205/89°
Deformation zone: Not defined
Fracture orientation set: NE
Fracture minerals: Adularia, albite, hematite, chlorite/corrensite

Figure A-108. *Sealed fracture with adularia, albite and hematite with later chlorite/corrensite. The diameter of the drill core is c 5 cm.*

Sample: **KFM06A 622.31–622.36 m**
Rock type: Metagranite
Fracture: Crushed zone
Orientation: 192/79°
Deformation zone: Not defined
Fracture orientation set: NS
Fracture minerals: Quartz, albite, adularia, chlorite/corrensite

Figure A-109. *Crushed zone with quartz, albite, adularia, chlorite/corrensite and rock fragments. The width of the picture is c 12 cm.*

Sample: **KFM06A 653.26–653.33 m**
Rock type: Metagranite
Fracture: Sealed and open fractures
Orientation: 217/86°
Deformation zone: Not defined
Fracture orientation set: NE
Fracture minerals: Adularia, albite, hematite, quartz, calcite, pyrite

Sequence of mineralizations:

1. Adularia + albite + hematite
2. Quartz
3. Calcite + pyrite

Figure A-110. *Sealed fractures with adularia, albite and hematite have been reactivated during crystallization of a quartz coating on which calcite and pyrite have crystallized. The diameter of the drill core is c 5 cm.*

Sample: **KFM06A 743.39–743.52 m**
Rock type: Metagranite
Fracture: Open fracture
Orientation: 027/75°
Deformation zone: Not defined
Fracture orientation set: NE
Fracture minerals: Quartz, calcite, pyrite

Sequence of mineralizations:

1. Quartz
2. Calcite + pyrite

Figure A-111. *Fracture with thin coating with euhedral quartz crystals on which calcite and pyrite have crystallized. The diameter of the drill core is c 5 cm.*

Sample: **KFM06A 768.87–769.04 m**
Rock type: Metagranite
Fracture: Sealed fracture
Orientation: 207/80°
Deformation zone: Not defined
Fracture orientation set: NE
Fracture minerals: Prehnite, clay minerals, hematite

Sequence of mineralizations:

1. Prehnite
2. Clay minerals + hematite (alteration products)

Fracture filled with prehnite that partly has been altered into clay minerals. The clay is very Mg-rich and resembles vermiculite in chemical composition. The origin of the Mg could be chlorite that now has been completely decomposed. The remaining prehnite is very low in Fe but contains micrograins of hematite.

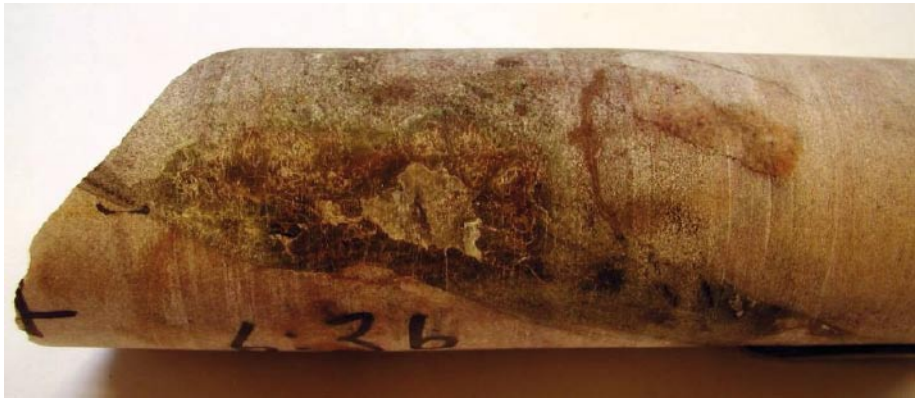

Figure A-112*. Thick mineral filling of prehnite, clay minerals and hematite. The diameter of the drill core is c 5 cm.*

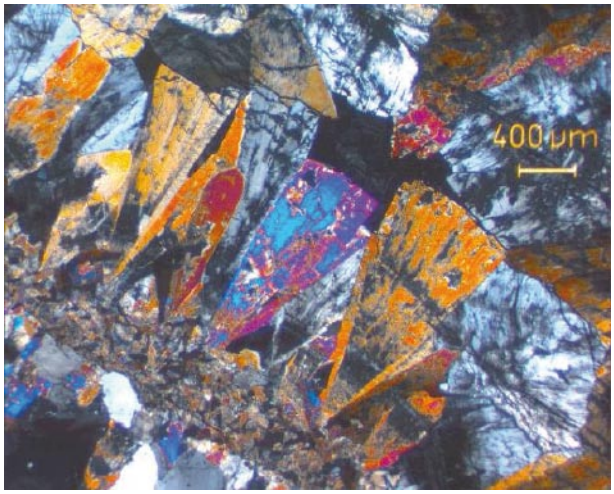

Figure A-113. *Partly altered prehnite. Photomicrograph with crossed polars.*

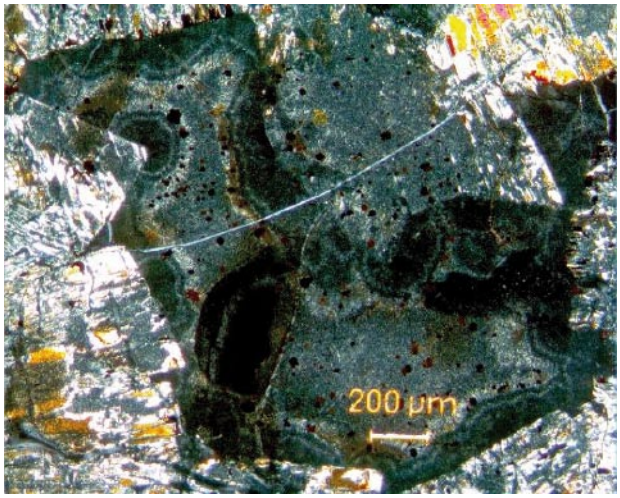

Figure A-114. *Clay mineral surrounded by altered prehnite crystals . Photomicrograph with crossed polars.*

Sample: **KFM06A 770.32–770.42 m**
Rock type: Metagranite
Fracture: Crushed zone
Orientation: 226/84°
Deformation zone: Not defined
Fracture orientation set: NE
Fracture minerals: Calcite, quartz, adularia, chlorite/corrensite

Figure A-115. *Crushed zone with rock fragment and calcite, quartz, adularia and chlorite/ corrensite. The width of the picture is c 20 cm.*

Sample: **KFM06A 794.78–794.88 m**
Rock type: Metagranite
Fracture: Open fracture
Orientation: 266/75°
Deformation zone: Not defined
Fracture orientation set: EW
Fracture minerals: Pyrite, calcite

Sequence of mineralizations:

1. Pyrite
2. Calcite

Figure A-116. *Open fracture with thin layer of platy calcite crystals that have crystallized over pyrite. The diameter of the drill core is c 5 cm.*

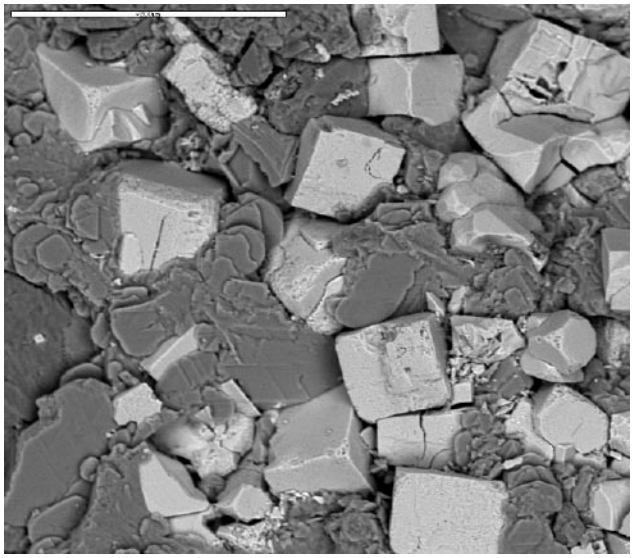

Figure A-117. *Platy calcite crystals covering cubic pyrite. The bar is 200 µm. Back-scattered electron image.*

Sample: **KFM06A 963.99–964.03 m**
Rock type: Metagranite
Fracture: Sealed fracture
Orientation: 231/69°
Deformation zone: Not defined
Fracture orientation set: NE
Fracture minerals: Adularia, hematite, chlorite, clay mineral

Sequence of mineralizations:

1. Adularia, hematite, chlorite/clay mineral

The rock is cut by thin fractures sealed with adularia, hematite and a clay mineral.

Highly altered wall rock with saussuritized plagioclase and chloritized biotite. The microcline is relatively unaltered. Epidote occurs abundantly in the wall rock.

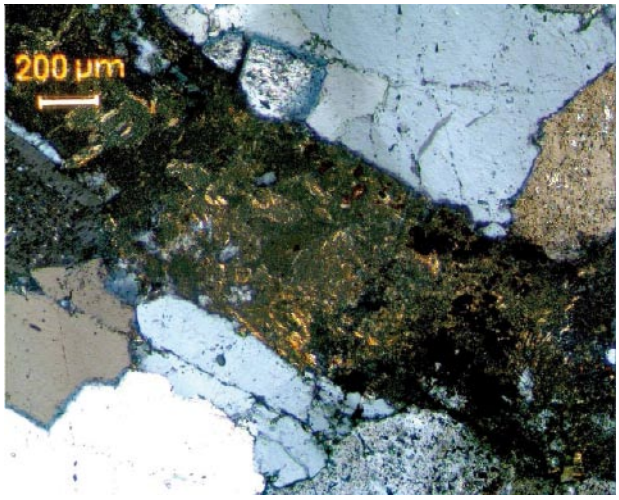

Figure A-118. *Thin fractures sealed with adularia, hematite, chlorite and a clay mineral.*

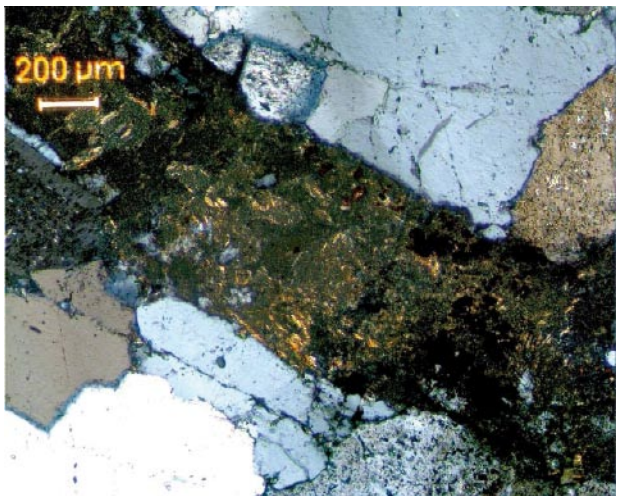

Figure A-119. *Fracture filled with chlorite, clay mineral and hematite. Photomicrograph with crossed polars.*

Appendix 2

SEM-EDS analyses

Sample	Mineral	Na_2O	MgO	Al_2O_3	SiO_2	K_2O	CaO	TiO_2	MnO	FeO	Total	Comment
KFM05A 109.75A	Adularia	1.5	*	18.1	65.1	15.9	*	0.1	*	*	100.0	
KFM05A 111.56A	Adularia	*	0.5	18.4	63.0	15.6	*	0.2	*	1.4	98.9	In illite
KFM05A 702.42H	Analcime	8.8	*	18.9	50.1	0.1	*	*	*	*	77.9	
KFM05A 702.42I	Analcime	10.5	0.1	19.6	50.4	*	*	*	*	*	80.8	
KFM05A 692.00D	Allanite	*	*	8.2	33.1	*	12.5	0.7	*	11.5	81.8	La_2O_3 = 5.1; Ce_2O_3 = 9.9; ThO_2 = 1.0
KFM05A 692.00E	Allanite	0.3	0.2	10.4	34.1	*	13.0	0.6	0.2	13.1	85.8	La_2O_3 = 4.5; Ce_2O_3 = 7.6; ThO_2 = 0.9; Nd_2O_3 = 1.7
KFM04A 179.70a	Calcite	*	*	0.3	0.6	*	53.1	*	0.2	*	54.4	
KFM04A 179.70b	Calcite	*	*	0.2	*	*	54.6	*	*	*	54.7	
KFM04A 179.70c	Calcite	*	*	*	*	*	55.0	*	*	*	55.3	
KFM04A 212.77b	Calcite	*	*	*	*	*	49.2	*	*	*	49.6	
KFM04A 179.70d	Chlorite	*	15.4	24.4	32.8	*	0.5	*	0.2	17.7	88.0	
KFM04A 179.70e	Chlorite	*	14.9	21.8	32.8	0.1	0.6	*	0.3	17.7	88.2	
KFM04A 226.20c	Chlorite	*	11.6	17.8	34.1	0.8	1.2	*	0.3	23.3	89.1	
KFM04A 226.20e	Chlorite	*	12.8	17.3	26.5	0.1	0.2	*	0.6	27.4	85.0	
KFM05A 689.33A	Chlorite	1.4	11.8	14.6	25.5	*	0.1	*	0.7	31.2	85.3	In biotite
KFM05A 692.00A	Chlorite	*	11.0	21.6	24.9	*	*	*	0.8	34.4	92.8	with epidote
KFM05A 692.00B	Chlorite	*	11.4	20.8	24.7	*	*	*	0.7	33.9	91.6	In wall rock
KFM05A 692.00C	Chlorite	*	12.8	15.7	28.8	0.2	0.1	*	0.5	34.4	92.6	In wall rock
KFM05A 702.42E	Chlorite	0.9	13.5	16.0	26.1	*	*	0.1	0.7	29.6	87.1	In wall rock
KFM05A 737.78A	Chlorite	*	10.9	18.8	23.8	*	*	*	0.5	30.9	85.2	In wall rock
KFM05A 737.78B	Chlorite	*	10.7	18.6	23.4	*	*	*	0.6	31.1	84.5	

Sample	Mineral	Na_2O	MgO	Al_2O_3	SiO_2	K_2O	CaO	TiO_2	MnO	FeO	Total	Comment
KFM05A 938.00	Unknown Clay mineral	*	3.8	7.3	30.5	0.3	8.1	*	*	7.9	73.0	Ce2O3 = 10.54; Nd2O3 = 7.02
KFM05A 109.75B	Chlorite/corrensite	1.1	1.7	12.1	24.1	*	0.1	*	0.1	50.8	90.2	
KFM05A 109.75C	Chlorite/corrensite	1.2	1.6	12.3	23.8	*	0.1	*	0.1	51.0	90.3	
KFM05A 109.75D	Chlorite/corrensite	1.3	2.1	12.4	25.3	*	0.2	*	0.1	46.9	88.4	
KFM05A 146.40	Chlorite/corrensite	0.9	5.1	9.4	33.8	0.2	1.2	*	0.5	30.9	81.9	From surface sample
KFM05A 232.95A	Chlorite/corrensite	0.8	8.7	10.6	35.5	0.2	2.2	*	0.2	31.8	90.1	
KFM05A 232.95B	Chlorite/corrensite	0.7	12.7	13.6	31.1	*	1.1	*	0.3	30.2	89.7	
KFM05A 232.95C	Chlorite/corrensite	*	11.7	13.2	31.8	0.1	0.9	0.1	0.4	27.4	85.7	
KFM05A 395.75A	Chlorite/corrensite	1.5	20.6	13.9	37.8	0.1	1.1	*	0.2	17.0	92.4	In micro vein
KFM05A 428.00A	Chlorite/corrensite	0.9	18.3	13.5	34.7	*	1.3	*	0.3	21.5	90.4	
KFM05A 428.00B	Chlorite/corrensite	0.7	21.9	12.7	35.9	*	1.1	*	0.3	11.5	84.3	
KFM05A 428.00C	Chlorite/corrensite	0.7	18.1	12.6	33.5	*	1.0	*	0.4	18.9	85.3	
KFM05A 428.00D	Chlorite/corrensite	0.8	17.4	12.6	34.3	0.5	1.0	*	0.3	18.4	85.3	
KFM05A 938.00	Chlorite/corrensite	*	4.4	10.3	30.3	0.2	2.0	*	0.0	35.5	83.0	
KFM05A 702.42A	Chlorite/corrensite	0.9	23.4	13.6	33.4	*	0.2	*	0.2	16.7	88.4	
KFM05A 702.42B	Chlorite/corrensite	0.7	4.1	13.1	30.0	0.5	1.7	*	0.2	38.8	89.3	
KFM05A 702.42C	Chlorite/corrensite	0.9	22.8	13.0	33.1	*	0.2	*	0.2	17.6	87.6	
KFM05A 702.42D	Chlorite/corrensite	0.6	3.0	14.6	26.3	0.2	1.2	*	0.2	41.6	87.7	
KFM05A 702.42F	Chlorite/corrensite	*	21.1	13.0	33.1	*	0.1	*	0.1	19.6	87.1	
KFM05A 702.42G	Chlorite/corrensite	*	18.6	13.2	34.0	0.1	0.8	*	0.2	16.7	83.6	
KFM05A 938.00	Hematite	*	0.2	0.6	1.0	*	*	0.4	*	86.2	88.5	
KFM04A 226.20f	Epidote	*	*	21.2	35.9	*	22.5	*	*	14.9	94.7	
KFM04A 226.20g	Epidote	*	*	24.0	31.1	*	22.9	*	0.3	12.0	96.4	
KFM05A 692.00F	Epidote	*	*	23.7	37.8	*	23.0	0.1	0.2	13.8	98.5	In chlorite in wall rock
KFM05A 737.78C	Epidote	*	*	24.3	38.2	*	22.8	*	0.3	12.3	98.0	

Sample	Mineral	Na_2O	MgO	Al_2O_3	SiO_2	K_2O	CaO	TiO_2	MnO	FeO	Total	Comment
KFM05A 111.56B	Illite	*	6.1	14.5	32.9	4.9	*	1.2	0.3	22.0	82.0	
KFM04A 226.20d	Laumontite	*	*	21.3	49.9	0.2	11.3	*	*	*	82.7	
KFM05A 395.75B	Prehnite	0.5	*	21.4	42.4	0.1	26.2	*	*	3.1	93.3	
KFM05A 689.33B	Prehnite	0.7	*	23.1	43.7	0.2	25.6	*	*	1.0	93.8	In adularia vein
KFM05A 689.33C	Prehnite	0.5	*	21.2	40.2	0.1	24.6	*	*	1.1	87.3	
KFM05A 689.33D	Prehnite	0.6	*	18.6	39.5	0.1	24.4	*	*	4.9	88.0	
KFM05A 689.33E	Prehnite	0.4	*	21.4	40.4	0.1	24.8	*	0.1	1.3	88.0	
KFM05A 689.33F	Prehnite	0.6	*	17.2	39.6	*	24.5	*	*	7.2	88.7	
KFM05A 692.00G	Prehnite	*	*	20.9	43.4	*	26.1	0.2	*	5.3	95.8	In chlorite in wall rock
KFM05A 737.78D	Prehnite	*	*	22.0	42.2	*	25.7	*	*	2.9	92.9	
KFM05A 737.78E	Titanite	*	0.1	7.1	29.8	*	26.4	27.4	*	*	91.4	In wall rock

* = Below detection limit.

Appendix 3

Calcite, stable isotopes

Sample	$\delta^{13}C$ PDB	$\delta^{18}O$ PDB	$^{87}Sr/^{86}Sr$	Comment
KFM01B 25.30 m	–7.5	–10.8	0.714460	
KFM01B 417.53 m	–5.2	–18.7	0.709264	
KFM04A 347.32 m	–13.0	–13.6		
KFM04A 232.80 m	–17.1	–11.4		
KFM04A 235.50 m	–4.2	–9.7	0.715579	
KFM04A 294.50 m (A)	–26.4	–12.7		
KFM04A 294.50 m (B)	–26.8	–12.3		
KFM04A 295.67 m	–14.1	–13.4	0.715168	
KFM04A 296.50 m	–13.6	–13.5	0.715491	
KFM04A 306.40 m	–30.5	–12.7	0.715118	
KFM04A 414.10 m	–11.1	–13.2		
KFM05A 146.40 m (A)	–13.2	–12.4	0.715590	Eq-sca
KFM05A 146.40 m (B)	–13.5	–12.4		Eq-gran
KFM05A 395.75 m	–3.2	–13.4	0.709085	
KFM05A 702.74 m	–15.3	–13.5	0.716106	Eq-sca
KFM05A 719.12 m (A)	–22.5	–12.7	0.714891	Open fracture
KFM05A 719.12 m (B)	–9.4	–16.7	0.709287	Sealed fracture
KFM05A 938.00 m	–6.3	–13.2	0.715327	Eq
KFM06A 106.94 m	–15.1	12.4		With asphaltite
KFM06A 110.49 m	–19.0	–13.0		
KFM06A 170.06 m	–11.3	–11.9		Euhdral with corrensite
KFM06A 142.27 m (A)	–12.3	–11.9		
KFM06A 142.27 m (B)	–6.8	–10.8		Later than A
KFM06A 331.88 m (A)	–18.0	–13.1		
KFM06A 331.88 m (B)	–14.3	–13.5		Later than A
KFM06A 336.68 m	–18.1	–11.8		
KFM06A 348.06 m	–15.7	–13.1		Breccia sealing
KFM06A 352.27 m	–16.8	–13.6		
KFM06A 356.53 m	–16.2	–12.0		

Appendix 4

Calcite chemistry, ICP-MS

Drillcore		KFM01B	KFM04A	KFMO4A	KFM04A	KFM04A	KFM05A	KFM05A	KFM06A	KFM06A	KFM06A	KFM06A
Depth		417.53	226.98	294.5	294.67	306.4	702.74	719.12	106.94	331.88	348.06	356.53
Element												
Na	ppm	45	24	47	29	52	131	61	91	84	58	115
Mg	ppm	113	320	17	12	< 2	45	38	182	12	12	209
Al	ppm	50	124	< 50	< 50	110	< 50	< 50	243	< 50	< 50	193
K	ppm	80	62	62	74	64	78	96	109	80	87	144
Ca	ppm	408,500	419,800	414,900	421,000	417,100	420,500	417,100	412,000	412,400	340,900	404,000
Sc	ppm	0.47	< 0.01	< 0.01	< 0.01	< 0.01	< 0.01	< 0.01	1.31	0.04	0.46	0.62
Mn	ppm	1,537	14	681	165	294	713	720	432	597	436	617
Fe	ppm	780	760	814	764	790	946	774	1,609	838	705	910
Rb	ppm	0.09	< 0.01	0.11	< 0.01	< 0.01	0.06	0.04	0.07	0.05	0.12	0.65
Sr	ppm	248	334	54	22	21	49	186	32	41	50	38
Y	ppm	9.01	4.53	9.67	1.24	3.02	44.96	0.34	15.55	13.04	22.04	35.00
Ba	ppm	< 1	< 1	< 1	< 1	< 1	< 1	< 1	< 1	< 1	< 1	< 1
La	ppm	1.14	0.17	13.81	2.42	5.18	29.92	0.25	8.25	34.95	20.01	8.15
Ce	ppm	2.12	< 0.01	42.92	6.31	12.39	139.90	0.27	28.33	86.11	62.09	43.37
Pr	ppm	0.20	0.02	5.62	0.70	1.69	19.32	< 0.01	3.92	9.57	7.16	6.96
Nd	ppm	1.66	0.82	27.04	3.83	9.88	105.70	0.16	21.81	40.45	30.51	39.72
Sm	ppm	0.51	0.24	4.71	0.74	1.65	23.13	0.07	6.41	6.53	7.71	10.38
Eu	ppm	0.05	< 0.01	0.34	< 0.01	0.04	1.25	< 0.01	0.31	0.29	0.32	0.72
Gd	ppm	0.62	0.23	3.87	0.40	1.19	18.13	< 0.01	5.44	5.31	6.47	10.10
Tb	ppm	0.02	< 0.01	0.27	< 0.01	0.04	1.62	< 0.01	0.53	0.39	0.77	1.13
Dy	ppm	0.64	0.33	1.41	0.13	0.45	7.47	< 0.01	2.84	2.04	3.66	5.86

Drillcore Depth		KFM01B 417.53	KFM04A 226.98	KFMO4A 294.5	KFM04A 294.67	KFM04A 306.4	KFM05A 702.74	KFM05A 719.12	KFM06A 106.94	KFM06A 331.88	KFM06A 348.06	KFM06A 356.53
Element												
Ho	ppm	0.10	0.01	0.19	< 0.01	0.03	1.41	< 0.01	0.47	0.32	0.60	1.15
Er	ppm	0.43	0.20	0.55	0.01	0.18	3.59	< 0.01	1.25	0.93	1.88	3.32
Tm	ppm	0.02	< 0.01	0.01	< 0.01	< 0.01	0.39	< 0.01	0.12	0.07	0.19	0.47
Yb	ppm	0.54	0.24	0.49	0.07	0.29	3.16	0.01	1.26	0.82	1.80	3.32
Lu	ppm	0.02	< 0.01	0.04	< 0.01	< 0.01	0.46	< 0.01	0.15	0.09	0.23	0.52
Th	ppm	0.08	0.08	0.12	0.10	0.09	0.09	0.09	0.21	0.10	0.24	0.25
U	ppm	0.03	0.19	0.13	< 0.01	< 0.01	0.12	< 0.01	0.04	0.07	0.07	0.37

Appendix 5

Calcite chemistry, LA-ICP-MS traverses

	KFM06A 142.27 B1	KFM06A 142.27 B2	KFM06A 142.27 B3	KFM06A 142.27 B4	KFM06A 142.27 B5	KFM06A 142.27 B6	KFM06A 142.27 B7	KFM06A 142.27 B8
Ca43 (%)	40.0	41.8	50.8	43.1	43.2	41.8	44.6	51.0
Ca44	--IS--	--IS--	--IS--	--IS--	--IS--	--IS--	--IS--	--IS--
Sc45 (ppm)	25.2	152.0	66.8	56.5	70.1	68.9	72.1	97.0
Mn55 (ppm)	1,870.7	656.5	575.2	319.9	526.3	231.7	428.8	349.8
Fe57 (ppm)	636.7	1,815.0	< 140	< 50	< 150	< 500	< 180	< 70
Rb85 (ppm)	< 0.11	< 5	< 0.19	< 0.26	< 0.14	< 0.15	< 0.3	< 0.13
Sr88 (ppm)	58.8	31.0	64.9	53.9	47.5	33.3	55.5	55.3
Y89 (ppm)	114.9	106.1	58.9	41.6	68.5	163.4	76.3	56.6
Ba137 (ppm)	1.0	20.7	< 1.8	< 2.4	< 1.6	< 1.9	< 4	< 1.1
La139 (ppm)	39.8	< 150	20.9	17.4	16.9	13.8	18.8	16.8
Ce140 (ppm)	53.2	< 220	42.8	38.2	37.4	32.9	39.9	44.9
Pr141 (ppm)	6.7	21.8	5.7	5.9	5.1	4.2	6.6	6.2
Nd146 (ppm)	25.1	< 140	24.5	25.5	21.6	18.2	25.7	27.6
Sm147(ppm)	6.7	21.5	7.4	8.5	7.8	7.0	9.4	9.7
Eu153 (ppm)	0.8	1.8	0.6	0.8	0.9	0.6	1.1	1.1
Gd157 (ppm)	9.6	24.3	8.6	8.6	9.5	8.3	11.5	9.2
Dy163 (ppm)	18.3	23.8	16.0	12.4	16.5	27.2	20.0	19.4
Er166 (ppm)	13.2	13.5	9.5	8.1	11.2	29.9	13.9	11.8
Yb172 (ppm)	14.6	15.7	14.7	11.9	13.6	< 70	24.6	20.8
Pb208 (ppm)	0.2	0.3	< 0.11	< 0.11	< 0.09	< 0.8	< 0.5	< 0.13

	KFM06A 142.27 C1	KFM06A 142.27 C2	KFM06A 142.27 C3	KFM06A 142.27 C4	KFM06A 142.27 C5	KFM06A 142.27 C6	KFM06A 142.27 C7	KFM06A 142.27 C8
Ca43 (%)	41.7	48.7	42.3	45.7	41.5	48.8	47.0	45.2
Ca44	--IS--	--IS--	--IS--	--IS--	--IS--	--IS--	--IS--	--IS--
Sc45 (ppm)	56.1	54.7	69.9	54.9	50.1	6.3	5.4	10.9
Mn55 (ppm)	443.0	608.5	428.1	511.0	551.6	305.2	301.3	280.7
Fe57 (ppm)	84.3	< 220	< 70	66.5	5,684.8	< 270	< 800	< 1,700
Rb85 (ppm)	< 0.16	< 0.3	< 0.12	< 0.1	< 12	< 0.4	< 0.6	< 2.8
Sr88 (ppm)	56.3	117.7	63.2	38.5	43.7	38.9	46.7	39.8
Y89 (ppm)	64.6	35.9	61.0	39.9	79.7	27.2	36.1	41.7
Ba137 (ppm)	< 1.3	2.5	< 1.4	< 0.9	60.8	< 2.6	6.0	< 19
La139 (ppm)	24.0	11.3	29.2	8.0	36.1	30.5	31.2	26.4
Ce140 (ppm)	54.7	29.9	54.4	18.9	73.9	51.3	52.1	49.8
Pr141 (ppm)	7.1	4.0	7.7	2.8	8.9	6.2	7.4	7.4
Nd146 (ppm)	31.8	14.4	37.1	14.6	37.7	23.6	26.4	30.2
Sm147(ppm)	10.4	5.4	10.3	4.5	11.6	5.6	6.6	8.6
Eu153 (ppm)	1.0	0.5	1.0	0.6	0.9	0.4	0.5	0.7
Gd157 (ppm)	10.8	6.2	11.3	5.2	14.5	5.1	6.9	8.6
Dy163 (ppm)	17.7	9.9	16.5	11.2	16.3	4.9	6.0	7.5
Er166 (ppm)	11.6	6.0	10.3	6.6	9.7	2.9	3.4	3.6
Yb172 (ppm)	19.7	9.7	16.6	14.4	11.1	3.0	3.0	3.7
Pb208 (ppm)	< 0.1	< 0.6	< 0.07	< 0.04	1.2	< 0.09	< 0.1	< 0.4

	KFM06A 142.27 C9	KFM06A 142.27 D1	KFM06A 142.27 D2	KFM06A 142.27 D3	KFM06A 142.27 D4	KFM06A 142.27 D5	KFM06A 142.27 D6	KFM06A 142.27 D7
Ca43 (%)	44.4	46.9	45.6	42.1	43.5	43.6	43.7	45.4
Ca44	--IS--	--IS--	--IS--	--IS--	--IS--	--IS--	--IS--	--IS--
Sc45 (ppm)	6.8	2.7	0.9	3.4	0.6	0.8	11.6	4.9
Mn55 (ppm)	234.7	220.3	371.9	279.9	437.2	438.4	299.7	85.7
Fe57 (ppm)	< 210	309.8	30.8	27.8	32.3	< 40	< 1,800	< 110
Rb85 (ppm)	< 1.1	< 0.27	< 0.07	< 0.07	< 0.06	< 0.1	< 14	< 1.6
Sr88 (ppm)	33.7	21.7	53.7	36.9	90.3	53.3	73.2	< 40
Y89 (ppm)	26.5	10.8	45.4	25.7	79.6	87.3	46.2	< 40
Ba137 (ppm)	7.1	< 2.2	< 0.6	< 0.6	1.0	< 0.3	54.9	< 50
La139 (ppm)	21.8	27.6	32.6	12.0	93.9	24.9	35.0	14.1
Ce140 (ppm)	42.9	54.7	67.6	25.5	228.4	115.7	70.0	25.7
Pr141 (ppm)	5.7	6.7	12.3	3.8	32.9	26.8	10.5	< 4
Nd146 (ppm)	25.4	30.7	61.2	17.3	163.2	179.7	49.1	12.9
Sm147(ppm)	7.3	4.4	13.6	5.2	30.2	42.1	12.4	< 8
Eu153 (ppm)	0.5	0.2	0.7	0.3	2.1	3.1	0.6	< 0.7
Gd157 (ppm)	7.4	3.4	11.5	6.1	29.0	35.1	12.7	< 10
Dy163 (ppm)	5.5	2.1	7.5	4.9	14.0	15.6	8.0	< 25
Er166 (ppm)	2.7	1.1	4.3	2.5	6.6	7.9	4.1	< 8
Yb172 (ppm)	2.5	1.1	3.7	2.7	5.1	6.3	3.9	6.4
Pb208 (ppm)	< 2.1	< 0.13	< 0.03	< 0.026	< 0.12	< 0.03	< 0.27	< 0.12

	KFM06A 142.27 D8	KFM06A 324.54 A1	KFM06A 324.54 A2	KFM06A 324.54 A3	KFM06A 324.54 A4	KFM06A 324.54 A5	KFM06A 324.54 A6	KFM06A 324.54 A7
Ca43 (%)	45.3	41.6	44.7	44.6	45.3	41.1	41.0	38.1
Ca44	--IS--	--IS--	--IS--	--IS--	--IS--	--IS--	--IS--	--IS--
Sc45 (ppm)	7.2	0.8	0.7	< 0.5	0.6	4.7	19.0	6.7
Mn55 (ppm)	195.6	144.2	181.2	159.1	156.0	895.6	682.5	712.8
Fe57 (ppm)	181.6	< 1,200	1,802.9	< 190	151.3	284.7	162.2	12,123.4
Rb85 (ppm)	< 2.7	0.4	< 0.3	< 0.5	< 0.8	< 0.22	< 0.22	< 5
Sr88 (ppm)	37.1	32.2	41.3	29.0	32.4	56.9	55.4	33.2
Y89 (ppm)	23.9	8.4	9.6	8.2	8.4	400.8	372.8	38.0
Ba137 (ppm)	9.7	3.3	3.5	< 7	< 9	< 1.9	< 2	15.1
La139 (ppm)	21.4	16.1	18.4	17.5	18.5	38.4	47.6	26.0
Ce140 (ppm)	50.1	26.7	32.0	27.4	33.5	44.6	65.6	33.2
Pr141 (ppm)	6.6	3.7	4.3	4.2	5.2	7.9	10.7	4.5
Nd146 (ppm)	23.6	14.4	16.9	16.9	18.6	34.0	42.1	19.7
Sm147 ppm)	6.1	3.0	3.2	3.0	3.0	10.5	14.1	4.1
Eu153 (ppm)	0.5	0.2	0.2	0.2	0.2	1.8	2.1	0.4
Gd157 (ppm)	5.7	2.4	3.2	2.3	2.6	19.4	21.0	4.5
Dy163 (ppm)	4.9	1.4	1.4	1.2	1.5	49.2	69.8	6.9
Er166 (ppm)	2.2	0.8	0.9	0.7	0.8	54.2	91.8	5.8
Yb172 (ppm)	2.6	1.0	1.1	0.8	1.0	63.0	167.4	7.6
Pb208 (ppm)	< 0.12	< 0.09	< 0.13	< 0.15	< 0.22	< 0.031	< 0.1	< 0.15

	KFM06A 324.54 B1	KFM06A 324.54 B2	KFM06A 324.54 B3	KFM06A 324.54 B4	KFM06A 324.54 B5	KFM06A 324.54 B6	KFM06A 324.54 B7
Ca43 (%)	41.7	44.6	43.8	41.5	42.8	39.5	43.9
Ca44	--IS--	--IS--	--IS--	--IS--	--IS--	--IS--	--IS--
Sc45 (ppm)	< 1.7	< 0.4	< 0.7	< 1	4.5	6.9	5.6
Mn55 (ppm)	188.9	201.1	167.1	157.3	727.2	797.1	649.4
Fe57 (ppm)	371.0	< 21	719.6	134.7	1,762.7	149.9	723.7
Rb85 (ppm)	< 0.8	< 0.12	< 0.6	< 1	< 0.28	< 1.2	3.2
Sr88 (ppm)	44.8	93.2	34.2	28.1	40.0	28.9	24.9
Y89 (ppm)	11.7	27.5	9.1	9.8	168.2	257.9	< 240
Ba137 (ppm)	< 7	< 1.7	< 3	< 12	2.0	< 14	13.0
La139 (ppm)	23.4	64.0	16.0	9.4	80.3	< 50	55.3
Ce140 (ppm)	42.1	122.5	28.4	15.8	104.1	< 50	82.5
Pr141 (ppm)	5.7	17.5	3.6	2.3	15.4	< 8	< 12
Nd146 (ppm)	24.7	79.8	16.2	10.4	59.5	< 40	< 50
Sm147 ppm)	4.7	16.1	3.0	2.0	14.6	< 11	< 17
Eu153 (ppm)	0.3	0.8	0.2	0.2	1.3	< 1.6	< 1.6
Gd157 (ppm)	3.3	11.0	2.3	1.9	17.3	13.2	< 23
Dy163 (ppm)	1.9	5.2	1.3	1.3	29.2	39.9	< 31
Er166 (ppm)	0.9	1.8	0.8	1.1	22.4	47.3	< 26
Yb172 (ppm)	0.9	1.2	1.1	1.7	27.2	91.5	24.8
Pb208 (ppm)	< 0.21	< 0.1	< 0.3	< 0.28	< 0.4	< 0.4	0.1

Appendix 6

Asphaltite analyses, stable isotopes

Sample	$\delta^{13}C$ ‰ PDB
KFM01B 22.97–23.05 m	–30.0
KFM01B 25.30–25.43 m	–29.5
KFM03B 65.20–65.25 m	–29.8
KFM05A 109.75–109.90 m	–29.7
KFM05A 111.56–111.60 m	–29.6
KFM06A 106.18–106.36 m	–30.1
KFM06A 111.40–111.52 m	–30.0

Appendix 7

XRD analyses

	Ca	Qz	Plag	K-fsp	Pre	Lau	Sme	Chl/Corr	Py	Hm	Ill	X
KFM01B												
28.65–28.70 m		X		X				X			X	
47.90–48.00 m		X	X	X			X	X			X	
418.29–418.43 m	X	X						X				Amp
KFM04A												
296.50–296.65 m	X	X				X		X				
KFMO5A												
105.58–105.65 m		X	X	X				X			X	
111.56–111.60 m		X	X	X				X			X	
428.00–428.13A m	X	X			X			X				
428.00–428.13B m	X	X						X				
611.17–611.20 m		X	X			X		X		X		
629.21–629.33 m	X	X	X			X		X		X	X	
705.81–705.88 m	X	X		X		X		X				Apo
771.95–772.05 m	X	X	X					X				
985.80–985.92 m	X	X	X	X				X		X	X	
KFM06A												
145.62–145.73 m		X	X	X			X	X	X		X	
201.94–202.07 m		X		X			X				X	
268.48–268.71 m	X	X										
503.44–503.49 m	X	X	X	X								Bi
622.31–622.36 m		X	X	X				X				
770.32–770.42 m	X	X		X				X				

Ca = Calcite
Qz = Quartz
Plag = Plagioclase (Albite)
K-fsp = K-feldspar (Adularia)
Pre = Prehnite
Lau = Laumontite
Sme = Smectite
Chl = Chlorite
Corr = Corrensite
Py = Pyrite
Hm = Hematite
Ill = Illite
Amp = Amphibole
Apo = Apophyllite
Bi = Biotite

Appendix 8

Mössbauer analyses

Sample	Fe-mineral	Oxidation factor (sil)*	Oxidation factor (tot)**	Oxidation factor oxides***
KFM02A 118.25–118.70 m	chlorite	0.33	0.35	1
KFM02A 903.65–903.70 m	chlorite	0.28		trace magnetite
KFM03A 451.85–451.90 m	chlorite, epidote	0.30		trace magnetite
KFM03A 803.85–804.05 m	chlorite	0.12		trace FeOOH?
KFM04A 192.00–192.10 m	chlorite, epidote, hematite	0.42	0.67	1

* Fe^{3+} (sil)/Fe^{3+} (sil)+Fe^{2+} (sil).
** Fe^{3+} (sil)+Fe^{3+} (oxide)/100.
*** Fe^{3+} (ox)/Fe^{2+} (ox)+Fe^{3+} (ox).

Appendix 9

Chemical analyses of fracture fillings

Borehole Depth Minerals/ Comment		KFM01A 127.40 Ana,Qz, K-fsp,chl	KFM01A 148.40 Pre,Corr, Ana,Py	KFM01A 149.18 Pre,Corr, Ana,Py	KFM01A 179.35 Qz,Ab,Chl Ca,Hm	KFM01A 185.35 Pre,Chl,Ill Hm,MLC	KFM01A 188.1 Lau,Qz	KFM01A 269.90 Pre,Ana Corr,Ca Qz,Py	KFM01B 25.30 Asph	KFM01B 28.65 K-fsp
SiO2	%	59.4	44.7	40.9	51.6	38.9	53.8	32.6	1.4	73.5
Al2O3	%	15.3	20.3	18.9	16.7	19.4	21.5	15.0	0.3	13.1
CaO	%	0.72	17.70	12.70	3.04	9.75	11.10	19.20	2.32	0.74
Fe2O3	%	10.7	6.7	10.8	11.6	10.5	1.0	10.2	0.7	2.4
K2O	%	3.01	1.29	1.60	1.74	1.48	0.39	0.65	0.15	8.48
MgO	%	1.52	3.44	7.80	4.54	6.18	0.16	6.45	<0.04	0.63
MnO	%	0.0567	0.0851	0.1700	0.1670	0.1410	0.0065	0.1500	0.0094	0.0188
Na2O	%	5.14	1.14	0.39	5.07	0.20	0.35	1.15	<0.08	0.58
P2O5	%	0.0228	0.0098	0.0073	0.2260	0.0098	0.0078	0.0123	0.0065	0.0706
TiO2	%	0.0904	0.0391	0.0199	0.9190	0.0356	0.0152	0.0263	0.0070	0.2190
Summa	%	96.0	95.4	93.3	95.6	86.6	88.4	85.4	4.8	99.8
Ba	mg/kg	554	180	340	161	76.3	128	117	16.2	1.540
Be	mg/kg	1.27	5.45	9.89	3.79	14.7	2.06	5.01	<1	2.36
Co	mg/kg	<6	<6	<6	21.5	<10	<6	<6	<10	<6
Cr	mg/kg	18.2	24	17.9	21.9	<30	<10	57	<20	27.3
Cs	mg/kg	32.7	9.21	3.02	n.a.	11.3	n.a.	8.58	n.a.	5.91
Cu	mg/kg	37.2	13.8	7.05	11.4	96.2	6.17	39.7	248	41.7
Ga	mg/kg	16.7	32.5	37.9	31.4	7.36	26.7	21.6	<2	13
Hf	mg/kg	2.31	0.416	0.818	2.38	0.907	0.264	0.666	<0.2	5.61
Mo	mg/kg	<2	<2	14.5	50.7	<5	<2	5.05	<4	<2
Nb	mg/kg	6.7	3.24	0.933	8.73	<0.5	0.959	0.882	<0.4	9.54
Ni	mg/kg	<10	<10	<10	19.1	<30	<10	13.8	<20	<10
Rb	mg/kg	99.5	39.1	47.9	106	141	20.6	26.5	<4	181
Sc	mg/kg	1.64	<1	<1	36.2	<3	<1	<1	<2	5.63
Sn	mg/kg	1.56	2.45	<1	6.05	2.77	<1	<1	5.22	19.6
Sr	mg/kg	52.3	22.6	54	193	79.7	338	53	9.01	50.4
Ta	mg/kg	0.53	0.367	0.137	0.771	<0.1	0.0987	0.094	<0.1	0.872
Th	mg/kg	1.51	0.247	0.53	2.9	<0.3	0.853	1.18	0.581	14.1
U	mg/kg	6.68	6.69	5.46	12.1	8.4	0.461	3.41	1.36	15.8
V	mg/kg	21.2	87.9	177	100	100	<2	50	24.8	18.6
W	mg/kg	6.18	4.6	1.85	2.95	11.3	1.04	2.56	22.2	1.42
Y	mg/kg	13.1	8.94	18	34.3	28.2	2.14	12.3	11.4	41.9
Zn	mg/kg	21.8	32.1	73.7	109	133	<10	93.9	94.2	78.2
Zr	mg/kg	47.1	2.36	6.8	97.7	6.57	12.4	10.6	12	211
La	mg/kg TS	30	4.52	10.8	41.8	45.6	6.6	25.3	4.16	114
Ce	mg/kg TS	56.1	13.1	24.9	62.4	182	15.2	47.9	9.34	170
Pr	mg/kg TS	5.08	1.41	2.43	8.27	12	1.46	5.16	<2	24.2
Nd	mg/kg TS	18.3	6.4	10.6	32.7	43.3	4.57	22.2	2.35	85
Sm	mg/kg TS	3.97	1.69	4.24	6.39	8.69	0.817	3.34	<0.6	12.7
Eu	mg/kg TS	0.501	0.177	<0.05	1.08	0.949	<0.05	0.262	<0.08	0.796
Gd	mg/kg TS	3.21	1.54	3.32	6.36	10.1	0.96	2.79	<0.6	9.11
Tb	mg/kg TS	0.468	0.14	0.414	0.799	1.1	0.119	0.222	0.235	1.2
Dy	mg/kg TS	2.26	1.17	2.46	4.47	4.3	0.574	1.53	1.38	5.94
Ho	mg/kg TS	0.467	0.219	0.526	0.961	0.981	0.107	0.317	<0.1	1.26
Er	mg/kg TS	1.17	0.52	1.18	3.13	3.24	0.588	0.939	<0.2	3.39
Tm	mg/kg TS	<0.1	0.142	0.227	0.491	<0.3	<0.1	<0.1	<0.2	0.647
Yb	mg/kg TS	1.51	0.911	1.13	3.34	2.21	<0.2	0.896	<0.4	4.77
Lu	mg/kg TS	0.148	0.0964	0.121	0.537	0.177	<0.03	0.0616	<0.06	0.756

Ab=albite, Amp=amphibole, Ana=analcime, Apo=apophyllite, Asph=asphaltite, Chl=chlorite, Corr=corrensite, Hm=hematite, Ill=illite, K-fsp=K-feldspar, Lau=laumontite, MLC=Mixed layer clay, Mus=muscovite, Pl=plagioclase, Pre=prehnite, Qz=quartz, Sme=smectite.

Cont.

Borehole Depth Minerals/ Comment		KFM01B 47.90	KFM01B 49.39 Asph,qz, K-fsp,chl	KFM01B 418.29	KFM02A 118.25 Qz,Ab, K-fsp,Ill	KFM02A 423.65 Qz,Ab K-fsp,Ca	KFM02A 476.75 Qz,Corr, Apo,Ca	KFM02A 516.09 Ca,Chl, Corr,Qz	KFM02A 893.45 Apo,Chl
		<0.5mm				Chl		Ab,K-fsp	
SiO2	%	49.2	34.6	35.6	71.8	70.6	40.1	40.0	51.0
Al2O3	%	16.5	8.7	13.1	14.2	12.5	11.9	16.4	1.2
CaO	%	1.82	0.25	6.04	0.45	0.88	6.79	12.40	22.70
Fe2O3	%	15.0	1.4	15.3	2.0	5.9	14.2	9.1	1.4
K2O	%	6.39	7.15	0.36	8.10	5.19	4.73	1.61	4.61
MgO	%	3.23	0.24	18.50	0.82	2.26	12.10	7.68	0.85
MnO	%	0.0747	0.0111	0.3730	0.0233	0.1240	0.3010	0.2860	0.0411
Na2O	%	1.09	0.15	0.34	1.07	2.13	0.18	2.37	0.21
P2O5	%	0.2870	0.0304	0.2300	0.0822	0.0815	0.1100	0.1290	0.0208
TiO2	%	0.9470	0.0686	0.5010	0.1250	0.2960	0.5580	1.0000	0.1190
Summa	%	94.5	52.7	90.3	98.7	100.0	91.0	90.9	82.2
Ba	mg/kg	681	1,480	33.2	1,220	1,430	317	207	247
Be	mg/kg	4.09	0.761	2.49	2.07	1.38	1.24	5.12	<1
Co	mg/kg	13.6	<6	80	<7	<6	21.6	17.8	<10
Cr	mg/kg	25.6	15.8	244	242	<10	617	294	<20
Cs	mg/kg	11.2	n.a.	<0.1	15.7	0.305	9.7	0.367	0.277
Cu	mg/kg	n.a.	12.2	n.a.	20.5	16.1	606	37.1	1490
Ga	mg/kg	32.5	<1	37	32.8	42.5	30	32.8	<2
Hf	mg/kg	2.73	2.16	0.998	7.26	11.5	0.942	6.93	3.26
Mo	mg/kg	2.46	<2	<2	<3	<2	<2	<2	<5
Nb	mg/kg	6.36	0.496	3.15	9.8	30.4	20.6	36.1	2.82
Ni	mg/kg	13.7	133	175	<10	<10	90.3	41.3	69.3
Rb	mg/kg	397	163	11.4	254	133	340	48.5	439
Sc	mg/kg	42.6	4.01	71.7	2.81	6.59	31.8	41.6	<2
Sn	mg/kg	14	<1	9.82	1.42	3.73	25.4	16.3	21.5
Sr	mg/kg	81.6	17.9	31.6	50.4	60.7	27.6	359	20.3
Ta	mg/kg	0.443	<0.06	0.295	1.12	2.72	23.1	5.15	0.209
Th	mg/kg	5.04	7.45	5.31	2.39	10.8	1.12	7.2	4.1
U	mg/kg	22.1	6.12	7.21	4.54	39.7	1.37	20.9	1.7
V	mg/kg	73	24.8	149	38.2	14.6	183	156	5.19
W	mg/kg	8.99	2.28	1.03	1.54	7.9	1.79	2.07	12.6
Y	mg/kg	56.9	52.9	19	25.4	39.1	35.4	54.2	212
Zn	mg/kg	124	39	311	56.5	87.5	285	196	194
Zr	mg/kg	152	116	18.7	250	353	24.9	197	87.3
La	mg/kg TS	88.6	31	9.04	12.9	38.4	43.8	37	815
Ce	mg/kg TS	148	44.8	21.3	25.6	74.6	44.4	57	1060
Pr	mg/kg TS	17.2	3.26	2.86	2.97	7.8	4.79	6.82	97.2
Nd	mg/kg TS	76.9	26	11.6	11	34.1	23	27.2	373
Sm	mg/kg TS	15.8	<0.4	2.35	2.72	7.23	4.88	6.87	58.4
Eu	mg/kg TS	1.79	0.285	0.558	0.383	0.909	<0.04	0.609	9.4
Gd	mg/kg TS	14.2	6.47	2.53	1.72	6.26	4.73	6.41	58.8
Tb	mg/kg TS	1.98	1.06	0.384	0.373	1.07	0.684	1.06	7.2
Dy	mg/kg TS	9.51	7.25	2.67	3.03	6.99	5	7.65	32.4
Ho	mg/kg TS	1.83	1.49	0.544	0.828	1.52	1.08	1.74	5.58
Er	mg/kg TS	4.48	3.13	1.65	2.76	4.76	3.94	6.27	12.9
Tm	mg/kg TS	0.742	0.456	0.261	0.496	0.783	0.486	1.12	1.5
Yb	mg/kg TS	4.34	2.9	1.73	3.8	4.65	5.37	9.84	6.38
Lu	mg/kg TS	0.635	0.396	0.279	0.641	0.634	0.686	1.54	0.85

Ab=albite, Amp=amphibole, Ana=analcime, Apo=apophyllite, Asph=asphaltite, Chl=chlorite, Corr=corrensite, Hm=hematite, Ill=illite, K-fsp=K-feldspar, Lau=laumontite, MLC=Mixed layer clay, Mus=muscovite, Pl=plagioclase, Pre=prehnite, Qz=quartz, Sme=smectite.

Cont.

Borehole Depth Minerals/ Comment		KFM03A 644.17	KFM03A 643.80 Ca,Qz,Ab K-fsp,Chl	KFM03A 803.85 Qz,Ab, Chl	KFM03B 65.2 Ca,Qz,Ab K-fsp,Chl	KFM05A 111.56 Qz,K-fsp, Asph,Ill	KFM05A 629.21 Ca,Qz,Ab, Lau,Corr,	KFM06A 145.62 Qz,Ab K-fsp,Sme	KFM06A 770.32 Ca,Qz, K-fsp
			Corr, Hm		Corr, Ill	<0.125mm	Hm, Ill	Corr,Py,Ill	Corr
SiO2	%	31.5	29.9	54.6	64.7	66.6	45.5	44.5	50.8
Al2O3	%	12.8	11.3	14.0	15.7	13.1	10.5	17.2	15.2
CaO	%	8.61	12.70	1.55	1.30	0.21	5.81	0.71	9.83
Fe2O3	%	22.7	17.7	15.6	4.7	3.3	13.9	14.7	4.6
K2O	%	2.07	2.20	3.02	5.20	9.85	2.18	4.77	8.08
MgO	%	9.60	8.10	4.96	2.30	0.63	9.41	7.36	2.05
MnO	%	0.3100	0.3000	0.2370	0.0000	0.0281	0.1550	0.1200	0.0776
Na2O	%	0.99	1.10	3.24	3.80	0.18	1.43	0.32	1.79
P2O5	%	0.0941	0.0398	0.1100	0.4600	0.0271	0.0164	0.0041	0.0404
TiO2	%	0.9320	0.9000	0.6910	0.5000	0.2240	0.0637	0.0492	0.0933
Summa	%	89.6	84.2	98.0	98.7	94.1	89.0	89.7	92.6
Ba	mg/kg	704	551	292	313	1,770	419	215	797
Be	mg/kg	13.6	11.1	3.19	2.88	1.22	3.74	14.5	3.38
Co	mg/kg	43.2	38.3	10.9	13.6	<6	<7	211	<6
Cr	mg/kg	940	816	74.1	17	413	1760	19	36.2
Cs	mg/kg	8.35	5.02	2.77	7.05	2.56	1.71	14.1	0.865
Cu	mg/kg	n.a.	249	114	162	<6	18.9	77.6	208
Ga	mg/kg	36.5	29.8	88.9	11.2	12.8	47.2	70.5	27.6
Hf	mg/kg	3.25	2.7	8.14	3.38	3.69	3.77	1.17	3.73
Mo	mg/kg	11.6	<2	8.13	<2	2.37	<3	8.07	5.88
Nb	mg/kg	18	33.6	54	30.5	9.82	3.15	7.92	17.1
Ni	mg/kg	231	183	52	<10	<10	19.5	109	18.4
Rb	mg/kg	128	116	118	135	326	86.8	259	186
Sc	mg/kg	61.7	47.4	17.5	12.8	8.13	3.17	151	4.44
Sn	mg/kg	11.2	5.78	15.4	9.03	12.9	4.24	93.1	8.37
Sr	mg/kg	128	110	69.6	74.9	15.8	102	53.2	490
Ta	mg/kg	5.26	4.14	3.35	4.31	0.748	0.263	0.767	1.59
Th	mg/kg	11.4	6.8	1.3	8.07	9.77	6.93	2.06	14.7
U	mg/kg	2200	2310	3.32	14.5	3.25	69.4	17.8	12.8
V	mg/kg	244	195	74.2	35.1	19.1	22	430	32.9
W	mg/kg	16.9	11.5	4.01	4.69	1.77	8.01	0.626	6.09
Y	mg/kg	217	198	34.2	39.5	39.7	134	104	90
Zn	mg/kg	1210	234	158	148	110	201	96.3	170
Zr	mg/kg	102	91	287	125	133	104	26.3	105
La	mg/kg TS	105	70.8	8.36	12	46.9	201	3.78	24.9
Ce	mg/kg TS	105	73.3	21.1	15.9	95.9	1090	14.6	46.7
Pr	mg/kg TS	13.3	10.4	6.65	3.32	11.3	41.9	1.83	6.33
Nd	mg/kg TS	50.8	40.6	14.6	14.4	38.2	191	7.92	23.2
Sm	mg/kg TS	14.4	12.7	4.06	2.98	7.36	39.8	3.77	5.21
Eu	mg/kg TS	2.23	2.17	0.555	0.814	0.529	3.13	0.394	0.423
Gd	mg/kg TS	18.9	19.5	0.855	4.54	6.58	47.7	7.63	6.91
Tb	mg/kg TS	4.22	4.12	<0.1	0.762	0.996	4.76	1.44	1.46
Dy	mg/kg TS	29.9	31.4	4.71	5.52	5.75	15.6	10.6	11.5
Ho	mg/kg TS	7.17	7.19	1.13	1.23	1.14	2.57	2.42	2.65
Er	mg/kg TS	24.5	23.7	3.04	3.91	3.11	4.85	9.04	8.44
Tm	mg/kg TS	4.02	4.24	0.668	0.738	0.537	0.396	1.43	1.43
Yb	mg/kg TS	30	28.7	3.76	4.66	3.22	3.2	11.2	9.88
Lu	mg/kg TS	4.84	4.85	0.537	0.733	0.435	0.353	1.66	1.24

Ab=albite, Amp=amphibole, Ana=analcime, Apo=apophyllite, Asph=asphaltite, Chl=chlorite, Corr=corrensite, Hm=hematite, Ill=illite, K-fsp=K-feldspar, Lau=laumontite, MLC=Mixed layer clay, Mus=muscovite, Pl=plagioclase, Pre=prehnite, Qz=quartz, Sme=smectite.